ISSN 1994-3237
Volume 44(1), 2011

Abstract Volume & Program

26th Himalaya-Karakoram-Tibet Workshop

Canmore, Alberta, Canada

July 12-13, 2011

JHES

Journal of Himalayan Earth Sciences

Edited By
Guilmette, C., Larson, K.
Unsworth, M., Grudjic, D.
Hébert, R., Godin, L.
Coutand, I., Kellett, D.

Understanding the origins of Eo- and Neohimalayan granitoids in Eastern Tibet

Amos Aikman[1], T. Mark Harrison[2]

[1] Research School of Earth Sceinces, The Australian National University, Canberra, A.C.T. 0200, Australia
[2] Dept. of Earth and Spa ce Sciences, UCLA, Los Angeles, CA 90095 USA; tmark.harrison@gmail.com

The magmatic history of the eastern Himalaya is only now being studied to the extent that the rest of the range has been documented but has already revealed several surprises. Perhaps the most paradoxical occurrences are the Eocene igneous complexes which outcrop within the Tethyan Himalaya. In context of a N-S transect from the Main Central Thrust (MCT) to the Indus Tsangpo suture (ITS), we have studied two of these centers, the Dala igneous complex and the Yala-Xiangbo granitoids, and conclude that they arose from very different processes.

The Dala granitoids formed from Gangdese-type magmas that assimilated approximately 50% crustal material from the Greater Himalayan Crystallines (GHC) and/or Tethyan Himalayan Sequence (THS) prior to emplacement at relatively shallow crustal levels. In contrast, the Yala-Xiangbo granitoids are a series of leucocratic sills, dykes and small plutons that, although structurally similar to the North Himalayan granites (NHG), were emplaced 15 to 30 m.y. earlier. The Dala granitoids, in particular, represent a mode of Eocene magmatism undocumented elsewhere in the Himalaya.

Also observed are anatectic granitoids similar to the High Himalayan Leucogranites (HHL) and North Himalayan Granites (NHG) commonly found across the Himalayan Arc. The Miocene Arunachal Leucogranites (AL) and Tsona Leucogranites (TL) outcrop, respectively, within the Arunachal Greater Himalayan Crystalline (GHC) sequence and adjacent the South Tibetan Detachment. They are equivalent to the HHL in terms of emplacement style and structural position. While the Tsona leucogranites formed by vapour-absent melting of nearby units, as has been generally documented for the HHL, the Arunachal leucogranite suite formed by a combination of both vapour-absent muscovite melting and vapour-present melting of the Lesser Himalayan series. Although once the preferred model for Himalayan leucogranite formation, vapour-present melting of Himalayan sequences has since been largely abandoned in favour of vapour-absent melting of micas to explain the genesis of the HHL and NHG. We suggest that vapour-present melting may be more widespread in the Himalaya than currently thought.

We conclude that by ca. 45 Ma, thickened THS metasediments were already in the hanging wall of the main Himalayan decollement. During the Eohimalayan episode, the eastern Himalaya experienced amphibolite-grade metamorphism and localised peraluminous granitoid magmatism. Subsequently, a period of tectonic quiescence occurred in the northern Himalaya simultaneous with shortening occurring further south. The Neohimalayan history of the eastern Himalaya is similar to other parts of the range where deformation and magmatism were intimately associated in the frontal part of the range. Exhumation in the North Himalaya appears to have largely been driven by thrusting along the ITS.

The results of this study suggest that the prevailing view of post-collisional granitic magmatism, developed largely from investigations in the central Himalaya, does not well-describe the easternmost segment of the Himalayan Arc. Particularly puzzling is the origin of Eocene igneous complexes which outcrop within the Tethyan Himalaya, as the heat source needed to generate Eohimalayan peraluminous magmatism (and regional metamorphism) in the eastern Tethyan Himalaya is not predicted by existing models. However, tomographic images reveal a persistent lithospheric weakness, coincident with the Ninety East Ridge, which intersects the eastern Himalaya beneath our study area. This feature may have localized heat-flow and magmatism beneath the eastern Himalaya throughout the Tertiary.

Miocene exotic taxa in the Indian Himalaya and subtle aspects of India-Asia collision

Ansuya Bhandari and B. N. Tiwari

Wadia Institute of Himalayan Geology, 33, Gen M S Road, Dehra Dun 248 001 Uttarakhand, India, ansuya12@rediffmail.com

India–Asia collision eliminated marine barrier and thus gave way to mixing of life on either landmasses and as a consequence succeeding horizons deposited in basins adjoining suture zone are characterized by their exotic fossil taxa. Following suturing, Ladakh Molasse Basin apparently served as the meeting ground for the fauna from both bio-provinces and thus eventually provides palaeontological view and constraints to the events that followed the collision. Studies on the similar lines of the fauna from basins on the southern flank of the Himalaya that are more or less coeval to Ladakh Molasse are more insightful in revealing the subtle details of geomorphological changes due to earliest phase of the collisional and deformational dynamics. Induction of exotic deinotheres, native African folivorous beasts, in Dharmsala Basin of Indian Himalayan region in early Miocene is a potential proxy to the fact that basin was having a well drained thick forest, and thus older levels of the region revealing barrenness indicate a big change in the intervening interval. Similarly cyprinids and other species known to have roots and better dispersal history in Asian territories in the north are now well represented in Miocene Dharmsala assemblage; realization of the fact that surface water streams' bound fishes reaching in the Himalayan region from Tibet and across areas of the Asia impels to visualize surface water streams following available slopes due to post-collisional tectonics, that is, an embryonic antecedent river system.

Our explanation regarding occurrence of exotic Dharmsala cyprinids through connecting streams in conjunction with their Oligo-Miocene records from Ladakh and earliest phase of Himalayan Orogeny is apparently tenable. Similarly, disjunct distributions of the extant Malayan freshwater fishes in the Indian shield region — core issue explained by Hora's Satpura Hypothesis (now annulled) — can better be explained by taking into account orogeny driven multiple river reorganizations that are known to have taken place.

River capture in the Easternmost Himalaya: Testing erosion-tectonic feedback models using palaeo-Brahmaputra deposits of the Bengal Basin, Bangladesh

Laura Bracciali[1,2], Yani Najman[2], Randall R. Parrish[1], and Matthew S.A. Horstwood[1]

[1] NERC Isotope Geosciences Laboratory, British Geological Survey, Keyworth, Nottingham, NG12 5GG, UK, laur@bgs.ac.uk
[2] Lancaster Environment Centre, Lancaster University, Lancaster, LA1 4YQ, UK

Fluvial drainages impact on, and are impacted by, surface uplift, exhumation and strain, and thus an investigation of their evolution provides a key to understanding crustal deformation processes and erosion-tectonic-climate interactions. In the context of the protracted India-Asia collision, the unusual drainage configuration near the eastern syntaxial region of the Himalaya (Fig. 1) has been interpreted either as distorted drainage resulting from crustal shortening and lateral extrusion of crustal material (Hallet and Molnar 2001) or as the result of river capture events tectonically induced by surface uplift, with the more northerly basins' evolution related to regional-scale uplift of Tibet, and the more southerly captures (including the Yarlung Tsangpo by the Irrawaddy and finally the Brahmaputra River) to sub-regional uplift at the eastern syntaxis (Clark et al. 2004). A further twist to the latter is that one such capture event, that of the Yarlung Tsangpo by the Brahmaputra, has potentially resulted in extremely rapid recent exhumation of the Indian plate metamorphic rocks of the Namche Barwa Eastern syntaxis by focused weakening of the crust due to very rapid fluvial incision and erosive thinning of strong upper crust due to the capture event (erosion-tectonic coupling model, Zeitler et al. 2001). Hence, determining if and when this river capture event occurred is key to testing these models of crustal deformation. Additionally, constraining the timing of the exceptionally rapid exhumation in the syntaxis that we see today, is crucial to relate or refute any connection of rapid erosion to a capture event.

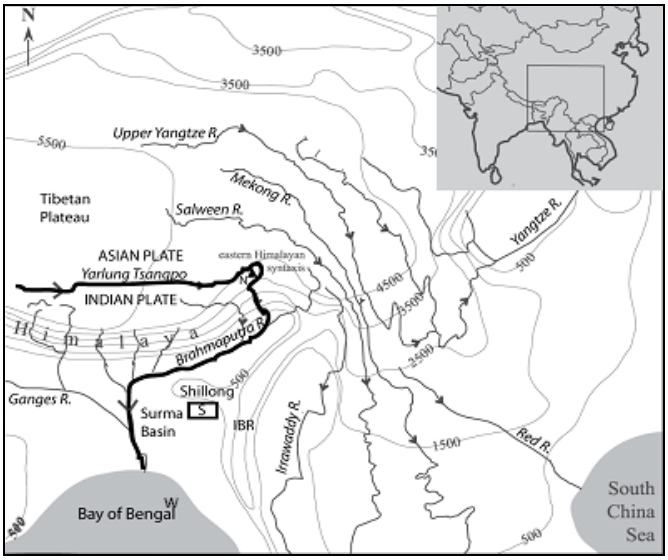

Figure 1. Major fluvial drainage systems of the eastern Himalayan-Tibet region (adapted from Clark et al. 2004). The Yarlung Tsangpo-Brahmaputra River is traced in thicker outline. The east-flowing Yarlung Tsangpo lies along the suture zone separating metamorphosed Indian plate Himalayan material to the south from Asian Plate Trans-Himalayan arc material to the north. The river then crosses the rapidly exhuming Namche Barwa of the Eastern Himalayan syntaxis (triangle with small 'N'). At this location the Yarlung drops into a steep gorge before flowing south, transverse to the Himalaya, as the Brahmaputra.
Rectangle labelled "S" is Surma Basin; Shillong = Shillong Plateau; IBR = Indo-Burman Ranges.

The Yarlung Tsangpo follows the line of the India-Asia suture zone, draining the Jurassic-Paleogene Trans-Himalayan arc of the Asian plate (Liang et al. 2008; Chiu et al 2009) to the north of the suture and the northern part of the Tethyan Himalaya of the Indian plate to the south of the suture (Hodges 2000). The Brahmaputra prior to capture would have drained the southern Himalayan slopes composed only of Precambrian-Palaeozoic Indian crust (Hodges 2000), much of it metamorphosed to high grade during the Oligo-mid-Miocene. On the assumption that capture took place, the first arrival of detritus carried by the Yarlung Tsangpo detritus (with its Cretaceous-Paleogene juvenile crust fingerprint) in the Neogene deposits of the palaeo-Brahmputra river in Bangladesh (Surma Basin, Fig. 1; Najman et al. 2008 and references therein) should date the capture event.

Input from the eastern syntaxis can be identified in the Brahmaputra sedimentary record by the appearance of rapidly exhumed mineral grains (those with short lag times, i.e. the difference between the

mineral cooling age and the host sediment depositional age) and very young grains (<10 Ma and in particular <6 Ma; Burg et al. 1998; Ding et al. 2001; Booth et al. 2004, 2009) which would demonstrate that the syntaxis has been rapidly exhuming since Plio-Pleistocene times (and possibly as early as late Miocene). This source now dominates the detritus in the Brahmaputra sediment budget downstream of the syntaxis with material from the Asian plate being subordinate (Stewart et al. 2008).

To address the river capture and the erosion-tectonic coupling hypotheses, U-Pb LA-MC-ICP-MS dating of detrital zircon grains (from palaeo-Brahmputra sediments as well as sands from modern rivers draining the Trans-Himalaya and Himalayan southern slopes) is integrated with microtextural analysis in a revised approach to the use of detrital zircon data as applied to provenance studies. Detrital zircon data (from mantles/cores of grains as well as from thin rims) are complemented by the novel application of U-Pb dating to rutile detrital grains. In this ongoing multi-technique study, Ar-Ar dating of detrital white mica and zircon fission-track thermochronology will also be used to assess the timing of rapid exhumation of the syntaxis.

References

Booth, A.L. et al., 2004, U-Pb zircon constraints on the tectonic evolution of Southeastern Tibet, Namche Barwa Area, American J. Science, 304, 889-929.

Booth., A.L., Chamberlain, C.P., Kidd, W.S.F. and Zeitler, P.K., 2009, Constraints on the metamorphic evolution of the eastern Himalayan syntaxis from geochronologic and petrologic studies of Namche Barwa, Geological Soc. America Bull., 121, 385-407.

Burg, J-P. et al., 1998, The Namche Barwa syntaxis: evidence for exhumation related to compressional crustal folding, J. Asian Earth Sciences, 16, 239-252.

Chiu, H-Y. et al., 2009, Zircon U–Pb and Hf isotopic constraints from eastern Transhimalayan batholiths on the precollisional magmatic and tectonic evolution in southern Tibet, Tectonophysics, 477, 3–19.

Clark, M.K. et al., 2004, Surface uplift, tectonics, and erosion of eastern Tibet from large-scale drainage patterns, Tectonics, 23, TC1006, doi:10.1029/2002TC001402.

Ding, L., Zhong, D., Yin, A., Kapp, P. and Harrison, T.M., 2001, Cenozoic structural and metamorphic evolution of the eastern Himalayan syntaxis (Namche Barwa), Earth and Planetary Science Letters, 192, 423-438.

Hallet, B., and Molnar, P.J., 2001, Distorted drainage basins as markers of crustal strain east of the Himalaya, J. Geophysical Research, 106, 13697-13709.

Hodges, K.V., 2000, Tectonics of the Himalaya and southern Tibet from two perspectives, Geological Soc. America Bull., 112, 324-350.

Liang, Y-H. et al., 2008, Detrital zircon evidence from Burma for reorganization of the Eastern Himalayan river system, American J. Science, 308, 618-638.

Najman, Y. et al., 2008, The Paleogene record of Himalayan erosion: Bengal Basin, Bangladesh, Earth and Planetary Science Letters, 273, 1-14.

Stewart, R.J. et al., 2008, Brahmaputra sediment flux dominated by highly localized rapid erosion from the easternmost Himalaya, Geology, 36, 711–714.

Zeitler, P. et al., 2001, Crustal reworking at Nanga Parbat, Pakistan-Metamorphic consequences of thermal-mechanical coupling facilitated by erosion, Tectonics, 20, 712-728.

Tectonic discontinuities within the Greater Himalayan Sequence in Western Nepal: insights on exhumation mechanisms

Rodolfo Carosi [1], Chiara Montomoli [1], Dario Visonà [2]

[1]Dipartimento di Scienze della Terra, via S. Maria, 53, 56126, Pisa, Italy carosi@dst.unipi.it
[2] Dipartimento di Geoscienze, Università di Padova Via Gradenigo, 6 35131, Padova, Italy

The Greater Himalayan Sequence (GHS), one of the main tectonic units of the Himalayan range, shows an impressive continuity running from east to west for more than 2000 kilometers. However, the thickness of the crystalline rocks decreases from 20-30 Km in the eastern Himalayas up to nearly 2 km in western Nepal (Carosi et al., 2007; 2010). Large volumes of granites were intruded in its upper portion, below the South Tibetan Detachment System (STDS; Burchfield et al., 1992; Searle, 1999; Beaumont et al., 2001; Carosi et al., 2002; Grujic, 2006; Godin et al., 2006 with references) but moving westward, toward Dolpo and Mugu- Karnali regions (Nepal) granites became scarcer (Leech, 2008). The ductile fabric within the GHS is due by a general shear as a consequence of the contemporaneous motion of the STDS and Main Central Thrust (MCT) at nearly 23-17 Ma (Grujic et al., 1996; Carosi et al., 2006; Larson & Godin, 2009). However, the deformation within the crystalline rocks is not only referable to a simple fabric related to a top-to-the south sense of shear developed in the time span of activity of the STDS and MCT.

Several shear zones and/or thrusts have been recognized within the GHS. Most of them have been regarded as out of sequence thrusts with respect to the MCT (Mukherjee et al., 2011 with references therein). However, geological investigations in the GHS of Western Nepal allow the authors to identify different generations of shear zones with different kinematics and different ages.

A high-temperature top-to-the SW shear zone (Toijem shear zone) has been recently documented in the core of the GHS in lower Dolpo (western Nepal), whose activity has been constrained at circa 26 Ma (Carosi et al., 2010) before the onset of shearing of the MCT. The Toijem shear zone is responsible for the exhumation of the hanging wall rocks before the well-known period of exhumation by extrusion or channel flow of the GHS by the contemporaneous activity of the Main Central Thrust and South Tibetan Detachment System.

Going to the west, in the Mugu-Karnali valley a km-thick shear zone with a top-to the SW sense of shear is again located in the middle part of the GHS nearly separating the upper part of the GHS (with the occurrence of sillimanite along the foliation) from a lower part mainly made by kyanite-bearing gneiss and micaschist. Its preliminary U-Th-Pb age brackets its activity in the STDS-MCT time span. This shear zone is similar to the one described by Yakymchuck (2010) in the Karnali valley few dozen kilometres to the west of Mugu-Karnali.

However, in Western Nepal, shear zones within the GHS are not all related to top-to-the South shearing: in the uppermost part of the GHS, north of Jumla village a ductile shear zone, involving tourmaline-bearing leucogranites shows a top-to-the SE sense of shear and stretching lineation pointing to an orogen-parallel extension. U-Pb age on zircons constrains its activity < 20 Ma.
A cross-cutting undeformed dyke in the GHS of lower Dolpo, emplaced at nearly 17 Ma point to the end of ductile deformation in the GHS at that time.

Recent field and satellite-image investigations documented a large granitic body (nearly 110 km^2) intruding both the uppermost portion of the GHS and the lower portion of the Tibetan Sedimentary Sequence (Bertoldi et al., 2011). U-Pb-Th ages from zircons and monazites extracted from the main granitic body and dykes intruded in the TSS point to an emplacement age at ~ 22-24 Ma. This age constraint represents a pin point for the upper limit of the movement of the STDS (or at least of the lower

ductile shear zone) in western Nepal with important consequences for the exhumation history and mechanisms of the GHS.

A number of observations, pointing to a more complex deformation history of the GHS, could place a possible limit of channel flow exhumation and even to extrusion of the crystalline unit in western Nepal: (1) The limited thickness of the GHS (largely below the 20-30 km required for an active channel flow; Godin et al., 2006); (2) the exhumation of the upper portion of the GHS happened before the MCT-STDS activity (e.g. Tojiem shear zone); and (3) the extensional decoupling of TSS and GHS for a very short time span (1-2 Ma only); (4) the occurrence of ductile shear zones at the top of GHS with an age < 20 Ma with orogen-parallel displacement and top-to-the South-East sense of shear.

References

Beaumont, C., Jamieson, R.A., Nguyen, M.H., and Lee, B. , 2001, Himalayan tectonics explained by extrusion of a low- viscosity crustal channel coupled to focused surface denudation, Nature, 414, 738–742.

Bertoldi, L., Massironi, M., Visona', D., Carosi, R., Montomoli, C., Gubert, F., Naletto, G., Pelizzo, M.G., 2011, Mapping the Buraburi granite in the Himalaya of Western Nepal: remote sensing analysis in a collisional belt with vegetation cover and extreme variation of topography, Remote Sensing of Environment, 115, 1129-1144.

Burchfiel, B. C., Z. Chen, K. V. Hodges, Y. Liu, L. H. Royden, D. Changrong, and Xu, L., 1992, The South Tibetan Detachment System, Himalayan Orogen: Extension contemporaneous with and parallel to shortening in a collisional mountain belt, Geol. Soc. Am. Spec. Publ., 269, 41.

Carosi, R., Montomoli, C. and Visonà, D., 2002, Is there any detachment in the Lower Dolpo (western Nepal)?, C.R. Geoscience, 334, 933-940.

Carosi, R., C. Montomoli, and Visonà, D. 2006, Normal- sense shear zones in the core of Higher Himalayan Crystallines (Bhutan Himalaya): Evidence for extrusion?, Geol. Soc.London, Spec. Publ., 268, 425-444.

Carosi, R., Montomoli, C. and Visonà, D., 2007, A structural transect in the Lower Dolpo: Insights on the tectonic evolution of Western Nepal, J. Asian Earth Sci., 29, 407–423.

Carosi, R., Montomoli, C., Rubatto, D., and Visonà D., 2010, Late Oligocene high-temperature shear zones in the core of the Higher Himalayan Crystallines (Lower Dolpo, Western Nepal). Tectonics, 29, TC4029, doi:10.1029/2008TC002400.

Godin, L., D. Grujic, R. D. Law, and M.P. Searle (2006), Channel flow, ductile extrusion and exhumation in continental collision zones: an introduction, Geol. Soc. Spec. Publ., 268, 1-23.

Grujic, D. (2006), Channel flow and continental collision tectonics: an overview. Geol. Soc. Spec. Publ., 268, 25-37.

Larson, K.P. and Godin, L., 2009, Kinematics of the Greater Himalayan sequence, Dhaulagiri Himal: implications for the structural framework of central Nepal, Journal of the Geological Society, London, 166, 25-43.

Leech, M.L., 2008, Does the Karakoram fault interruptmid- crustal channel flow in the western Himalaya?, Earth Planet. Sci, Letters, 276,314-322.

Mukherjee, S., Koyi, H. A., and Talbot C. ,2011, Implications of channel flow analogue models for extrusion of the Higher Himalayan Shear Zone with special reference to the out-of-sequence thrusting, Int J Earth Sci (Geol Rundsch), DOI 10.1007/s00531-011-0650-6.

Searle, M. P. 1999, Extensional and compressional faults in the Everest- Lhotse Massif, Khumbu Himalaya, Nepal, J. Geol. Soc. (Lond.), 156, 227-240.

Yakymchuck, C. J. A., 2010, Tectonometamorphic evolution of the Greater Himalayan Sequence, Karnali Valley, Western Nepal, MSc Thesis, 204 pages.

Karakorum fault slip-rate seems to be constant along strike over the last 200 ka

M.-L. Chevalier[1], P. Tapponnier[2], J. Van der Woerd[3], F.J. Ryerson[4], R.C. Finkel[5], Haibing Li[1]

[1] Key Laboratory of Continental Dynamics, MLR, Institute of Geology, CAGS, 26 Baiwanzhuang st, Beijing 100037, China, mlchevalier@hotmail.com
[2] Earth Observatory of Singapore, Singapore 639798
[3] Institut de Physique du Globe de Strasbourg, 67084 Strasbourg, France
[4] Atmospheric, Earth and Energy Division, Physical and Life Sciences directorate, Lawrence Livermore National Laboratory, Livermore, CA 94550, USA
[5] Earth and Planetary Science Department, University of California, Berkeley, CA 94720, USA

Determining the slip-rate history along the Karakorum Fault is fundamental to understanding its present-day kinematic role in the deformation of Tibet. InSAR data suggest that the Karakorum Fault is barely active (1±3 mm/yr) while field observations and high-resolution satellite images inferred a slip-rate of ~30 mm/yr. Geodetic and Quaternary geologic studies suggest slip-rates between 3.4±5 mm/yr and 11±4 mm/yr (GPS), and 4±1 mm/yr and 10.7±0.7 mm/yr (cosmogenic ^{10}Be), respectively. Whether slip-rate variability exists along strike and/or time, or simply results from different techniques/timescales, remains unknown. We present new ^{10}Be cosmic-ray surface exposure ages for 127 quartz-rich samples collected on 3 lateral moraines and 3 alluvial sites along the southern segment of the right-lateral Karakorum fault (the Menshi-Kailas basin) and along the normal fault in the Pulan graben in western Tibet. These dates constrain the age of fluvial and glacial geomorphic features right-laterally or vertically offset by the fault by varying amounts from 7±1 m to 430±30 m (right-lateral) and up to 53±5 m (vertical). From the 30° Karakorum Fault bend at Baer (80.5°E), to Mount Kailas, the slip-rate along the Karakorum fault varies from 5.7±3.4 - 9.4±2.5 mm/yr to >8.2 – 15.1 mm/yr (total slip on two parallel fault strands). In the Pulan graben, the normal fault slip-rate is >1.5±0.3 mm/yr. Our data suggest that the Quaternary slip-rate in the Menshi-Kailas Basin is at least 2 to 10 times faster than the geodetic InSAR rate and the slowest GPS rate. It is also consistent with our previous rate obtained further north (10.7±0.7 mm/yr) and with the highest GPS rate. Therefore, it might suggest that the Karakorum fault slip-rate is constant along strike.

Determination of three-dimensional in situ stresses from anelastic strain recovery (ASR) of Wenchuan Earthquake Fault Scientific Drilling-1 (WFSD-1)

Junwen Cui[1], Weiren Lin[2], Lianjie Wang[3], Zhemin Tang[1], Lu Gao[4], Wei Wang[3], Dongsheneg Sun[3], Zongfan Li [5], Jingchun Zhou[3], Huashan Qian[6], Hua Peng[3], Kemei Xia[5] and Ke Li[5]

[1] State Key Laboratory of Continental Dynamics, Ministry of Land and Resources; Institute of Geology, Chinese Academy of Geological Sciences; Beijing 100037, China
[2] Kochi Institute for Core Sample Research, Japan Agency for Marine-Earth Science and Technology (JAMSTEC) Nankoku, 783-8502, Japan
[3] Institute of Geomechanics, Chinese Academy of Geological Sciences, Beijing 100081, China
[4] China University of Geosciences (Beijing), Beijing 100081, China
[5] Regional Geological Survey Party of Sichuan Province, Chengdu 610213, Sichuan, China
[6] Beijing Supcompute Com.,Beijing 100083, China

The stress existing in the crustal rock mass is called in-situ stress. The ASR (short for anelastic strain recovery) technique is widely used in deep 3-D stress measurements of rocks in crustal drilling, especially in seismic fracture zones with complex geologic conditions and broken formations. Well WFSD-1 is the first among the 4 scientific boreholes drilled in the project "Scientific Drilling in Seismic Fracture Zones of Wenchuan", which was implemented soon after the great May 12 earthquake. It is located at Hongkou Township, Dujiangyan City, Sichuan Province, in the hanging wall of the causative Yangxiu-Beichuan fault with relatively large horizontal dextral displacement and vertical displacement. The well depth is 1201 m and the vertical depth is 1179 m. Following the requirements of the ASR method, a total of 7 samples were collected, yielding the orientations of the maximum principal stress σ_1 as 291 ~ 325° (N35 ~ 69ºW), averaging 309°. With deepening of the borehole, they show a trend from NW to NWW. The values of the maximum, intermediate and minimum principal stresses, the vertical stress, and the maximum and minimum horizontal stresses (σ_1, σ_2, σ_3, σ_v, σ_H and σ_h respectively) at the 7 measuring points were calculated based on the average density of rocks provided by logging data, and the principal stresses and horizontal stresses roughly show linear relations with depth. The relations between σ_H, σ_v and σ_h reveal the vertical inhomogeneity of the structural state in Well WFSD-1. Generally, the relations between the horizontal and the vertical stress values show that at the depths of above 427–465 m, from 427–465 m to 800–1000 m 427–465 m, 800–1000 m and below 800–1000 m, they are $\sigma_v>\sigma_H>\sigma_h$, $\sigma_H>\sigma_h>\sigma_v$ and $\sigma_H>\sigma_v>\sigma_h$ respectively (Fig. 11, Table 2), indicating that above 427–465 m, it is in normal slipping; from 427–465 m to 800–1000 m and below 800–1000 m, they are in compressive and dextral strike-slip states respectively The ASR measurement results of WFSD-1 support the conclusion on the focal mechanism solution that the May 12 earthquake is dominated by thrusting accompanied by dextral strike-slip faulting. The orientations of σ_1 are roughly correlatable with the displacement direction of the Longmenshan area, which indicates that there are indeed movements from NW to SE, i.e. compression of the Songpan-Garzê block toward the Sichuan basin. Therefore, from a macroscopic view, the ASR technique can well be applied to the in-situ stress measurerment of cores deep in seismal fracture zones, serving as an important supplement to other methods.

How the paradoxal Longmen Shan belt has been built: through new petrological structural geochronological data?

Julia de Sigoyer[1], Audrey Billerot[2], Alexandra Robert[1], Stéphanie Duchêne[3], Olivier Vanderhaeghe[2], Manuel Pubellier[1], Patrick Monié[4]

[1] ENS-CNRS UMR 8538, Paris France, sigoyer@geologie.ens.fr
[2] G2R Nancy University, France
[3] GET Toulouse University, France

The paradox of a high eastern Tibetan plateau associated with very low convergence rate (Gan et al., 2007) has led to an underestimation of the seismic hazard in the Longmen Shan area (China) prior to the May 12th 2008, Mw 7.9 earthquake. This paradox has spawned a vigorous debate regarding the relative roles of upper-crustal faulting (Hubbard et al., 2009, Arne et al., 1997) of roughly pure-shear thickening of the Tibetan crust (Robert et al., 2010a, b,) and lower-crustal flow (Royden et al., 2008, Vanderhaeghe and Teyssier 2001) in building and maintaining a high Tibetan margin. Very few data exist regarding the timing and processes of thickening of this eastern Tibetan plateau. Compounding this difficulty is the complexity of structural and petrological records in this area, due to the polycyclic events that have affected this eastern Tibetan margin. Two main events are described (1) the Late Triassic to Late Jurassic Indosinian orogeny and the (2) Cenozoic orogeny (Himalayan collision). The recent uplit history of the Longmen Shan belt has been dated at ~11 Ma (Arne et al., 1997, Godard et al., 2009), however it is not clear how it is directly related to the thickening of eastern Tibetan margin. This study addresses the problem of thickening of this area through time; the aim is to identify the contribution of each event to the present thickening.

Our seismological experiment across the belt (Robert et al. 2010a) showed a sharp vertical offset of the Moho below the Longmen Shan belt, from thick (63 km) east Tibetan crust to a near-normal (44 km) Yangtze crust below the Sichuan basin.
Part of our scientific effort has been deployed to identify the nature of the basement on each part of this Moho step. With geochemical analysis (major trace isotopic) we have first identified that the Neoproterozoic Yangtze basement extended from the Pengguan crystalline massif in the Longmen Shan to the Gezong and Gongcai slices in the Danba area (Fig. 1).
Many Mesozoic granites (Fig 1) emplaced at the end of and after the Indosinian orogeny, between 228,4±1,9 and 153±3 Ma (Zhang et al., 2007, Roger et al 2004), crop out in this eastern border of the Tibetan plateau.

We review all available data on the Songpan Ganze granitoids and studied five new granitoids (Billerot Ph-D). Many different and incoherent sources have been proposed previously for all the granites in this area (Roger et al., 2004, Yuan et al., 2010, Zhang et al., 2007). We identified three different types of granitoids : (i) alkaline granites (ii) high-K calc-alkaline granites represented by the majority of granitoids and (iii) some S-type granites. We have shown that the different types of granitoids can coexist in the same locality. Three types of sources, that underwent various degrees of mixing, have been identified by their elemental and isotopic signatures: the undepleted mantle, the basal continental crust of the Yangtze craton and the Songpan Garze sediments. Two subduction zones were active during late Triassic in this area (Fig 1) we propose a context of slab retreat of the subduction zone for the majority of high-K calc-alkaline granites. The A type granites have an undepleted mantle signature (Yuan et al., 2010), probably due to the upwelling of the asthenosphere located under the subduction slab. This observation suggests the existence of a tear fault in the subduction zone preceding a slab break-off.

Our geochemical analyses on the eastern Tibetan margin suggest then that the nature of the basement is the same on both side of the Moho step. However, the western side has recorded the Triassic orogeny and an intense episode of magmatism (probably related to the slab break off). Whereas the eastern side has not been affected. The thermal and rheological consequence of this Triassic evolution (slab break-off or

delamination) has then to be considered In order to understand the the thickenning of the eastern Tibetan margin.

The thickening of the eastern Tibetan plateau is approached by a metamorphic study of the Longmen Shan (Wenchuan-Xuelongbao), Danba and Songpan Garze area. It indicates a much more important zone of high grade metamorphism compared to the previous studies of Zhou et al., 2008.
This metamorphism presents an invert gradient, identified in Danba, Xuelongbao and Wenchuan areas. Garnet, staurolite, biotite±kyanite assemblages allows the estimation of the peak conditions of this event at 580°C for 6 kbar, using several petrological tools (garnet-biotite thermometer and pseudosection using Perplex modelling). The peak of pressure is locally followed by a peak of temperature (about 700°C) at constant pressure that lead to the migmatization of metasediments in Danba. U-Pb ages (microsims) on overgrowing zircon attested a Triassic age (220 Ma) for the high grade metamorphism, as previously proposed by Huang et al.,2002 who related the high grade metamorphism to the Indosinian orogeny.
We identified a greenschist facies overprint of all the area (Songpan Garze-Danba and Longmen Shan internal zones Wenchuan-Xuelongbao zone and Pengguan massif). Analyses of the multiequilibrium between chlorite and phengite solide solution following Lanari et al (2010) method, allow the estimation of metamorphic conditions at 400°C for 5 Kbar for this last event.
U-Pb geochronological studies (Wallis et al., 2003, PhD Robert) indicate a 60-70 Ma event recorded in metamorphic monazites. We don't know whether these ages represent mixing ages or reflect a late Cretaceous reactivation of metamorphism.

While ^{39}Ar-^{40}Ar ages ranging between 75 and 27 Ma were obtained in the Danba area similar to the Itaya et al. (2009) ages. The oldest ages can be clearly interpreted as mixing ages between Indosinian (Triassic) event and Cenozoic reactivation (47-26 Ma).

According to these results a first event of crustal thickening occurred during Triassic time. This zone was probably reactivated by the end of Cretaceous when the Lhasa block was accreted to the Tibetan plateau. Then a second reactivation of deformation and metamorphism under greenschist facies conditions occurred between 47 to 27 Ma. It predates the final uplift phase of the Longmen Shan (since 11 Ma).

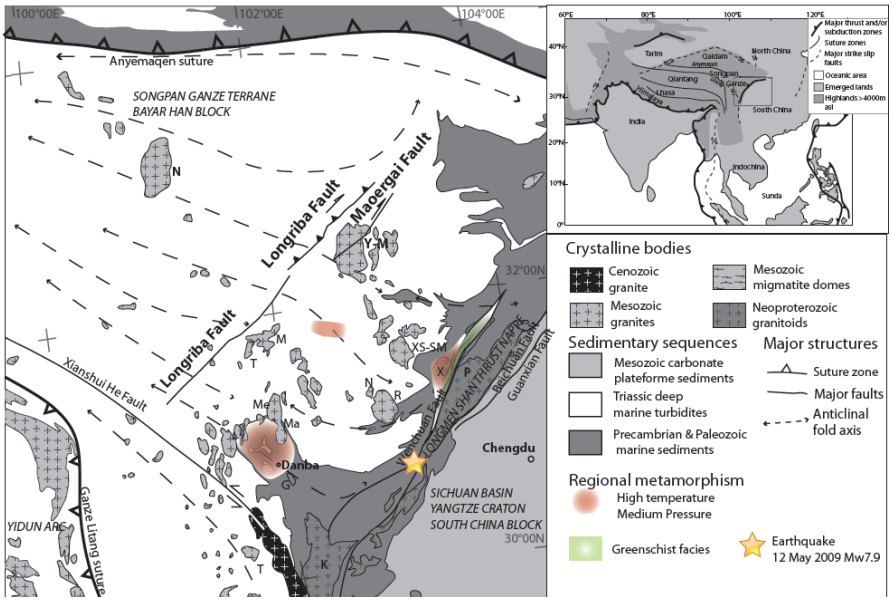

Figure 1 :Geological sketch map of the studied area. Letters represent granitic bodies : T= Tagong, Ma= Manai, M= Markam, R= Rilong, XS-SM= Xue Sheng and Sheng Meng, Y-M= Yaggon et Maoergai, N= Nyanbaoyeche**,** X= Xuelongbao, P= Pengguan, K= Kangding. Insert map represents the global context. See the two opposite suture north and south of the Songpan Garze.

References

Arne, D.; et al 1997. Differential exhumation in response to episodic thrusting along the eastern margin of the Tibetan Plateau. Tectonophysics,280, 239-256.

Gan, W.J., et al, J., 2007, Present-day crustal motion within the Tibetan Plateau inferred from GPS measurements: Journal of Geophysical Research-Solid Earth, v. 112.

Godard, V., Pik, R., Lave, J., Cattin, R., Tibari, B., de Sigoyer, J., Pubellier, M., and Zhu, J., 2009, Late Cenozoic evolution of the central Longmen Shan, eastern Tibet: Insight from (U-Th)/He thermochronometry: Tectonics, v. 28.

Hubbard, J., and Shaw, J.H., 2009, Uplift of the Longmen Shan and Tibetan plateau, and the 2008 Wenchuan (M=7.9) earthquake: Nature, v. 458, p. 194-197.

Itaya, T. et al, C., 2009, Regional-Scale Excess Ar wave in a Barrovian type metamorphic belt, eastern Tibetan Plateau: Island Arc, v. 18, p. 293-305.

Robert, A., Zhu, J., Vergne, J., Cattin, R., Chan, L.S., Wittlinger, G., Herquel, G., de Sigoyer, J., Pubellier, M., and Zhu, L.D., 2010a, Crustal structures in the area of the 2008 Sichuan earthquake from seismologic and gravimetric data: Tectonophysics, v. 491, p. 205-210.

Robert, A., Pubellier, M., de Sigoyer, J., Vergne, J., Lahfid, A., Cattin, R., Findling, N., and Zhu, J., 2010b, Structural and thermal characters of the Longmen Shan (Sichuan, China): Tectonophysics, v. 491, p. 165-173.

Roger F., Malavielle J., Leloup Ph., Calassou S., Xu Z, 2004 - Timing of granite emplacement and cooling in the Songpan-Garzê Fold Belt (eastern Tibetan Plateau) with tectonic implications, Journal of Asian Earth Sciences, Vol. 22, 465-481.

Royden, LH; Burchfiel, BC; van der Hilst, RD, 2008. The geological evolution of the Tibetan plateau. Science Vol.: 321 Is.: 5892, 1054-1058

Vanderhaeghe O., Teyssier C., 2001.Partial melting and flow of orogens. Tectonophysics 342, 451-472. 52 47

Wallis, S. et al, 2003. H. Cenozoic and Mesozoic metamorphism in the Longmenshan orogen: Implications for geodynamic models of eastern Tibet. *Geology*, 31, 745-748

Yuan, C., et al 2010. Triassic granitoids in the eastern Songpan Ganzi Fold Belt, SW China: Magmatic response to geodynamics of the deep lithosphere. Earth and Planetary Science Letters, Volume 290, Issue 3-4, 20 February 2010, Pages 481-492

Zhang H. F. et al 2007. A-type granite and adakitic magmatism association in Songpan Garze fold belt, eastern Tibetan Plateau : Implication for lithospheric delamination. Lithos 97, pp 323-335.

Zhou M.F, Yan D. P, Vasconcelos P. M, Li J.W, Hu R.Z, 2008 Structural and geochronological constraints on the tectono-thermal evolution of the Danba domal terrane, eastern margin of the Tibetan plateau. Journal of Asian Earth Sciences (33) 414-427.

Subduction-Related Metamorphism and Southwest Vergence in the Footwall Block Below Kaghan Eclogite Thrust Sheets, Swat, Pakistan, Western Himalaya

Joseph A. DiPietro, Amber R. King, James W. Wallace

Department of Geology, University of Southern Indiana, Evansville, IN 47712, USA, dipietro@usi.edu

The composite Loe Sar-Kotah dome is located at the northern edge of the Indian plate on the west flank of the Indus syntaxis in the Swat-Hazara part of the Pakistan metamorphic belt. The area is significant because it was autochthonous prior to Miocene southward displacement on the Panjal-Khairabad thrust, and because it forms part of the footwall block to eclogite-bearing thrust sheets presently exposed in the Kaghan region to the east. The rocks in the core of the dome were metamorphosed prior to the Oligocene with T-P estimates in the range of 600-700 °C and 9-14 kbar. The main focus of this report is on the Kotah dome which forms a satellite structure west of the larger Loe Sar dome.

The metamorphic core of the Kotah dome consists of Middle Permian Swat flaser granitic gneiss unconformably overlain by Late Permian Marghazar formation. The Marghazar consists of quartzo-feldspathic schist, amphibolite, and schistose marble and is roughly equivalent with the Panjal formation. In spite of penetrative deformation, the Marghazar formation shows evidence for rapid depositional facies changes and abrupt thickness variations. These characteristics, coupled with the presence of granitic pebbles and detrital zircon ages between 261 and 279 Ma (similar to the U-Pb zircon intrusive age of the Swat gneiss), suggest that rocks of the Marghazar formation filled down-dropped Late Permian extensional basins directly adjacent to up-thrown blocks of Swat gneiss. A 10 to 30 m thick amphibolite horizon forms the upper member of the Marghazar formation across the entire Loe Sar-Kotah dome directly below Triassic marble of the Kashala formation which surrounds the composite dome and forms part of the metamorphosed Tethyan shelf succession. A tourmaline granite gneiss locally intrudes the unconformity between Swat gneiss and the base of the Marghazar.

In the northern part of the dome, a layer of Swat gneiss less than 300 m thick is sandwiched below a 20-40 m thick layer of Marghazar formation composed mostly of amphibolite horizon, and above a much thicker (>500 m) section of Marghazar quartzo-feldspathic schist, amphibolite, and schistose marble. A series of intersecting cross sections combined into a fence diagram suggests that the layer of Swat gneiss forms a recumbent fold that extends about 8 km across the dome with southwest vergence. The fold does not appear to involve the amphibolite horizon, Kashala formation, or the stratigraphically overlying Saidu formation. The fold is believed to have nucleated by distributed shear across a pre-existing Late Permian normal fault that was oriented at a high angle to the shear direction and which originally separated an up-thrown block of Swat gneiss from a filled basin of Marghazar formation. Two additional west to southwest vergent folds are present in the Loe Sar dome. Field evidence suggests that the folds developed during prograde metamorphism and penetrative deformation when the Indian plate was underthrust beneath Indus ophiolitic mélange (DiPietro and Lawrence, 1991).

There are no metamorphic ages on rocks from the Kotah dome but a few 40Ar/39Ar hornblende ages from the Loe Sar dome average 38 ±5 Ma (Lawrence et al., 1985; Treloar and Rex, 1990; Baig, 1990). Peak metamorphic temperature estimates above 600 °C indicate that these are cooling ages that post-date fold development. The hornblende ages are consistent with a U-Pb LA-ICPMS zircon core age of 265 ±5.3 Ma and a rim age of 39.5 ±0.6 Ma from the tourmaline granite gneiss. The core age is identical with U-Pb zircon ages extracted from the Swat gneiss in the Loe Sar dome (DiPietro and Isachsen, 2001). The rim age likely dates crystallization of tourmaline-bearing melt. Given its age, the tourmaline gneiss is interpreted to have intruded following recumbent fold development. It is important to point out that the tourmaline granite gneiss, the amphibolite horizon, and the circa 38 Ma 40Ar/39Ar hornblende ages are restricted primarily to the region of the Loe Sar-Kotah dome. 40Ar/39Ar hornblende ages of rocks obtained to the east of the dome in the vicinity of the Indus syntaxis, and to the west of the dome in the Malakand thrust slice, are 51 ±2 Ma, 50 ±3 Ma, and 53 ±2 Ma. In addition, there are two undeformed, unmetamorphosed, intrusive rocks with U-Pb LA-ICPMS zircon ages of 48.1 ±0.8 Ma and 45.8 ±0.8 Ma.

These ages are consistent with previously published 40Ar/39Ar hornblende ages of 49 ±2 Ma, 50 ±2 Ma, and 51 ±2 Ma from the Indus syntaxis region (Treloar and Rex, 1990; Baig, 1990), and with a U-Pb zircon rim age of 47 ±3 Ma from the undeformed, unmetamorphosed, Malakand granite (Smith et al., 1994). Additionally, Treloar and Rex (1990) obtained 40Ar/39Ar hornblende ages of 67 ±2 Ma and 67 ±7 Ma.

Following W-SW-directed penetrative deformation in the Swat-Hazara metamorphic belt, the distribution of metamorphic ages implies that the Loe Sar-Kotah dome region remained buried and under metamorphic conditions until circa 38 Ma while surrounding areas were already undergoing metamorphic cooling beginning no later than 51 ±2 Ma. The circa 67 Ma hornblende ages suggest that metamorphic cooling could have begun as early as 67 Ma in at least part of the metamorphic belt. If India-Kohistan collision is considered to have occurred 52 ±3 Ma then collision did not produce metamorphism in this part of the Pakistan metamorphic belt. The Kohistan fault is a brittle, hard rock fault that separates the Kohistan arc complex from Indus mélange which is folded with the Indian plate. All three terranes truncate against the Kohistan fault (DiPietro et al., 2000; 2008). It is possible that the Indus suture zone in Pakistan is polygenetic (e.g. composed of remnants of the Late Cretaceous-Paleocene intra-oceanic subduction/obduction complex, and remnants of the Early Eocene and older accretionary prism associated with the Kohistan arc). Given available data, we currently favor the possibility that all (or most) of the exposed suture zone mélange is associated with Late Cretaceous-Paleocene intra-oceanic subduction and that this event initiated metamorphism in the Swat-Hazara metamorphic belt (DiPietro and Isachsen, 2001, DiPietro et al., 2008). Instead of causing metamorphism, the circa 52 Ma India-Kohistan collision may have instead driven exhumation and cooling in the Swat-Hazara metamorphic belt. In this scenario, the accretionary mélange to the Kohistan arc is largely or entirely buried with the northern margin of India below the obducted Kohistan arc complex. Kaghan eclogites underwent exhumation to amphibolite facies and were likely emplaced above previously deformed and metamorphosed Swat rocks circa 47 Ma (Wilke et al., 2010). Thus, the Kaghan rocks may have undergone a history similar to that of the Swat rocks and may have already been buried, possibly to eclogite facies, prior to India-Kohistan.

References

Baig, M.S., 1990, Structure and geochronology of pre-Himalayan and Himalayan orogenic events in the northwest Himalaya, Pakistan, with special reference to the Besham area [Ph.D. thesis]: Corvallis, Oregon State University, 397 p.

DiPietro, J.A., Ahmad, I., and Hussain, A, 2008, Cenozoic kinematic history of the Kohistan fault in the Pakistan Himalaya, Geological Society of America Bulletin, v.120, no.11/12, p.1428-1440, doi: 10.1130/B26204.

DiPietro, J.A., Hussain, A., Ahmad, I., Khan, A.M., 2000, The Main Mantle Thrust in Pakistan: Its character and extent. In: Khan, M. A., Treloar, M.P. Searle, and M.Q. Jan, eds., Tectonics of the Nanga Parbat Syntaxis and the Western Himalaya, Geological Society London Special Publication 170, p.375-393.

DiPietro, J.A., and Isachsen, C.E., 2001, U-Pb zircon ages from the Indian Plate in northwest Pakistan and their significance to Himalayan and pre-Himalayan geologic history, Tectonics, v. 20, no. 4, p. 510-525.

DiPietro, J.A., Lawrence, R.D., 1991, Himalayan structure and metamorphism south of the Main Mantle thrust, Lower Swat, Pakistan, Journal of Metamorphic Geology, v. 9, p. 481-495.

Lawrence, R.D., Snee, L.W., and Rosenberg, P.S., 1985, Nappe structure in a crustal scale duplex, Swat Pakistan, Geological Society of America Abstracts with Programs, v. 17, p. 640.

Smith, H.A., Chamberlain, C.P., Zeitler, P.K., 1994, Timing and duration of Himalayan metamorphism within the Indian plate, northwest Himalaya, Pakistan, Journal of Geology, v. 102, p. 493-508.

Treloar, P.J., and Rex, D.C., 1990, Cooling and uplift histories of the crystalline thrust stack of the Indian plate internal zones west of Nanga Parbat, Pakistan Himalaya, Tectonophysics, v. 180, p. 323-349.

Wilke, F.D.H., O'Brien, P.J., Gerdes, A., Timmerman, M.J., Sudo, M., and Khan, A., 2010, The multistage exhumation history of the Kaghan Valley UHP series, NW Himalaya, Pakistan from U-Pb and 40Ar/39Ar ages, European Journal of Mineralogy, v. 22 p. 703-719.

Catchment-wide erosion rates, glaciation, and topography of the central ladakh Range, India

Jason M. Dortch[1,2], Lewis A. Owen[1], Lindsay M. Schoenbohm[2], Marc W. Caffee[2]

[1] Department of Geology, University of Cincinnati, Cincinnati, OH45221, USA , Jason.dortch@utoronto.ca
[2] Department of Chemical and Physical Sciences, University of Toronto, Mississauga, ON L5L 1C6, Canada
[3] Dept of Physics/PRIME Laboratory, Purdue University, West Lafayette, IN 47906, USA

Introduction

Researchers have hypothesized that erosional unloading can influence rate and style of tectonic deformation, but this hypothesis remains controversial, and rates of erosion and sediment transfer need to be quantified to help test these models. The central Ladakh Range, located in the Transhimalaya of northern India, is an ideal setting to examine these models because the range has contrasting styles of deformation, unroofing history, and geomorphology on its northern and southern sides. The asymmetric topography and morphology of the Ladakh Range suggests that erosional unloading affects rock uplift on the northern side of the range. In this study, we aim to test this idea by comparing catchment-wide erosion rates, long valley profiles, equilibrium-line altitude's (ELAs), and basin statistics across the central Ladakh Range using ^{10}Be TCN methods, and morphometric analysis.

Previous work

Based on thermochronology data from zircon and apatite (U–Th/He) and apatite fission-track methods (AFT), Kirstein et al. (2006; 2009) argue that the central Ladakh Range has been tectonically tilted southward, which resulted in higher elevations on the northern side of the mountain range during the Late Palaeogene (Fig. 1). Using strath terrace incision rates, Dortch et al. (2011) argue the northern side of the range is actively uplifting at 0.6±0.1 km/Ma. Morphometric analysis of digital elevation models (DEMs) (Jamieson et al., 2004) shows that catchments on the southern side of the central Ladakh Range are significantly shorter, narrower, and have a lower mean elevation than the equivalent catchments on the northern side of the range. Owen et al. (2006) and Dortch et al. (2010) used ^{10}Be TCN dating to show that the most extensive preserved late Pleistocene glacial advances extended ~33 km at ~ 160 ka on the northern side and ~ 18 km during marine isotope stage (MIS)-8 on the southern side of the range. Morphostratigraphic correlation demonstrates that advances on the northern side of the mountain range were twice as extensive as those on the southern side, albeit still restricted to their valleys (Owen et al., 2006; Dortch et al., 2010).

Results

^{10}Be TCN analysis of 13 fluvial sediment samples from active channels in 6 catchments across the Ladakh Range constrains erosion rates for catchments on the northern side of the mountain range to 56±12 – 74±11 m/Ma, while rates for catchments on the southern side are 20±3 – 39±8 m/Ma. Minimum elevation from swath analysis shows that the range divide is shifted to the south by 3.5-11.8 kilometers (Fig. 2). Maximum elevation is unusually uniform and dips toward the southern side of the range. Moreover, maximum elevation and relief are strongly correlated with proximity to the Karakoram Fault. Elevation vs. catchment size statistics show a nearly parallel positive trend of maximum (R^2=0.86) and average (R^2=0.39) elevation increasing to the north side of the range. The ELAs of the 382 contemporary glaciers are remarkably consistent across the region, with an average of 5455±130 m. However, there is a distinct ELA gradient increasing to the north that closely follows the distribution of the highest topography, which suggests that glacier headwall height controls topography (Fig. 2).

The higher erosion rate to the north likely relates to tectonic tilting of the Ladakh Range, active rock uplift on the northern side of the range along the Karakoram Fault, and increased glaciation. The nearly parallel maximum and average elevations across the range suggests that greater erosion on the northern side of the range is not keeping pace with rock uplift. This is confirmed by catchment-wide erosion rates on the northern side of the range that are an order of magnitude slower (60-70 m/Ma) than rock uplift 600 m/Ma (Dortch et al., 2011a). Thus, we preclude the possibility of long-term denudational unloading from

having a significant influence on the tectonic tilting of the range. Moreover, because rock uplift is outpacing erosion and maximum topography follows the conditions of the glacial buzzsaw hypothesis, the average elevation must be increasing and will continue to do so until limited by the ELA as long as the northern side of the range remains tectonically active. Therefore, we suggest that the central Ladakh Range is a transient landscape moving toward a state of equilibrium between topography and glaciation.

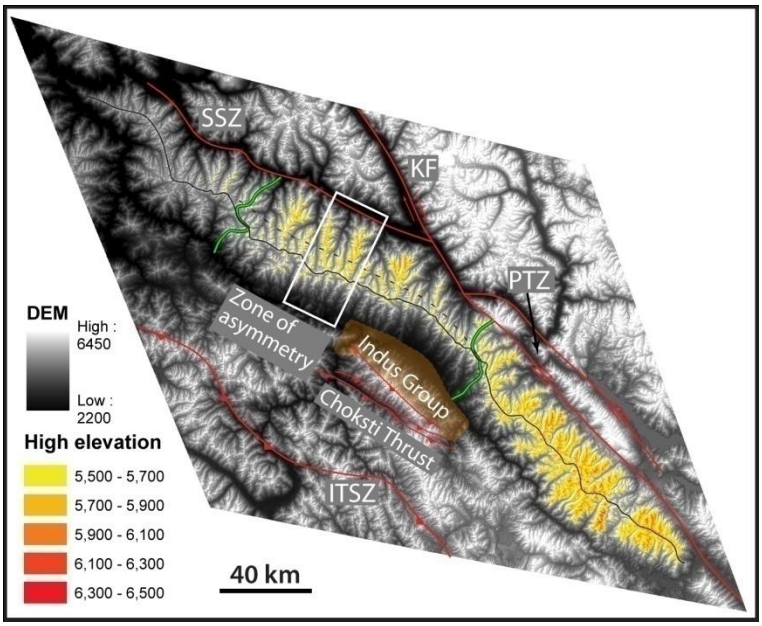

Figure 1. SRTM DEM highlighting the unequal distribution of high elevation across the central Ladakh Range. Topography with elevation > 5,500 m decreases dramatically with distance away from the Karakoram Fault. The asymmetric central Ladakh Range is marked by green lines. White box shows the location of the example swath profile in Figure 2.

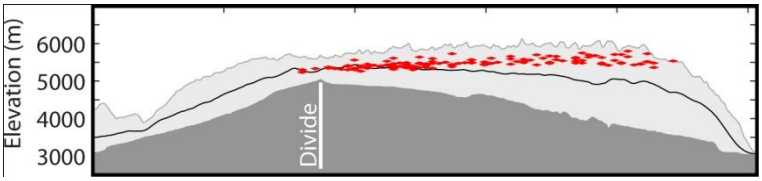

Figure 2. Swath profiles of the central Ladakh Range coded by boxes. Minimum elevation shown in dark gray and maximum elevation marked by medium gray line. Light gray between maximum and minimum elevations is relief. Average elevation marked by black line. Equilibrium-line elevations for contemporary glaciers are marked by red diamonds. Elevation error (± 20 m) and distance error (± 0.25 km) do not extent beyond red diamonds.

References

Dortch, J.M., Owen, L.A., Caffee, M.W., 2010. Timing and extent of Quaternary glaciation in the Nubra and Shyok valleys, northernmost Ladakh, India. Quaternary Research 74, 132–144.

Dortch, J.M., Owen, L.A., Dietsch, C., Caffee, M.W., Bovard, K., (2011a). Episodic fluvial incision of rivers and rock uplift in the Himalaya and Transhimalaya. Geological Society of London, DOI: 10.1144/0016-76492009-158.

Jamieson, S.S.R., Sinclair, H.D., Kirstein, L.A., Purves, R.S., 2004. Tectonic forcing of longitudinal valleys in the Himalaya: morphological analysis of the Ladakh Batholith, North India. Geomorphology 58, 49–65.

Kirstein, L.A., Sinclair, H., Stuart, F.M., Dobson, K., 2006. Rapid early Miocene exhumation of the Ladakh batholith, western Himalaya. Geologic Society of America 34, 1049–1052.

Kirstein, L.A., Foeken, J.P.T., van der Beek, P., Stuart, F.M., Phillips, R.J., 2009. Cenozoic unroofing history of the Ladakh Batholith, western Himalaya, constrained by thermochronology and numerical modeling. Geological Society of London 166, 667–678.

Owen, L.A., Caffee, M.W., Bovard, K.R., Finkel, R.C., Sharma, M.C., 2006. Terrestrial cosmogenic nuclide surface exposure dating of the oldest glacial successions in the Himalayan orogen: Ladakh Range, northern India. Geological Society of America, Bulletin 118, 383–392.

A new result of the crustal structure and variation of the Moho in central Tibet-revealed by the 300 km long deep seismic reflection profile

Rui Gao[1], Zhanwu Lu[1], Xiaosong Xiong[1], Whenhui Li[1], Gong Deng[1], Chen Chen[2] and Larry D Brown[2]

[1] Institute of Geology, Chinese Academy of Geological Sciences, 100037, China. gaorui@cags.net.cn
[2] Institute for the Study of the Continents, Cornell University, Ihtaca, NY 14853, USA

The Bangong-Nujiang Suture (BNS) resulted from the collision of the Lhasa terrane（LB）and Qiangtang terrane（QB）in the late Jurassic(Yin A. & Harrison T. M., 2000), was subsequently reactivated by strike slip deformation by the Himalayan collision. The QB has also been associated with the mantle suture between India and Asia, i.e. northern limit of penetration of the subducted Indian lithosphere beneath the Asian Tibetan crust. Partial melting zone in the lower crust of the LB is suspected to be one factor that may have limited seismic penetration in this region. The E-W trending Qiangtang central uplift, located in the interior of the Qiangtang terrane is interpreted as a major convergence structure associated with the west Kunlun orogenic belt (Gao, et al., 2000).

Understanding the composition and structure of the over thickened crust of the Tibetan plateau is fundamental to unraveling the mechanisms for uplift of the Tibetan plateau. Deep seismic reflection profiling is one of the internationally recognized advanced techniques that can reveal the fine structure of continental lithosphere.

In the early 1990s, deep reflection profiling was successfully carried out in the southern Tibetan plateau by the INDEPTH project, imaging the Main Himalaya Thrust which marks the underthrusting of the Indian plate beneath Himalaya. However, subsequent deep seismic by INDEPTH efforts within the interior of the Tibetan plateau was too limited to trace lower crustal structure near the Bangonghu-Nujiang suture (BNS) (Ross, et al., 2004).

As part of the new SINOPROBE-02 initiatiave (Sinoprobe-02) and with funding from the NSF of China (40830316), we collected a 310 km of deep seismic reflection profile is crossing Bangong-Nujiang suture and Qiangtang terrane, successfully revealed details of thecrustl structures down to the Moho and possible deeper. The profile starts west of the Silin Co in the northern Lhasa block, crosses the Bangong-Nujiang suture west of Lunpola, skirts the eastern extension of the central Qiantang anticline and ends at Dogai Coring just of south of Jinsha suture. Main acquisition methods are showed in Table1.

Recording system	408XL	Near offset(m)	225
Geophones(Hz)	10	seismic source(kg)	50(small)
Receiver group spacing(m)	50		200(middle)
Numbers of one receiver group	24		1000(large)
Number of channels	960(large)	shot spacing(m)	250(small)
	720(middle/small)		500(middle)
Record length(s)	60(large)		50000(large)
	30(middle/small)	shot depth(m)	30*1(small)
Sample interval(ms)	4(large)		50*2(middle)
	2(middle/small)		50*10(large)
Far offset(m)	47975(large)	fold	72(small)
	17975(middle/small)		36(middle)

Table 1: Acquisition parameters of the deep seismic reflection profile. We used large explosive (1000kg), deep drill (50m) and long spread (ac.50km) to get more deep reflection data.

The stack of 300 km long section provides us a with the first detailed image of this area. The result shows that (1) beneath the southernmost portion of the profile there are two sets of strong north-dipping

reflectors between 10 s-19 s TWT, which we interpreted to indicate that the LB may underthrust beneath the BNS; (2) there is a well-developed northward thrust beneath the shallow crust near the BNS; (3) there is a broad, gently folded reflection that presents close to the southern segment of the BNS at 10s and shallower to ca. 7 s crossing the BNS; (4) that the Moho reflection appears at 23-24 s in the southern of BNS, with an indication of the change in the Moho depth across the BNS, Moho reflection appears at 20 s. New data should provide us with the first detailed reflection image of crustal structure in Central Tibet.

References

Gao Rui, Huang Dongding, Lu Deyuan, Qian Guihua, Li Yingkang, et al., 2000, Deep seismic reflection profile across the juncture zone between the Tarim Basin and the West Kunlun Mountains, Chinese Science Bulletin, 45(24): 2281-2286.

Ross A, Brown Larry D., Pananont Passakorn, Nelson K. D., Klemperer Simon, et al., 2004. Deep reflection surveying in central Tibet: lower-crustal layering and crustal flow, Geophysical Journal International, 156(1): 115-128.

Yin A., Harrison T. M., 2000, Geologic evolution of the Himalayan-Tibetan orogen, Annual Review of Earth and Planetary Sciences, 28(1): 211-280.

Himalayan hinterland-verging superstructure folds related to foreland-directed infrastructure ductile flow: Insights from centrifuge analogue modelling

Laurent Godin[1], Chris Yakymchuk[1,2], Lyal B. Harris[3]

[1] Department of Geological Sciences and Geological Engineering, Queen's University, Kingston, Ontario K7L 3N6, Canada, godin@geol.queensu.ca
[2] Now at Department of Geology, University of Maryland, College Park, MD, 20742-4211, USA
[3] Institut national de la recherche scientifique, centre - Eau Terre Environnement, 490 de la Couronne, Quebec City, Quebec G1K 9A9, Canada

The orogenic superstructure (SS) and infrastructure (IS) constitute two levels of a mountain belt with contrasting structural styles. In several Himalayan transects, N-verging back folds, which oppose the orogenic vergence, dominate the SS. Competing explanations for these folds are tested using scaled centrifuge analogue models employing new materials and computed tomodensitometry (CT scanning) (Fig. 1) (Godin et al., 2011; Yakymchuk et al., in press). This technique provides insight into the progressive three-dimensional formation of mechanically active, buckle and kink folds of a stratified sedimentary sequence upon migmatitic gneisses in a large hot orogen.

Analogue materials with properties scaled to represent both the layered Tethyan sedimentary sequence (the SS) and the underlying lower-viscosity Greater Himalayan sequence (the IS) are used. Polydimethylsiloxane (PDMS), a low viscosity polymer simulating migmatites and melt pooling in the upper part of the IS, is incorporated on half the SS-IS interface to investigate its effects on superstructure fold geometry and superstructure-infrastructure decoupling efficiency.

Modelling suggests that SS folding occurs during bulk shortening accompanied by IS thickening before IS flow. Focused erosion then instigates IS lateral flow and stretching, decoupling of the SS, and transposition of the lower SS into a detachment zone. Decoupling at the IS-SS interface separates a SS dominated by older folds and an IS characterised by younger horizontal transposition and stretching of early folds. Extrusive ductile flow of the IS locally modifies fold vergence in the SS. The fold asymmetry is thus controlled by the efficiency of coupling between IS and SS; a low viscosity at the IS-SS interface favours complete decoupling and hinders modification of fold vergence, whereas a higher viscosity IS-SS interface favours fold vergence modification. Modelling supports a tectonic scenario in which Himalayan hinterland-verging folds are the product of early shortening of the SS followed by local modification of fold geometry when the IS subsequently stretches and flows during focused erosion and melt-enhanced IS weakening (e.g. Larson et al., 2010).

Models without PDMS, akin to localities without significant melts near the South Tibetan detachment, may also provide insight into the structural evolution of debated units such as the Haimanta Group in the Sutlej valley, NW India. The basal part of the Haimanta Group is similar to the Everest Series in eastern Nepal and to the Annapurna-Yellow Formation in central Nepal (as proposed by Gleeson and Godin, 2006) as well as the Chekha Group in eastern Himalaya (Kellett et al., 2010). In contrast, however, it displays minor differences in metamorphic grade with the uppermost Greater Himalayan sequence, despite being separated from it by a top-to-the-northeast shear zone. The Haimanta Group also distinguishes itself from the Greater Himalayan sequence by a distinct structural style, and a marked difference in exhumation path (Chambers et al., 2009). Our modelling suggests that without a weak layer (pooled crustal melts), the detachment is distributed over a broader zone, and can isolate part of the infrastructure in its hanging wall (Fig. 2). As such, the Haimanta Group may have initially evolved as part of the IS, but later became incorporated in the superstructure as the lower part of the infrastructure underwent later horizontal stretching flow.

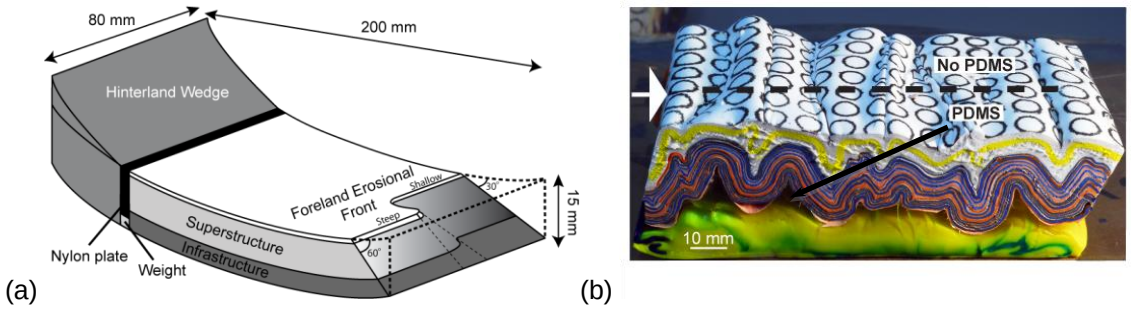

Figure 1. (a) Model set-up showing the collapsing wedge in the hinterland that activates layer-parallel shortening. Models consist of a 10 mm thick brittle-ductile superstructure overlying a 5 mm thick ductile infrastructure. The portrayed irregular erosion front was created on some models, while others contained an extra layer of polydimethylsiloxane (PDMS), a clear, low density and viscosity polymer, at the infrastructure-superstructure interface that simulates the presence of crustal melts. (b) Example of a model containing one half of clear PDMS at the interface between the layered sequence and ductile substrate and the other half with no PDMS along this interface.

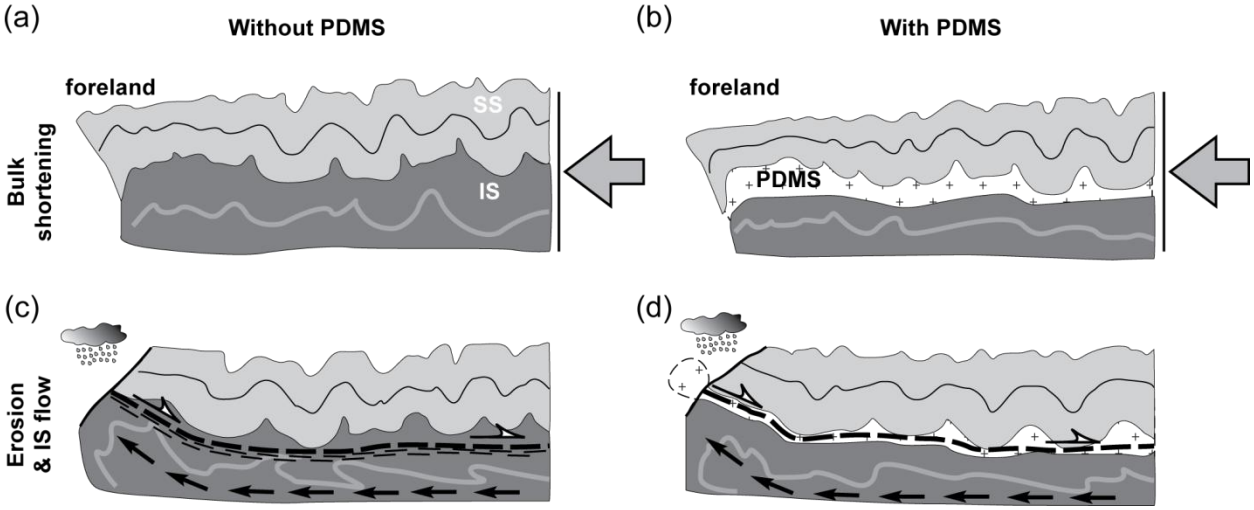

Figure 2. Sketches depicting deformation features developed in the models. (a) Without polydimethylsiloxane (PDMS) at the superstructure (SS) – infrastructure (IS) interface, initial shortening of the model develops buckle folds in the SS, while the IS material infills the SS anticlinal cores. (b) SS anticlines are cored by PDMS during early shortening, while the IS remains planar and horizontal, yet vertically thickens. (c) Once horizontal IS flow is triggered by focused foreland erosion (depicted by raining clouds), the IS-SS decoupling zone is localised in the upper part of the IS, and isolates the uppermost IS in the hanging wall of the detachment. (d) When PDMS is present, the detachment is localised within it; the entire IS is then confined to the footwall of the detachment, with only part of the PDMS isolated in the hanging wall.

References

Chambers, J., et al., 2009. Empirical constraints on extrusion mechanisms from the upper margin of an exhumed high-grade orogenic core, Sutlej valley, NW India. Tectonophysics 477, 77-92.

Godin, L., Yakymchuk, C. and, Harris, L., 2011. Himalayan hinterland-verging superstructure folds related to foreland-directed infrastructure plastic flow: insights from centrifuge analogue modelling. Journal of Structural Geology 33, 329-342.

Gleeson, T., Godin, L., 2006. The Chako antiform: A folded segment of the Greater Himalayan sequence, Nar valley, Central Nepal Himalayal. Journal of Asian Earth Sciences 27, 717-734.

Kellett, D.A.-M., et al. 2010. Metamorphic history of a syn-convergent orogeny-parallel detachment: The South Tibetan detachment system, Bhutan Himalaya. Journal of Metamorphic Geology 28, 785-808.

Larson, K. P., Godin, L., and Price, R. A., 2010. Kinematic compatibility in orogens: Linking the Himalayan foreland and hinterland in central Nepal. Geological Society of America Bulletin 122, 1116-1134.

Yakymchuk, C., Harris, L., and Godin, L., *in press*. Centrifuge modelling of deformation of a multi-layered sequence over a ductile substrate: 1. Style and 4D geometry of active cover folds during layer-parallel shortening. International Journal of Earth Sciences.

Resolving Conflicting Models for the Tectonic Assembly of the Eastern Himalaya

Lucy V. Greenwood[1], Randall R. Parrish[2], Tom W. Argles[1], Clare Warren[1], Nigel B.W. Harris[1]

[1] Department of Earth and Environmental Science, The Open University, Milton Keynes, MK7 6AA, United Kingdom, l.v.greenwood@open.ac.uk
[2] NERC Isotope Geosciences Laboratory, British Geological Survey, Keyworth, Notts NG12 5GG, United Kingdom

The tectonic evolution of the eastern portion of the Himalaya has been thrown into sharp relief with recent geological research in Bhutan prompting a reassessment of the classic work of Gansser (1983). The Bhutan Himalaya forms a unique sector along the orogenic front due to the existence of several klippen, a major out-of-sequence thrust fault and an apparently thickened, exhumed core (the Greater Himalayan Sequence or GHS). Unravelling the tectonic history in this region is crucial for understanding both heterogeneity and diachroneity of exhumation across the Himalaya.

Recent structural mapping across central Bhutan has revealed major new structures relating to the klippen. North-west verging nappes are seen in Tethyan carbonate and clastic sediments which structurally overlie migmatitic gneiss and leucogranite of the GHS (Figure 1). The recumbent folds verge in the opposite direction to the generally southward-verging orogen and may have been generated in response to top-to-the-north motion along the underlying South Tibetan detachment. Similarly-verging structures have been reported from central Nepal where their formation has been shown to be compatible with both wedge extrusion and channel flow models for the exhumation of the underlying mid-crustal gneisses (Kellett and Godin, 2009).

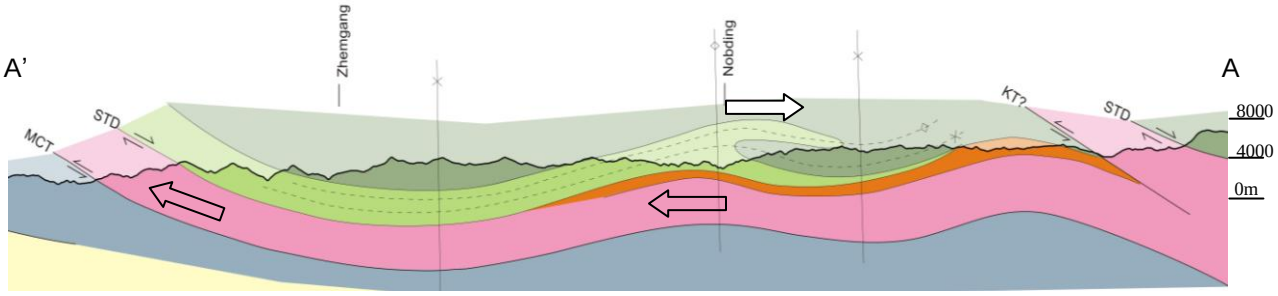

Figure 1. Cross Section south to north across central Bhutan. Arrows indicate direction of motion within each unit. No vertical exaggeration. Key as in Figure 2.

Mapping in the north and south of central Bhutan has led to the recognition of a single large allochthon extending from the Tang Chu in the north to the Black Mountains further south encompassing an area of ~80km x 10-50km (see Figure 2). Where the contact between these sediments and the GHS is exposed, there is clear evidence for localised top-to-the-north directed shear, apparently contrary to other recent findings (Long and McQuarrie, 2010).

The extensive leucogranite in the north (near the Tang Chu and shown mapped in Figure 2) along with thinner granite exposures outcropping at other basal sections of the allochthon all share similar chemistry and U-Pb zircon ages of ~18Ma indicating coeval crystallisation. Consequently an extensive, thin sheet of leucogranite underplating the allochthon can be envisaged, which may have played a significant role in the emplacement of the allochthon during the Early Miocene (e.g. Hollister and Crawford, 1986).

The results of this study provide constraints on the kinematics of continental collision and on tectonic models for the evolution of the eastern Himalaya including coupling of the upper and middle crustal and brittle and ductile deformation.

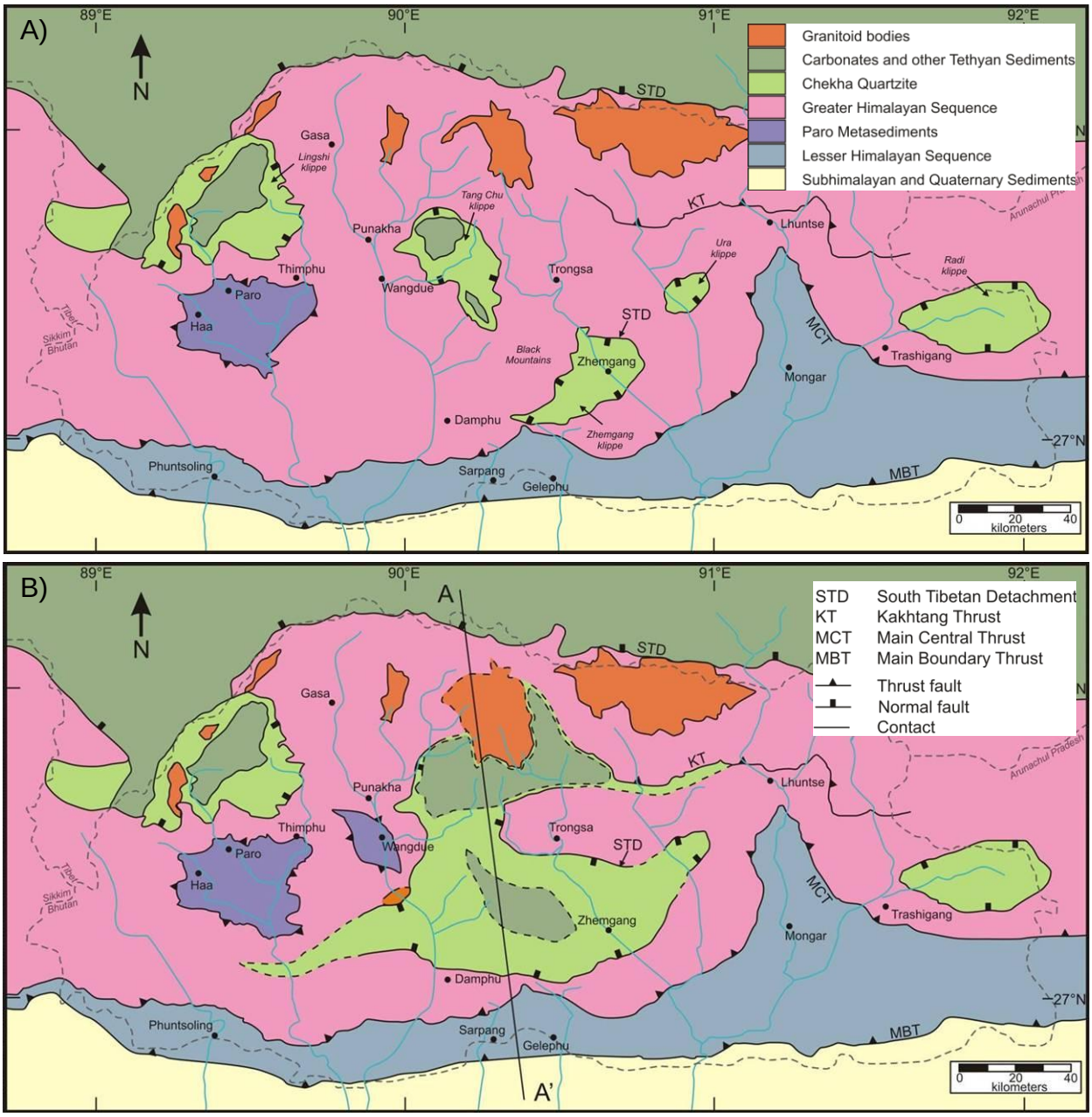

Figure 2. Redrawing the geological map of Bhutan: A) Geological map of Bhutan based on Grujic *et al*, 2002, Long and McQuarrie, 2010 and Gansser, 1983. Note the five isolated klippen and Kakhtang Thrust (KT). B) Revised map informed by field studies in 2009 and 2010. A-A' marks the line of cross section shown in Figure 1.

References

Gansser, A., 1983, Geology of the Bhutan Himalaya, Birkhauser Verlag Basel.

Grujic, D., Hollister, L.H. and Parrish, R.R., 2002, Himalayan metamorphic sequence as an orogenic channel: insight from Bhutan, Earth and Planetary Science Letters, 272, 105-117.

Hollister, L. S. & Crawford, M. L., 1986, Melt-enhanced deformation: a major tectonic process. Geology 14, 558-61.

Kellett, D.A. and Godin, L., 2009, Pre-Miocene deformation of the Himalyan superstructure, Hidden valley, central Nepal, Journal of the Geological Society, 166, 261-275.

Long, S. and McQuarrie, N., 2010, Placing limits on channel flow: Insights from the Bhutan Himalaya. Earth and Planetary Science Letters, 290, 375-390.

Pre-Collisional Evolution of the Himalayan-Tibetan System: Numerical Tests of Alternative Cretaceous-Tertiary Tectonic Settings

Carl Guilmette[1,2], Christopher Beaumont [1], Rebecca A. Jamieson [2]

[1] Department of Oceanography, Dalhousie University, Halifax, Canada, carl.guilmette@dal.ca
[2] Department of Earth Sciences, Dalhousie University, Halifax, Canada.

The Indus Yarlung Zangbo Suture Zone (IYZSZ) is a >2000 km long by roughly 30 km wide first-order tectonic structure (Fig. 1a) stretching across the southern Tibetan Plateau. It is interpreted to contain the remnants of the Neo-Tethys Ocean, which separated India from Eurasia (Lhasa Block) prior to the main continental collision. This once 4000 km wide ocean is thought to have vanished along at least two subduction zones during the Jurassic and the Cretaceous; one intraoceanic and one under the Eurasian margin. Relic Neo-Tethyan oceanic lithosphere has been preserved in the IYZSZ as the discontinuous Ladakh and Yarlung Zangbo Ophiolites (YZO). The sedimentary record and deformation structures within and south of the IYZSZ indicate that the obduction of the YZO over the Greater Indian passive margin had already started at 65 Ma (e.g. Ding et al. 2005). However, data from multiple sources, including UHP metamorphic ages from the Indian margin, support the onset of the main collision at around 55-50 Ma, 10-15 My later (e.g. Najman et al. 2010). Paleomagnetic data indicate that during that period, the convergence rate between India and Asia was on the order of 15 cm/y, suggesting that 1000-1500 km of convergence occurred between the obduction of the ophiolites and the onset of continental collision.

We investigate two tectonic hypotheses that may explain these observations, Cases 1 and 2 (Fig.1b). In Case 1, only one Andean-type subduction zone (SZ1) is active adjacent to the Eurasian (Tibetan) margin, whereas in Case 2 there is a second coeval intraoceanic subduction zone (SZ2). The generic upper-mantle-scale numerical models are designed to replicate four phases in the evolution of the system and to investigate the major system controls during these phases. These controls include rates of ocean floor spreading and subduction, slab pull and ocean ridge push forces, and the geometrical, rheological and thermal properties of the tectonic plates and their margins. During Phases 1 and 2, divergent kinematic velocity boundary conditions initiate continental rifting followed by oceanic spreading and the self-consistent growth of rifted continental margins and oceanic lithosphere. In Phase 3, the boundary conditions are changed to convergence with the inception of SZ1 (Case 1) and SZ1 and SZ2 (Case 2) subduction zones, followed by ocean closure and continent-continent collision in which India and Asia respectively correspond to the pro- and retro-sides of the system. The results are interpreted in terms of tectonic architecture, metamorphic P-T-t paths for the passive margins, and convergence rate variations at both trenches, and compared to relevant well documented natural examples like the India-Asia collision zone and the Gulf of Oman system.

The 2D upper-mantle scale thermo-mechanical finite element numerical models comprise a large-scale (LS) low-resolution model (10x2, 10x10 km elements) containing a nested (embedded) high-resolution (2x2 km) small-scale (SS) model. For each time step, the models are solved sequentially with the SS velocity and temperature boundary conditions derived from the LS model solution. The modelling techniques and model properties are similar to those of Beaumont et al. (2009) and Huismans and Beaumont (2008).

References

Beaumont, C., Jamieson, R.A., Butler, J.P., and Warren, C.J., 2009. Crustal structure: A key constraint on the mechanism of ultra-high-pressure rock exhumation. *EPSL, 287*, 116-129.

Ding, L., Kapp, P., Wan, X., 2005. Paleocene-Eocene record of ophiolite obduction and initial India-Asia collision, south central Tibet. *Tectonics*, 24, TC3001, 1-18.

Dupont-Nivet, G., Lippert, P.C., van Hinsberg, D.J.J., Meijers, M.J.M., Kapp, P., 2010. Palaeoloatitude and age of the Indo-Asia collision : paleomagnetic constraints. *GJI*, 182, 1189-1198.

Huismans, R. S., and Beaumont, C., 2008. Complex rifted continental margins explained by dynamical models of depth-dependent lithospheric extension, *Geology*, 36, 163-166.

Najman, Y., Appel, E., Boudagher-Fadel, M., Bown, P., Carter, A., Garzanti, E., Godin, L., Han, J.T., Liebke, U., Oliver, G., Parrish, R., Vezzoli, G., 2010. Timing of India-Asia collision: Geological, biostratigraphic and palaeomagnetic constraints. *JGR*, 115, B12416, doi:10.1029/2010JB007673.

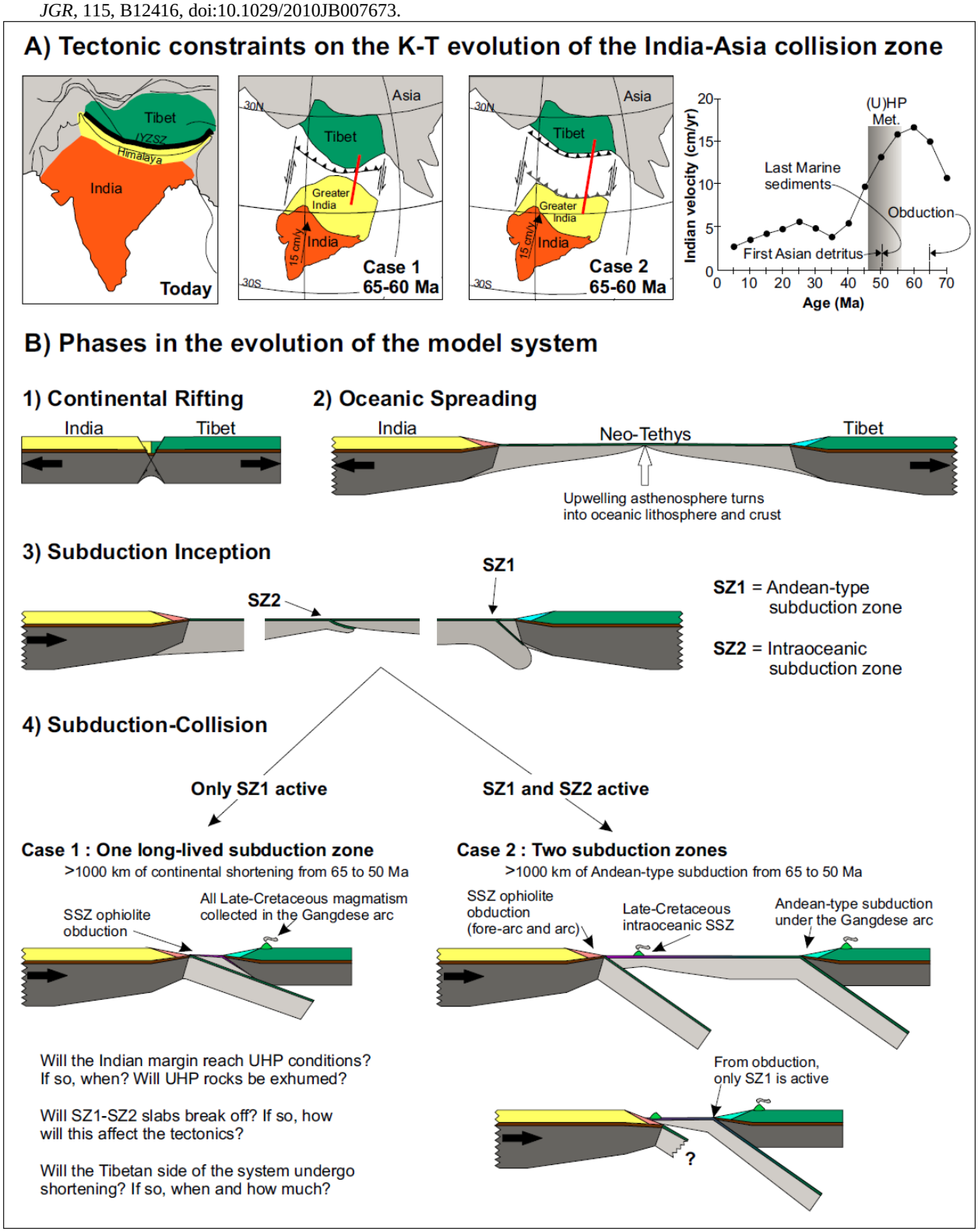

Figure 1: . A) Tectonic constraints on the Cretaceous-Tertiary evolution of the India-Asia collision zone. For paleomagnetic constraints, thermochronological ages and depositional ages see Ding et al. (2005), Dupont-Nivet et al. (2010), Najman et al. (2010), and references therein. B) Phases in the evolution of the model system. See text for explanation of Case 1 vs Case 2. SZ1, SZ2 = Andean and intraoceanic subdction zones, respectively; SSZ = suprasubduction zone.

Discovery of a dismembered metamorphic sole in the Saga ophiolitic mélange, South Tibet: Assessing an Early Cretaceous disruption of the Neo-Tethyan supra-subduction zone and consequences on basin closing.

Carl Guilmette[1], Réjean Hébert[1], Jaroslav Dostal[2], Aphrodite Indares[3], Émilie Bédard[1], Chengshan Wang[4]

[1] Département de géologie et de génie géologique, Université Laval, Québec, QC, Canada, e-mail : carl.guilmette.1@ulaval.ca
[2] Department of Geology, Saint Mary's University, Halifax, NS, Canada
[3] Earth Sciences Department, Memorial University of Newfoundland, St-John's, NL, Canada,
[4] Research Center for Tibetan Plateau Geology, China University of Geosciences, 29 Xueyuan Road, Haidian District, 100083 Beijing, China

Blocks of strongly foliated garnet- and clinopyroxene-bearing amphibolites have recently been discovered in the Saga ophiolitic mélange, South Tibet. The Saga ophiolitic mélange is a sheared serpentinite matrix mélange that crops out along the Yarlung Zangbo Suture Zone (YZSZ), South Tibet. The YZSZ is the youngest and the southernmost of all sutures stretching across the Tibetan Plateau and contains the remnants of the Neo-Tethys ocean which once separated India from the Lhasa block. The garnet- and clinopyroxene-bearing amphibolite blocks are interpreted as parts of a dismembered sub-ophiolitic metamorphic sole. They are mainly made of hornblende, diopside and garnet and were strongly metasomatized during retrogression. Thermobarometry and $^{40}Ar/^{39}Ar$ dating on hornblende indicate that they were metamorphosed to peak conditions in excess of 12 kbar and 850°C between 132 and 127 Ma. Major and trace element geochemistry suggest an N- to E-MORB nature for the protolith, which cannot rule-out a back- or inter-arc basin origin, like is seen in the East Scotia Sea. This data supports a model in which the back-arc YZSZ ophiolites (in the Xigaze area) were trapped in a fore-arc setting by the inception of a subduction at the back-/inter-arc ridge. The cause of this Early Cretaceous important tectonic event might be the presence of an oceanic plateau or hot-spot tracks in the Neo-Tethys and/or the collision of the Lhasa and Qiangtang blocks. Such a scenario provides an explanation for the absence (or rarity) of Late Cretaceous ophiolites along the YZSZ which are in majority of Late Jurassic Early Cretaceous age.

Laser-Ablation Split-Stream Petrochronology of Kangmar and Mabja North Himalayan Gneiss Domes

Bradley R. Hacker[1], Andrew Kylander-Clark[1], Jeffrey Lee[2], John Cottle[1], Michael Stearns

[1] Earth Science, University of California, Santa Barbara, CA 93106, USA, hacker@geol.ucsb.edu
[2] Geological Sciences, Central Washington University, Ellensburg, WA 98926, USA

North Himalayan gneiss domes are an important part of the Himalayan orogen providing windows into structural levels beneath the Tethyan Himalaya and may afford an opportunity to examine processes "farther upstream" from the Greater Himalayan Sequence. We used laser-ablation split-stream (LASS) ICP mass spectrometry to measure U/Th-Pb ages and compositions of monazite from garnet + aluminumsilicate ± staurolite pelites in the Kangmar and Mabja domes. Most of the monazites are situated in biotite, but rare grains are included in garnet. Textures indicate that the monazite-producing reaction in the rock matrix was apatite + biotite → muscovite + monazite. The monazites are typically ~100 microns in diameter in Mabja and <20 microns in Kangmar.

Previous work shows that mid-crustal rocks exposed in **Mabja Dome** record peak Barrovian P-T conditions around 8 kbar and 650–700°C coeval with vertical thinning and N–S stretching [Lee et al., 2004]. Zircon rims from two migmatitic gneisses deep in the section range from 35 to 21 Ma, and were interpreted to reflect distinct (re)crystallization events at 35 and 22 Ma [Lee and Whitehouse, 2007]. Extension-related, late-tectonic pegmatite dikes intruded from 28–23 Ma and post-tectonic granites crystallized from 16–10 Ma [Schärer et al., 1986; Zhang et al., 2004; Lee et al., 2006; Lee and Whitehouse, 2007; King et al., 2011]. Muscovite $^{40}Ar/^{39}Ar$ ages are 17 to 14 Ma [Lee et al., 2006] and biotites are 14 to 11 Ma [King et al., 2011].

Our LASS measurements show that staurolite- and sillimanite-bearing samples, typically with homogeneous garnet, have monazite with equivalent $^{208}Pb/^{232}Th$ and $^{206}Pb/^{238}U$ ages ranging from 29 Ma down to 20 Ma. The bulk of the ages are between 29 and 25 Ma, and spot ages <25 Ma are exclusively from samples with partially resorbed garnets that have homogeneous major-element compositions. All monazites have negative Eu/Eu*, but variable HREE + Y contents. Other measured elements—e.g., LREE—show minor differences among grains. Spot ages older than ~25 Ma show a wide range of Y and HREE concentrations, whereas spot ages younger than ~25 Ma are correlated with progressively higher Y and HREE contents. These garnet features, monazite trace-element signatures, and monazite ages suggest that prograde metamorphism was still underway at 29 Ma, but that decompression or cooling was occurring by 25 Ma, consistent with the interpretation that peak metamorphism and mid-crustal ductile extension began at ~35 Ma, was ongoing at ~23 Ma, and had ceased by ~16 Ma [Lee and Whitehouse, 2007]. One sample with prograde-zoned garnet, the coldest peak metamorphic temperature (620°C), and a muscovite $^{40}Ar/^{39}Ar$ age of 15 Ma has monazites as young as 17–14 Ma that may be related to the final post-tectonic stages of magmatism.

Previous work shows that mid-crustal rocks in **Kangmar Dome** were colder than in Mabja, reaching peak conditions of 8.5 kbar and 625°C prior to and during ductile N–S extension [Lee et al., 2000]. $^{40}Ar/^{39}Ar$ muscovite and biotite ages are similar to Mabja, but decrease up section from 16 to 11 Ma [Lee et al., 2000].

Our LASS measurements show that Kangmar monazites have negative Eu anomalies and mild Y+HREE suppression produced by the presence of? cogenetic plagioclase and garnet like those from Mabja, but they are not zoned in Y and show markedly less variation in composition. Monazite from three kyanite-grade pelites and one garnet-grade pelite are 20 to 16 Ma—similar to the youngest monazite from Mabja. No grains older than 20 Ma were found. These monazite trace-element signatures and ages suggest that prograde metamorphism at Kangmar was later than in Mabja, but of similar duration—or, perhaps because of their small size—closed after prograde metamorphism.

References

King, J., N. Harris, T. Argles, R. Parrish, and H. Zhang, 2011, Contribution of crustal anatexis to the tectonic evolution of Indian crust beneath southern Tibet, *Geological Society of America Bulletin, 123* (1-2), 218-239.

Lee, J., B.R. Hacker, W.S. Dinklage, P.B. Gans, A. Calvert, Y. Wang, J. Wan, and W. Chen, 2000, Evolution of the Kangmar Dome, southern Tibet: Structural, petrologic, and thermochronologic constraints, *Tectonics*, *19*, 872–895.

Lee, J., B.R. Hacker, and Y. Wang, 2004, Evolution of the North Himalayan Gneiss Domes: Structure and metamorphic studies in Mabja Dome, southern Tibet, *Journal of Structural Geology*, *26*, 2297-2316.

Lee, J., W. McClelland, Y. Wang, A. Blythe, and M. McWilliams, 2006, Oligocene-Miocene middle crustal flow in southern Tibet: Geochronologic studies in Mabja Dome, in *Channel Flow, Ductile Extrusion and Exhumation in Continental Collision Zones, Geological Society of London Special Publication, v. 268*, edited by R.D. Law, M.P. Searle, and L. Godin, pp. 445-469.

Lee, J., and M.J. Whitehouse, 200, Onset of mid-crustal extensional flow in southern Tibet; evidence from U/Pb zircon ages, *Geology (Boulder)*, *35* (1), 45-487.

Schärer, U., R.-H. Xu, and C.J. Allegre, 1986, U-(Th)-Pb systematics and ages of Himalayan leucogranites, South Tibet, *Earth and Planetary Science Letters*, *77*, 35–48.

Zhang, H., N. Harris, R.R. Parrish, S. Kelley, L. Zhang, N. Rogers, T. Argles, and J. King, 2004, Causes and consequences of protracted melting of the mid-crust exposed in the North Himalayan antiform, *Earth and Planetary Science Letters*, *228*, 195-212.

Is the deformation around the MCT, 2D or 3D deformation?

Daigoro Hayashi

Simulation Tectonics Laboratory, Faculty of Science, University of the Ryukyus, Okinawa 903-0129 Japan, daigoro@sci.u-ryukyu.ac.jp

The channel flow model (Beaumont et al.,2001, 2004)and its early model, wedge extrusion model (Grujic et al.,2002; Jessup et al., 2006) are attractive models to explain the Himalayan and Tibetan enigma. The kinematic vorticity number Wk analysis is one of the most important method to prove these models from geological side, because from Wk we know the ratio between pure shear and simple shear. According to Jessup et al. (2006) they measured the low Wk in the MCTZ in southern area of Everest that should show high Wk according to the channel flow model. The discrepancy may be resolved if we accept the logics emphasized by Li, C. and Jiang,D. (2011) in which recent methods measuring Wk are only valid in 2D but invalid for 3D deformation. But if 2D deformation occur around natural metamorphic zones, e.g. MCTZ or STDS, the recent methods measuring Wk can work. Unfortunately we do not have the 3D strain analysis method using rigid particles, but we have the other 3D method using passive marker (Hayashi, 2001, 2008). Hayashi (2008) showed that the deformation was 3D in the HHC, MCTZ and LHC around the southern area of Annapurna in Fig.3, therefore we should develop fast a new method to measure Wk in the genuine 3D deformation.

3D strain analysis method using passive marker is briefly explained hereafter. Quartz grain is used as a passive strain marker which is assumed to deform from its initial ellipse shape to the final ellipse.

2D strain analysis

The fabric method (Wheeler, 1986) is used for 2D strain analysis where calculation is performed by computer, since the method does not need the graphical and other manual operations but needs algebraic treatment only. Figure 1 explains the fabric method. Marker ellipses are deformed by "deformation tensor D". The deformed marker ellipses are averaged into a fabric ellipse. On the other hand, we can calculate a strain ellipse from the deformation tensor D. The fabric method maintains that the fabric ellipse is identical to the strain ellipse under the next four conditions. (1) Initial shape of marker is ellipse.(2) There is no initial foliation within markers.(3) There is no competency contrast between markers and matrix.(4) Markers are deformed in homogeneous finite strain. (Wheeler, 1986).

3D strain analysis

Least square method (Hayashi, 1994,2001) is used for 3D strain analysis. After the 2D strain analysis, we have already obtained the direction of long axis and the axial ratio of the strain ellipses on the planes A, B and C as shown in Fig.2. The following procedure is necessary to obtain the 3D strain. (1) Calculate the relative axial length of the strain ellipses by GS method (refer Hayashi, 1994,2001).(2) Calculate the shape tensor of the strain ellipsoid that is constructed from the strain ellipses by the least square strain technique.

(3) Calculate the axial lengths X, Y and Z using the eigen values of the shape tensor of the strain ellipsoid. Supposing that λ_1, λ_2 and λ_3 are the eigen values of the shape tensor and that $\lambda_1 \le \lambda_2 \le \lambda_3$,we have the axial lengths of the strain ellipsoid as

$X = \sqrt{\frac{1}{\lambda_1}}$, $Y = \sqrt{\frac{1}{\lambda_2}}$, $Z = \sqrt{\frac{1}{\lambda_3}}$,where X>Y>Z.

(6) Calculate the direction of X, Y and Z of the strain ellipsoid using the eigen vectors of the shape tensor. The direction of X, Y and Z equals that of the eigen vectors which correspond with λ_1, λ_2 and λ_3, respectively.

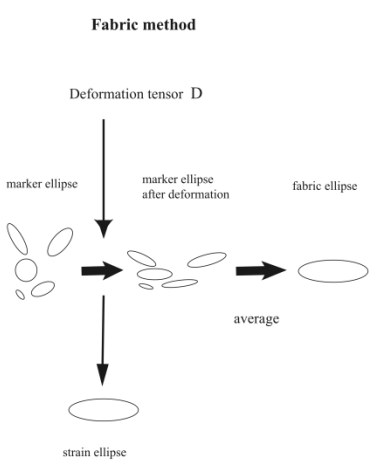

Fig.1

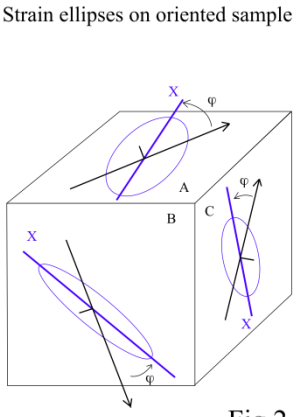

Fig.2

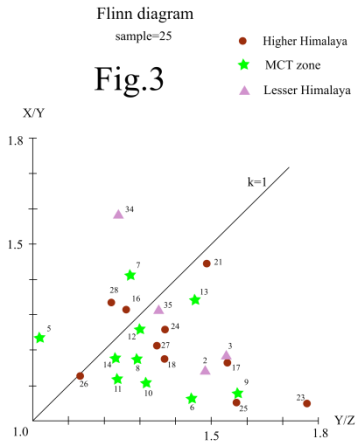

Fig.3

References

Hayashi,D., 2001. The technique that constructs strain ellipsoid from three strain ellipses measured on non-parallel sections based on the least square method and the factors that control precision of strain. Bulletin of the Faculty of Science, University of the Ryukyus, 71, 47-70. (http://ir.lib.u-ryukyu.ac.jp/) enter English page

Hayashi,D., 2008. Tectonic significance of Main Central Thrust around Annapurna detected by 3D strain analysis. Bulletin of the Faculty of Science, University of the Ryukyus, 86, 5-17. (http://ir.lib.u-ryukyu.ac.jp/) enter English page

Jessup,M.J., Law,R.D., Searle,M.P., Hubbard,M.S.,2006,Structural evolution and vorticity of flow during extrusion and exhumation of the Greater Himalayan Slab, Mount Everest Massif, Tibet/Nepal : implications for orogen-scale flow partitioning.Channel flow, ductile extrusion and exhumation in continental collision zones. Geological Society, London, Special Publications, vol.268,379-413.

Li,C. and Jiang,D.,2011,A critique of vorticity analysis using rigid clasts.Journal of Structural Geology 33,203-219.

Wheeler,J., 1986. Average properties of ellipsoidal fabrics: implications for two- and three- dimensional methods of strain analysis. Tectonophysics, 126, 259-270.

The Indus-Yarlung Zangbo ophiolite belt: A Mariana arc-backarc system analog

Réjean Hébert[1], Rachel Bezard[1], Carl Guilmette[1,2], Jaroslav Dostal[3], Chengshan Wang[4]

[1] Département de géologie et de génie géologique, Université Laval, Québec, QC G1V 0A6, Canada, rejean.hebert@ggl.ulaval.ca
[2] Department of Earth Sciences, Dalhousie University, Halifax, NS B3H 4J1 , Canada
[3] Department of Geology, St. Mary's University, Halifax, NS B3H 3C3, Canada
[4] Research Center for Tibetan Plateau Geology, China University of Geosciences, Beijing 100083, China

Current investigation of the 2500+ km long Indus-Yarlung Zangbo Suture Zone (IYZSZ) has shown that it is very complex in terms of geochronology and metamorphic and igneous history. Two ophiolite sub-groups are recognized within the IYZSZ. Sub-group 1 is Mid- to Late Jurassic (150-177 Ma) in age and ill-defined because only few sequences have been found and studied so far. Sub-group 1 is probably derived from the destruction of a marginal basin comprising intra-oceanic arc and fore-arc settings. Spontang and Zedong sequences are examples of this sub-group. Sub-group 2 is Lower Cretaceous (120-130 Ma) and represents the destruction of a marginal basin comprising an arc-back-arc system. These ophiolites are spatially associated with ophiolitic mélanges and flysch respectively representing the reworking of the Cretaceous ophiolites and Indian continental margin and the Neo-Tethyan ocean floor. Most ophiolitic sequences belong to Lower Cretaceous sub-group such as Xiugubagu, Saga, Xigaze, etc... Amphibolite and garnet amphibolite blocks (123-130 Ma) found within the ophiolitic mélange share similar geochemical attributes with sub-group 2 ophiolites. Their protoliths were probably generated within back-arc spreading center and metamorphosed in a nascent subduction zone at depth around 50 km. Some younger radiometric ages suggest events at 80 and 90 Ma which could represent the entry of Indian continental margin into the intra-oceanic subduction zone and/or obduction of ophiolites. However these ages seem to be very rare throughout the whole suture zone and are therefore considered as resulting from local metamorphic events.

IYZSZ ophiolites reveal geochemical features related to the interplay between India and Eurasian plates once separated by the large Tethys Ocean and associated smaller basins such as the Neo-Tethys marginal sea. We present series of geochemical diagrams showing the diversity of geodynamic settings for ophiolite massifs and related ophiolitic mélanges. We conclude that ophiolites are fragments of arc and backarc features which were assembled in a way similar to modern Mariana arc-backarc system. Ba/Ta, Th/Nb, Nb/Yb ratios and normalized multielement diagrams illustrate various crustal-derived material input into mantle sources as a result of evolution of supra-subduction zone factory. Tectonically associated OIB-type magmatic rocks should not be ascribed to ophiolite sequences because they result from a Lower Cretaceous plume which was active within Neo-Tethys basin. We propose a time-framed model for development and partial destruction of the Mariana-type system (Figure 1).

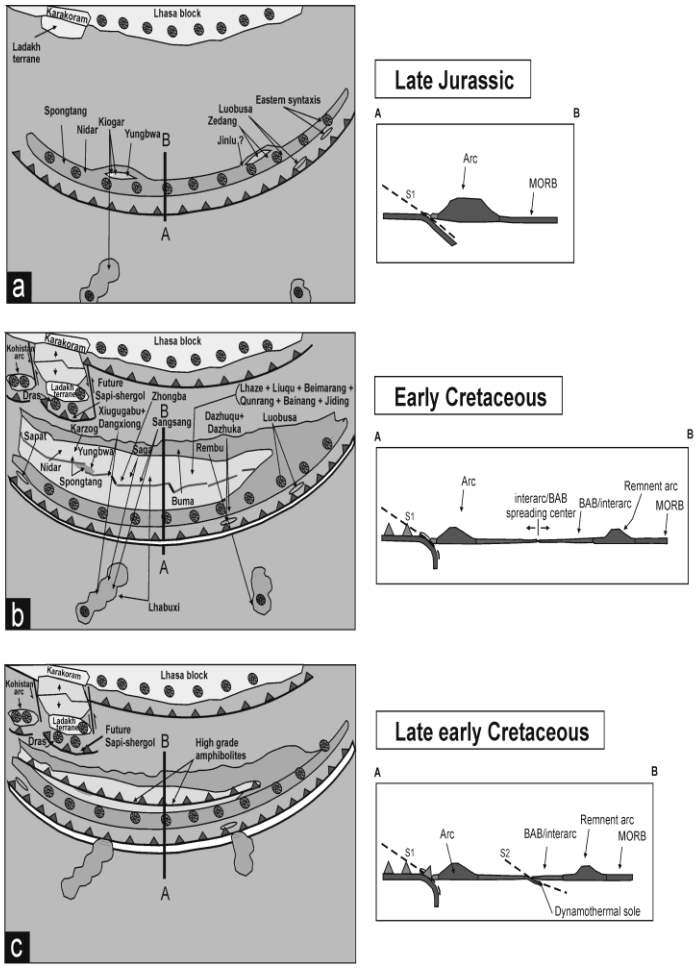

Figure 1. . Schematic reconstructions of the Neo-Tethys basin for the Jurassic and Cretaceous times. This model is based on rock geochemical affinities and available ages. Most ophiolites were formed in the Mariana-type intraoceanic suprasubduction zone developing over a hypothetic north-dipping subduction zone. OIB-related sequences could be associated with a hotspot.

Constraints to the timing of India–Eurasia collision? a re-evaluation of evidence from the Indus Basin sedimentary rocks of the Indus–Tsangpo Suture Zone, Ladakh, India.

Alex Henderson[1], Yani Najman[1], Randy Parrish[2], Gavin Foster[3], Eduardo Garzanti[4], Darren Mark[5]

[1] Lancaster Environment Centre, Lancaster University, Lancaster LA1 4YQ. y.najman@lancs.ac.uk
[2] NIGL, BGS-Keyworth, Nottingham, UK.
[3] National Oceanography Centre Southampton, Southampton University, UK.
[4] Dip Scienze Geologiche, University Milano-Bicocca, Milan, Italy.
[5] SUERC, East Kilbride, Scotland.

The Cenozoic Indus Basin Sedimentary Rocks (IBSR) are preserved in the Indus Suture zone, Ladakh. They have been used in previous research to constrain the timing of India-Asia collision as having occurred by 50 Ma, based on provenance studies which determine the earliest occurrence of mixed Indian and Asian detritus in the sedimentary record (Clift, 2002), and/or earliest evidence of Asian detritus deposited on the Indian plate (Clift, 2002; Clift et al., 2001). Our new study (Henderson et al., 2010a; Henderson et al., 2010b; Henderson et al., 2011) disagrees with these previous findings and we conclude that the sedimentary record in this region cannot be used to constrain India-Asia collision at 50 Ma in the manner previously utilised.

The Chogdo Formation of the IBSR, lying immediately beneath the 50 Ma aged Nummulitic limestone (Green et al., 2008), is proposed to contain both Indian (ophiolitic) and Asian (granitoid) derived material (Clift, 2002), and to lie in sedimentary contact with the underlying Indian plate Lamayuru Formation and ophiolitic melange (Clift, 2002; Clift et al., 2001), thus apparently providing two constraints to the time of collision.

Using the provenance techniques we employed (U-Pb on detrital zircon, Sm-Nd on detrital apatite), we were unable to discern any unequivocal evidence of Indian detritus in the Chogdo Formation, and concur with previous work (Wu et al., 2007), that interprets the Formation as overwhelmingly Asian-derived. We suggest that the ophiolitic detritus recorded in the Chogdo Formation, previously interpreted as derived from the Indian plate Spontang ophiolite, could equally well be derived from local sources in the suture zone, associated with the Dras arc, and do not provide conclusive evidence of Indian input. Thus we do not consider that the Chogdo Formation constrains the time of collision by containing both Indian and Asian detritus.

Given the overwhelmingly Asian provenance of the Chogdo Formation, its proposed stratigraphic position, in sedimentary contact with the underlying Indian plate, would provide another line of evidence to date the time of collision at prior to 50 Ma. For this evidence to be upheld, it must be shown that a) the material beneath the contact is indeed Indian rather than Asian plate, b) the material above the contact is indeed Chogdo Formation rather than younger Indus Basin Sedimentary rocks and c) that the contact is sedimentary rather than tectonic. After characterising the sedimentology, and isotopic, geochemical and petrographic signatures, of the various Indus Basin Sedimentary Rocks in the "type section" in the Zanskar River gorge, we studied the critical basal contact of the Chogdo at the three locations where previous work had indicated the formation lay over Indian plate Lamayuru Formation or ophiolitic melange associated with the Indian plate. These locations lie between the villages of Upshi and Lato on the Manali-Leh highway and between the villages of Chilling and Sumda in the Zanskar Gorge.

At the first location, on the Manali-Leh Highway, we consider that the Formation below the contact (which we suggest is a tectonised unconformity) is IBSR rather than Lamayuru Formation, based on the U-Pb ages of its detrital zircons, and its petrography, which show Asian rather than Indian affinities. We agree with previous work, that the formation above the contact is IBSR, as evidenced by its Asian-derived signature. However, the presence of mudstone enriched in Cr and Ni, limestone conglomerate clasts, detrital white micas, petrography with characteristics of a dissected arc provenance, absence of interbedded limestones, and the presence of a 48.4 +/-1.4 Ma detrital zircon makes the suggested correlation of this unit to the 50 Ma aged Chogdo Formation with its undissected arc petrography,

unenriched Cr and Ni concentrations and interbedded limestone units, unlikely. Rather, we prefer to correlate this unit with younger sediments higher up the IBSR succession.

At the second location, near the villages of Chilling and Sumda, the Chogdo Formation is considered to lie in sedimentary contact above both the Lamayuru Formation and Indian plate ophiolitic melange. However, our provenance analysis, based on petrography and U-Pb ages of detrital zircons, indicate that the unit above the contact is of Indian rather than Eurasian plate derivation, entirely unlike the defined Eurasian-derived Chogdo Formation in the "type section" of the Zanskar Gorge. We therefore do not consider it to be Chogdo Formation and this location cannot be used to constrain the timing of India-Asia collision in the manner previously proposed.

We therefore conclude that there is currently no evidence in the region for mixing of Indian and Eurasian detritus in the >50 Ma aged Chogdo Formation, nor evidence for Asian-derived Chogdo Formation overlying Indian plate in sedimentary contact. Thus, previously proposed constraints to the time of collision at ca 50 Ma, based on these data, in our view should be reconsidered.

References

Clift, P., Carter, A., Krol, M., Kirby, E., 2002, Constraints on India-Eurasia collision in the Arabian sea region taken from the Indus Group, Ladakh Himalaya, India. The tectonic and climatic evolution of the Arabian Sea region, Geological Society of London Special Publication, 195, 97-116.

Clift, P.D., Shimizu, N., Layne, G.D. and Blusztajn, J., 2001, Tracing patterns of erosion and drainage in the Paleogene Himalaya through ion probe Pb isotope analysis of detrital K- feldspars in the Indus Molasse, India, Earth and Planetary Science Letters, 188, 475-491.

Green, O.R., Searle, M., Corfield, R.I. and Corfield, R.M., 2008, Cretaceous-Tertiary carbonate platform evolution and the age of the India-Asia collision along the Ladakh Himalaya (Northwest India), Journal of Geology, 16, DOI: 10.1086/588831.

Henderson, A., Foster, G.L. and Najman, Y., 2010a, Testing the application of in situ Sm–Nd isotopic analysis on detrital apatites, A provenance tool for constraining the timing of India–Eurasia collision, Earth and Planetary Science Letters, 297, 42-49.

Henderson, A.L. et al., 2010b, Geology of the Cenozoic Indus Basin sedimentary rocks: Paleoenvironmental interpretation of sedimentation from the western Himalaya during the early phases of India-Eurasia collision, Tectonics, 29, TC6015 doi 10.1029/2009TC002651.

Henderson, A.L., Najman, Y., Parrish, R., Mark, D. and Foster, G.L., 2011, Constraints to the timing of India–Eurasia collision; a re-evaluation of evidence from the Indus Basin sedimentary rocks of the Indus–Tsangpo Suture Zone, Ladakh, India, Earth Science Reviews, in press, doi:10.1016/j.earscirev.2011.02.006.

Wu, F.Y., Clift, P.D. and Yang, J.H., 2007, Zircon Hf isotopic constraints on the sources of the Indus Molasse, Ladakh Himalaya, India, Tectonics, 26, ISI:000246146800004

Tectonic consequences of partial melting: comparison of the Coast Orogen, British Columbia with the Higher Himalaya Crystallines.

Lincoln S. Hollister

Department of Geosciences, Princeton University, Princeton, NJ 08544, USA, linc@princeton.edu

The recognition that a small amount of melt greatly weakens rock was first made not far from the site of this conference, in the Coast Orogen of British Columbia. This phenomenon is now recognized as a necessary condition for channel flow to occur. Although many question the concept of channel flow, I believe most of us are persuaded by the preponderance of evidence from the Higher Himalaya Crystallines (HHC) that channel flow occurred there. The question is whether channel flow, as described for the HHC, has occurred in the Canadian Cordillera, or anywhere else. There is no question that melt weakening, even for a few percent melting, is fundamental for controlling deformation and flow of rock, and there is no question that the crystalline cores of British Columbia had been partially melted.

In addition to the role of melt in deformation, a key observation for the Coast Orogen of British Columbia was that the rocks had decompressed by some 4 kbar while they remained at high temperature. Near isothermal decompression is also recognized in the HHC of Bhutan; there, the amount of decompression was 5-7 kbar. In the Coast Orogen, it is now recognized that the decompression resulted from a combination of tectonic and erosional denudation during Eocene crustal scale extension. The extension appears to have created the pressure difference that drove lower crustal flow westward and into the domes, with accompanying decompression.

Because of the similarities of the deformation, metamorphic, and decompression phenomena in the Coast Orogen and of the HHC, it is reasonable to infer common elements in their histories. The Coast Orogen began with crustal thickening and finished with tectonic thinning by whole lithosphere extension. Erosion accompanied the extension. In the Himalayas, erosion certainly now plays a role in the exhumation. Earlier tectonic exhumation is also demonstrated by the north dipping south Tibetan detachment systems. However, a fundamental difference is that the Coast Orogen evolved mainly during transpression and transtension, and the Himalayas are now dominated by orthogonal convergence. Another important difference is that the crustal thickness of western British Columbia, following extension, was 34 km thick, whereas the Himalayas, still growing, are over 70 km thick. The Himalayas and the Tibetan Plateau have yet to collapse to normal crustal thickness. If the future collapse were to be by extension rather than denudation, the HHC would still occur at the surface and would preserve the metamorphic and deformation history of the earlier channel flow event.

In any case, the presence of partial melt, accompanied by isothermal decompression, appears to signal the flow of low viscosity (partially melted) rock toward lower pressures. For the HHC the pressure gradient was from deep under the Tibetan Plateau to the Himalayan mountain front. For the Coast Orogen, the pressure gradient was from the base of the crust east of the axis of the Coast Mountains to the break away caused when top to east normal shear began.

Petrology of the ultramafic rocks from the Waziristan Ophiolite, NW Pakistan

M. Qasim Jan[1], Said Rhaim Khan[2] and M. Asif Khan[1]

[1] National Centre of Excellence in Geology, University of Peshawar, Peshawar 25120, Pakistan, mqjan@yahoo.com
[2] Geological Survey of Pakistan, Azad Kashmir Regional Directorate, Chak Shezad Town, Islambad, pakistan

Waziristan is the 2nd largest (~1800 km^2 in area) of the ophiolites exposed along the western plate boundary of the Indian Plate and involved in the India-Afghan collision (Figure 1). Spread across the border between the Waziristan Tribal Agency, Pakistan, and Khost Province, Afghanistan, the ophiolite body is probably an extension of the Khost ophiolite (Cassaingeau, 1979; Gnos et al., 1997). The ophiolite is one of the three major thrust sheets derived from the Neothyteys and emplaced onto the western passive-margin outer shelf of the Indian Plate in Pakistan. The Waziristan ophiolite (WO) is the uppermost thrust sheet, followed eastwards by the Kurram-Khaisora nappe derived from Triassic-Paleocene Outer Shelf, and westwards by the Kahi nappe derived from a Cretaceous oceanic fore-deep sequence (Robinson et al., 2000; Khan et al., 2003). The ophiolite was intially obducted at 90 Ma within an intraoceanic setting (Gnos et al., 1997), but emplacement onto the Indian-Plate shelf sequence is dated at Late Paleocene (Beck et al., 1995; 1996).

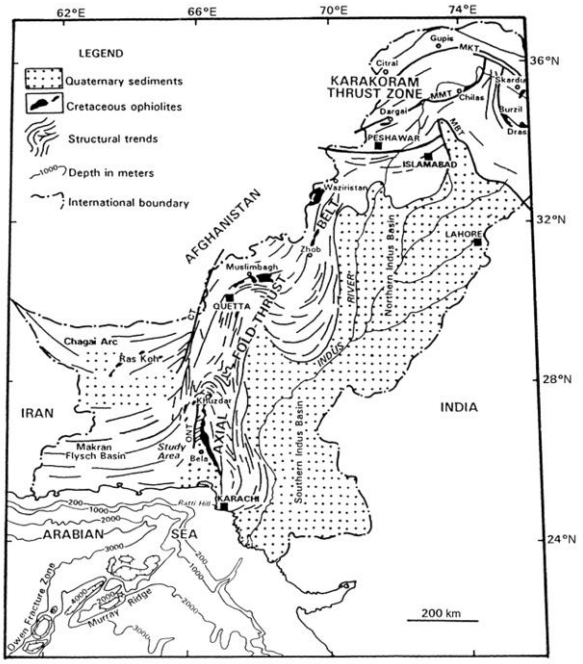

Figure 1. Simplified geological map of Pakistan showing Cretaceous ophiolites at the western-northwestern plate boundary of the Indian plate (Asrarullah and Abbas, 1979).

WO is internally divisible into three thrust sheets (nappe); these, from east to west (i.e., lower to upper), include, Vezhda Sar, Boya and Datta Khel nappes. Despite strong tectonic dismemberment, the WO, includes all the principal lithological elements of a type ophiolite, i.e., ultamfic rocks, gabbros, sheeted dykes, plagiogranite, pillowed basalts and pelagic sediments. This paper is restricted to the ultramafic rocks in terms of their petrology and mineralogy.

The Vezhda Sar nappe, which forms the eastern edge of the WO and is thrust over the outer shelf sediments of the Indian Plate, is composed entirely of pillow basalts. Ultramafic rocks in this nappe are restricted to exotic blocks dispersed in the pillow basalts. The Boya nappe, which forms the central part of the WO is strongly dismembered, giving the appearance of a typical mélange. Here, the ultramafic rocks are irregularly distributed as fault-bounded blocks within a larger mass of pillow basalt. However, an intact ophiolite section occurs in the basal part of the nappe at Mami Rogha. This sequence is composed of ultramafic rocks at the base, followed upwards by isotropic gabbros, and pillow basalts capped by pelagic sediments. In the Datta Khel nappe, the ophiolite sequence starts with gabbros at the base, and the ultramafic rocks occur only as fault-bounded blocks, irregularly distributed in the thrust sheet.

Ultramafic rocks in the ophiolites and oceanic crust are commonly of two types; granular- and layered peridotites, respectively occuring below and above the petrological Moho. The former, having annelaed under high temperature, are commonly refered to as the mantle (tectonized) peridotites, while the latter are considered to have crystallized as comulates from a basaltic magma in the ophiolite magma chamber. A great majority of the WO ultramafic rocks are characterized by a cumulus textures typical of the crustal untramafic rocks in ophiolites and oceanic crust. The mantle peridotites are either not exposed or not sampled. The ultramafic cumulates in the WO include wherlite (olivine, diopside with enstatite, magnetite and chrome spinel as accessories), harzburgite (olivine, enstatite, with minor accessroes of diopside and chrome spinel), and dunite (olivine with minor clinopyroxene); wherlite being the most common and dunite being the least. Chromitite forms lensoide bodies (up to 3 m thick), layers (cm scale), veins and stringers associated with dunites. It consists of chromite and olivine or secondary chlorite and serpentine.

Olivine and chrome spinels from the ultramafic rocks of the WO have been analyzed for mineral chemistry. Olivine in the silicate rocks is characterized by a high foresterite content, but with a narrow range, i.e., Fo 90-91. Orthopyrexene in the harzburgite is similarly magnesian (En 90-91).The peridotites locally contain swarms of pyroxenite dykes comprising enstatite ± olivine ± opaque oxide. The olivine in the chromitites is more magnesian (Fo 92 to 96) due probably to Mg – Fe exchange with chromite during subsolidus re-equilibution.

Chromite shows considerable variation in Cr# (100 Cr/(Cr + Al) and Mg # (Mg/ (Mg+Fe^{2+}). The Cr # ranges from 84 to 45 in chromitites and 74 to 21 in accessory chromite. Similarly, Mg # ranges from 44 to 55 in chromite in chromitites and 76 to 47, in accessory chromite. Several workers (i.e., Dick and Bullen, 1984, Jan and Windley, 1991) have suggested that large variations in chromite compsoition, especially in Cr #, may be suggestive of a complex origin.

References

Asrarullah, A.Z., and Abbas, S.G., 1979, Ophiolites in Pakistan; an introduction: in Farah, A., and DeJong, K. A., eds., Geodynamics of Pakistan: Quetta, Geological Survey of Pakistan, 181-192.

Beck, R. A., and 17 others, 1995, Stratigraphic evidence for an early collision between northwest India and Asia, Nature, 373, 55-58.

Beck, R. A., Burbank, D. W., Sercombe, W. J., Khan, M.A., and Lawrence, R.D. 1996, Late Cretaceous ophiolite obduction and Paleocene India-Asia collision in the westernmost Himalaya, Geodinamica Acta, 9, 114-144.

Cassaingeau, C., 1979. Contribution a l'étude des sutures Inde-Eurasie, la zone de suture de Khost dans le Sud-Est de l'Afghanistan. L'Obduction L'Obduction Paleocene et la tectonique tertiaire. Unpublished Ph. D dissertation, Montpellier, France, p. 145.

Dick, H. J. B. and Bullen, T. 1984, Chromium spinel as a petrologic indicator in abyssal and alpine-type peridotites and spatially associated lavas. Contribution to Mineralogy and Petrology, 86, 54-76.

Gnos, E., Immenhauser, A., Peters, T., 1997, Late Cretaceous/Early Tertiary convergence between the Indian and Arabian plates recorded in ophiolites and related sediments, Tectonophysics, 271, 1–19.

Jan, M. Q. and Windley, B. F. 1990, Chromian spinel-Silicate chemistry in ultramafic rocks of the Jijal Complex, Kohistan islanad arc, Pakistan. Journal of Petrology, 31, 667-715.

Khan, M. A., Abbasi, I. A., Qureshi, A. W. and Khan, S. R. , 2003. Tectonics of Afghan-India Collision Zone, Kurram-Waziristan Region, N. Pakistan. Proceedings of ATC, 1-14.

Robinson, J., Beck, R. A., Gnos, E. and Vinvent, R. K., 2000. New structural and stratigraphic insights for northwestern Pakistan from field and Landsat Thematic mapper data, Geological Society of America Bulletin, 112, 3, 364-374.

Strain partitioning during dome formation in the Himalaya: Insights into the Ama Drime Massif and Leo Pargil dome, NW India

Micah Jessup[1], Jackie Langille[1], , John Cottle[2], Graham Lederer[2], Talat Ahmad[3]

[1] University of Tennessee, Knoxville, TN 37996, USA, mjessup@utk.edu
[2] University of California, Santa Barbara, CA 93106, USA
[3] University of Delhi, Delhi -110007, India

Migmatite-cored domes such as Leo Pargil dome (Thiede et al., 2006; Hintersberger et al., 2010), Ama Drime Massif (Cottle et al., 2009; Kali et al., 2010; Langille et al., 2010) and the Gurla Mandhata core complex (Murphy et al., 2002) were exhumed along shear zones that accommodated orogen-parallel extension. These domes are bounded by shear zones that provide snapshots of different stages in the kinematic evolution of the orogen in the transition zone between crustal shortening in the foreland and orogen-parallel extension in southern Tibet.

The Ama Drime Massif, Tibet is a north-south trending range that developed during orogen-parallel extension that post-dates (~12 Ma) south-directed extrusion of the GHS. It is bounded by two oppositely dipping shear zones, the Ama Drime detachment (ADD) and Nyonno Ri detachment. The ADD is a west dipping, north-south striking shear zone that juxtaposes upper amphibolite facies migmatitic gneiss in the hanging wall with granulite facies migmatitic gneiss in the footwall. The ADD is a 100-300 m-thick mylonite zone of interlayered quartzite, marble, calc-silicate and leucogranites. Two-feldspar thermometry on asymmetric strain induced myrmekite provides a minimum temperature estimate (370-435ºC) for top-down-to-the-west sense of shear. Assuming a dip of 30º, these and other estimates of deformation temperature yield displacement estimates of 21-42 km during orogen-parallel extension (Langille et al., 2010). Mean kinematic vorticity estimates, using the rigid grain and quartz grain shape techniques, indicate that early deformation included a high contribution (49-66%) of pure shear (Langille et al., 2010).

The Leo Pargil dome, NW India is a northeast striking elongate dome that is composed of a leucogranite injection complex that records protracted melting during the Miocene (Leech, 2008; Langille et al., in prep), potentially synchronous with south-directed extrusion of the GHS. Two oppositely dipping high strain zones, the Leo Pargil shear zone (Thiede et al., 2006) to the northwest and the Qusum shear zone (Zhang et al., 2000) to the southeast, bound the dome. The Leo Pargil shear zone is a zone of distributed (>500 m) deformation that consistently records top-down-to-the-west -northwest sense of shear and juxtaposes amphibolite facies rocks in the footwall with low-grade metasedimentary rocks in the hanging wall. Quartz LPO data from quartzites that are interlayered with leucogranites yield estimates of 500-650°C while quartz and feldspar textures indicate some overprinting of lower temperature (500-280°C) conditions during exhumation.

Exhumation of the Ama Drime Massif occurred during orogen-parallel extension that clearly post-dates south-directed extrusion of the GHS between the STDS and MCTZ. The Leo Pargil dome appears to share a melting history that is similar to the Greater Himalayan Series, but the kinematic link between melting and exhumation during orogen-parallel extension is more complex. The Leo Pargil dome was exhumed from depths near the base of the Tethyan Sedimentary Series by a distributed shear zone. In contrast, the Ama Drime Massif was exhumed from some of the deepest positions that are exposed in the central Himalaya (Cottle et al., 2009; Langille et al., 2010; Kali et al., 2010).

References

Cottle, J.M., Jessup, M.J., Newell, D.L., Horstwood, S.A., Noble, S.R., Parrish, R.R., Waters, D.J., Searle, M.P., 2009, Geochronology of granulitized eclogite from the Ama Drime Massif: implications for the tectonic evolution of the South Tibetan Himalaya, Tectonics, 28, 1−25.

Hintersberger, E., Thiede, R. C., Strecker, M. R., and Hacker, B., 2010, E-W extension in the NW Indian Himalaya, Geological Society of America Bulletin, 122, 1499-1515.

Langille, J., Jessup, M., Cottle, J., Newell, D., Seward, G., 2010, Kinematics of the Ama Drime Detachment: Insights into orogen-parallel extension and exhumation of the Ama Drime Massif, Tibet-Nepal, Journal of Structural Geology, 32, 900-919.

Langille, J., Jessup, M., Cottle, J., Lederer, G., Ahmad, T., in prep, Timing of metamorphism, melting, and exhumation of the Leo Pargil dome, NW India, Journal of Metamorphic Geology.

Leech, M. L., 2008, Does the Karakoram fault interrupt mid-crustal channel flow in the western Himalaya? Earth and Planetary Science Letters, 276, 314-322.

Murphy, M. A., Yin, A., Kapp, P., Harrison, T. M., Manning, C. E., Ryerson, F. J., Lin, D., Jinghui, G., 2002, Structural evolution of the Gurla Mandhata detachment system, Southwest Tibet; implications for the eastward extent of the Karakoram fault system. Geological Society of America Bulletin, 114, 428−447.

Thiede, R. C., Arrowsmith, J. R., Bookhagen, B., McWilliams, M., Sobel, E. R., Strecker, M. R., 2006, Dome formation and extension in the Tethyan Himalaya, Leo Pargil, northwest India, Geological Society of America Bulletin, 118, 635−650.

Zhang, J., Ding, L., Zhong, D., Zhou, Y., 2000, Orogen-parallel extension in Himalaya: Is it the indicator of collapse or the product in process of compressive uplift? Chinese Science Bulletin, 45, 114-120.

The ascertainment and petrogenesis of Cenozoic Kuzigan A-type granitoids from NW India-Asia collision zone, Xinjiang, China

Shan Ke

School of Earth Science and Mineral Resources, China University of Geosciences, Beijing, 100083, China, keshan@cugb.edu.cn

The Kuzigan complex is located at the middle-east Pamir Syntaxis and distributed along the Karakorum fault. They are LREE-enriched peralkalic syenites and alkalic syenitoids with potassium feldspar, plagioclase, quartz, biotite and aegirine-augite as their common minerals. The chemical compositions of Kuzigan complex vary widely in SiO_2 (54.2 to 74.8%), and enriched in K_2O+Na_2O (7.29 to 11.95%) and K_2O ($K_2O/Na_2O>1$). Based on filed observation, petrography and geochemistry of Kuzigan complex, this complex is A-type granitoids emplaced at ~11Ma (SHRIMP U–Pb zircon).

However, compared with typical world A-type granites, this complex has its own special characteristics with high K_2O, MgO, $(La/Nb)_N$, Ba, Sr, Eu, La/Yb, Sr/Y, lower FeO^T/MgO and very small negative Eu anomaly. These are considered to be controlled mainly by its source rocks and melting conditions (e.g. high pressure). We suggest that Kuzigan A-type granitoids were the product of partial melting of mafic eclogite at the base of the thickened crust, with no plagioclase in the source but garnet and rutile in the residue. According to its tectonic setting, this kind of A-type granitoids was not formed at the end of orogeny but a magmatic product induced by the regional extension (e.g. large scaled strike-slip movement of the Karakorum) during the orogenic process.

South Tibetan detachment system in Sikkim: stuck between a massif and a cross-structure.

Dawn Kellett[1], Djorge Grujic[2], John Cottle[1], Isabelle Coutand[2]

[1] Department of Earth Science, University of California, Santa Barbara, CA 93106, USA, dkellett@geol.ucsb.edu
[2] Department of Earth Sciences, Dalhousie University, NS, B3H 4J1, Canada

The Sikkim, India segment of the South Tibetan detachment system is cut by two major strike-perpendicular structures. To the west, the N-S-striking Nyönni Ri detachment has unroofed the Ama Drime metamorphic massif with top-east displacement (Jessup et al., 2008), and to the east, the Yadong cross-structure apparently offsets the South Tibetan detachment system by > 50 km (Edwards and Harrison, 1997; Wu et al., 1998). The South Tibetan detachment system itself comprises a brittle-ductile fault with Tethyan sedimentary sequence black shale in the hanging wall and garnet-biotite-sillimanite gneiss and leucogranite of the Greater Himalayan sequence in the footwall. The top ~500 m of the footwall has been deformed into a mylonite layer with top-to-the-north sense of shear.

Zircon from a weakly-deformed leucosome in footwall garnet-biotite-sillimanite gneiss yields SHRIMP U-Pb ages for rims ranging 28.5-15.5 Ma. Weakly-deformed leucogranite dykes which cross-cut the mylonitic foliation in host gneiss contain zircons with rims as young as 13.0 Ma. A cordierite-bearing granite, which may reflect crystallization at low pressure (~4 kbar, e.g. Streule et al., 2010) yields U-Pb ages for zircon rims as young as 13.4 Ma. The lack of mylonitisation the leucogranites indicates that little ductile shearing occurred following their crystallization. Zircon crystallization temperatures, determined by measurement of Ti-in-zircon, are 660-810 °C during 34-13 Ma. Muscovite from four of these samples yield $^{40}Ar/^{39}Ar$ cooling ages of c. 13.1 Ma, with an estimated closure temperature for Ar diffusion of 430-490 °C. Apatite fission track ages from the same granites indicate cooling below 120 °C at c. 8-6 Ma.

Monazite were analyzed *in situ* in three host garnet-biotite-sillimanite gneisses by LA-ICP-MS. Monazite included in garnet yield Th-Pb ages of 36-23 Ma. In general, monazite Th-Pb ages range from 36-14.5 Ma. Youngest monazite ages in the host gneiss are associated with ductile deformation and older than the youngest zircon ages in leucogranite, in agreement with structural observations that little ductile deformation proceeded leucogranite emplacement.

Taken together, these data provide constraints on long-lived partial melting in the uppermost Greater Himalayan sequence between 34-13 Ma, as well as the cooling history of rocks unroofed by this segment of the South Tibetan detachment system. Latest deformation in the footwall of the South Tibetan detachment system constrains initiation of both the Nyönni Ri detachment, and the Yadong cross-structure, to younger than 13 Ma. Activation of the Nyönni Ri detachment before 11 Ma (Kali et al., 2010; Leloup et al., 2010) marks a major transition in tectonic transport in the eastern Himalaya from N-S to E-W. However, the South Tibetan detachment system in the Bhutan Himalaya, east of the Yadong cross-structure, was active after 11 Ma (Kellett et al., 2010). Thus the transition from NS-directed to EW-directed deformation in the eastern Himalaya was not synchronous.

References

Edwards, M.A. and Harrison, T.M., 1997, When did the roof collapse? Late Miocene north-south extension in the high Himalaya revealed by Th-Pb monazite dating of the Khula Kangri granite, Geology, 25, 6, 543-546.

Jessup, M.J., Newell, D.L., Cottle, J.M., Berger, A.L., Spotila, J.A., 2008, Orogen-parallel extension and exhumation enhanced by denudation in the trans-Himalayan Arun River gorge, Ama Drime Massif, Tibet-Nepal, Geology, 36, 587-590.

Kali, E., et al., 2010, Exhumation history of the deepest central Himalayan rocks, Ama Drime range: Key pressure-temperature-deformation-time constraints on orogenic models, Tectonics, 29, 10.1029/2009TC002551.

Kellett, D.A., et al., 2010, Metamorphic history of a syn-convergent orogen-parallel detachment: The South Tibetan detachment system, Bhutan Himalaya, JMG, 28, 785-808.

Leloup, P.H. et al., 2010, The South Tibet detachment shear zone in the Dinggye area Time constraints on extrusion models of the Himalayas, EPSL, 29, 10.1016/j.epsl.2009.12.035.

Streule, M.J., Searle, M.P., Water, D.J., Horstwood, M.S.A., 2010, Metamorphism, melting, and channel flow in the Greater Himalayan Sequence and Makalu leucogranite: Constraints from thermobarometry, metamorphic modeling and U-Pb geochronology, Tectonics, 29, doi:10.1029/2009TC002533.

Wu, C., Nelson, K.D., Wortman, G., Samson, S.D., 1998, Yadong cross structure and South Tibetan Detachment in the east central Himalaya (89°-90°E), Tectonics, 17, 28-45.

Geochemistry, Petrogenesis and Tectonic environments of JAL-NIAT amphibolites, Southeast Kohistan, Pakistan

M. Ahmed Khan[1], Saif ur Rehman[1], Khalid Mehmood[1], M. Asif Khan[2], Naveed Ahsan[3]

[1] Department of Earth Sciences, University of Sargodha, Sargodha, Pakistan, drahmadkhan@hotmail.com
[2] National Centre of Excellence in Geology, University of Peshawar, Pakistan.
[3] Institute of Geology, University of Punjab, Lahore, Pakistan

The intra-oceanic Kohistan island arc was initiated during the Cretaceous as a result of northward movement of the Indian Plate and sandwiched between Indian plate and Eurasian plate. The Kohistan sequence represents rocks of a young arc crust comprising amphibolites, diorites, metanorites and associated volcanic rocks. Amphibolites are prominently found along the southern belt of Kohistan sequence which extends from Afghanistan though Bajaur, Dir, Swat, Indus Valley, Babusar up to Nanga Parbat.

Kamila Amphibolite Unit (KAU) a strip (maximum 50×50 Km) of amphibolites constitutes the southeastern part of Kohistan and confined between Main Mantle Thrust (MMT) in south and Chilas Complex in north, along the southern part of Kohistan terrain (Fig 1). It lies on Jijal complex along MMT in Indus valley. The amphibolites are distinguished by mafic-ultramafics rocks of Sapat Complex at the base from MMT, the Spat Complex is composed of a variety of lithologies including dunite, pyroxenites, peridotites, chromitite, gabbros and anorthosite and these ultramafic rocks generally occur as lensoid bodies within the layered and isotropic gabbroic rocks.

Kamila Amphibolite Unit, part of Kohistan terrane represents thick pile of meta-volcanics with mafic-ultramafic base (Spat Complex) along the Main Mantle Thrust. KAU is intruded by diorites, granitoids and trondjhemites of Thak intusive complex. KAU is subdivided into four distinct units on the basis of distinct characters and new data from this study; Babusar amphibolites, Niat amphibolites, Jal amphibolites from south to north respectively with a thin slice of Sumal amphibolites within Jal-Niat amphibolites (Fig 1). Jal-Niat amphibolites are generally fine grained, banded and strongly foliated and fall in tholeiite group and show enrichment in HFSE (Zr, Y, P, Nb) and depletion in LILE (Rb, Pb, Th, K). MgO versus Zr plot indicate primitive to more evolved compositional pattern through intermediate stage. HFSE enrichment deciphers more heterogeneous and enriched mantle source like MORB for Jal-Niat amphibolites. Average concentration of TiO_2 (1.99 wt% for Niat amphibolites and 1.56 wt% for Jal amphibolites) and K_2O (0.14 wt% for Niat amphibolites and 0.20 wt% for Jal amphibolites) exhibit MORB like composition where as average Y/Nb ratio (8.9 for Niat amphibolites and 8.4 for Jal amphibolites) are close to N-MORB(12). Zr/Y vs Zr plot characterized the studied rocks as MORB and fall in ocean floor basalt (OFB) on Ti/100, Zr, Sr/2 triangle.

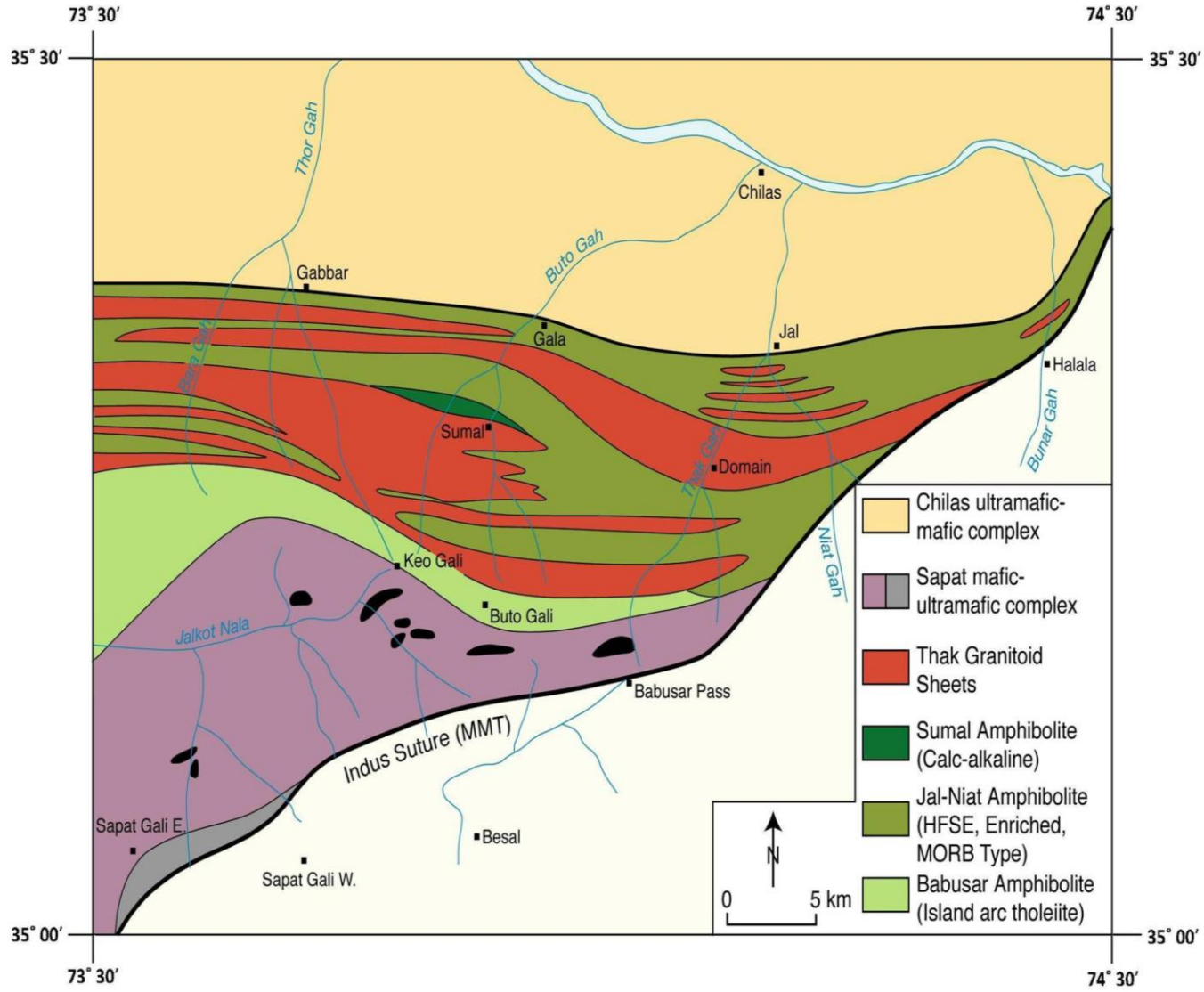

Figure 1. Geological Map of Kamila Amphibolite Unit bounded by MMT in south and Chilas Complex in north.

Interaction between the Himalayan and India-Afghan Collision Tectonics at the NW margin of the Indian Plate in the Kurram Region, NW Pakistan

M. Asif Khan, Muntazir Abbas

National Centre of Excellence in Geology, University of Peshawar, Peshawar 25120, Pakistan, masifk@upesh.edu.pk

The NW Himalayas in Pakistan, with a minor component extending into the NE Afghanistan present a number of tectonic flexures, which yield orographic trends markedly different from the NW-SE trending Kashmir-Zanskar Himalayas in the east. West of the Western Himalayan Syntaxis, the ~200 km wide Himalayan orogen, bounded by the Indus Suture in the north and the Salt-Range Frontal Thrust in the south is oriented WSW-ENE (Coward et al., 1988). The Kurram-Waziristan Ranges at the western margin of the Kohat Plateau in the NW Himalayan foreland trend NNE-SSW, almost at right angle to the Himalayan trend in the north (Meisner et al., 1975; Beck et al., 1996), forming a local syntaxial bend referred to as the Kurram Reentrant. This change in the orographic trends owes to two separate but coeval collisional tectonic regimes; India-Kohistan-Karakoram collision in the north (Coward et al., 1988) and India-Afghan collision in the west (Beck et al., 1995; 1996). The Kurram region NW of the Kohat Plateau, the focus of this study, represents the junction point between the collisional orogens resulting from these two collision events.

Three tectonic blocks are in contact with each other in the Kurram-North Waziristan region; 1) Spinghar block in the north, 2) Western Samana block in the middle and the 3) Kurram-Waziristan block in the south. The northern two blocks are characterized by WNW-ESE trends, in continuation with the orographic trend of NW Himalayas, while the southern block has NNE-SSE structural trend, contrasting with the Himalayan trend but parallel to the western ophiolite belt, contiguous with the Chaman transform fault. The Spinghar Block (stranding the border area between the Kurram Agency, Pakistan and Nangarhar Province, Afghanistan) is westerly extension of the Inner Lesser Himalayas in NW Pakistan (i.e., Lower Hazara-Peshawar Basin Zone) comprising low-grade metamorphic rocks (Precambrian Landikotal-Manki-Hazara slates) overlain by a Palaeozoic sequence. The Spinghar Thrust separates the Spinghar and Samana blocks and is western equivalent of the Nathiagali-Histartang Thrust that marks the boundary fault between the Inner and Outer Lesser Himalayas and separates the Internal Himalayas from the Outer Himalayas as defined by Coward et al. (1988). The Samana Block is part of the Outer Lesser Himalayas, and comprises carbonate-dominated Jurassic-Upper Palaeocene lithologies. The Samana Block, instead of being bounded by the Main Boundary Thrust (MBT) at its southern margin, as is the case in the Kohat-Potwar Plateau, is abutted against the Kurram-Waziristan Block along the Kurram Fault. The Sub-Himalayas are therefore missing in the Kurram Agency. The Waziristan-Kurram Block consists of a tectonic collage of thrust sheets derived from the shelf-oceanic basin transition zone in the Neotethys at the western margin of the Indian Plate and includes 1) Tani Formation, 2) dismembered ophiolite, 3) Triassic-Palaeocene Kurram-Khaisora Group and 4) Cretaceous Kahi Group (Satara-Zakha, Shinkai Post and Khajori Post formations), with Indian Plate passive-margin inner shelf autochthonous sequence exposed in window structures beneath these thrust sheets.

The typical passive margin shelf-sequence of the Hill Ranges in Outer Lesser Himalayas (i.e., Samana-Kotal Pass-Kalachitta-Margala Ranges) is characterized by a major Early Palaeocene unconformity marked by Hangu Formation (Pivnik and Sercombe, 1993). Subsequent sequence from Middle Palaeocene Lokhart Limestone to Middle Eocene Kohat Formation lacks any distinct unconformity (Izatt, 1990). In Samna Hill Ranges, west of Hangu, Beck et al. (1995; 1996) recognized that the Late Palaeocene Patala Formation is unconformably deposited on top of the Kurram Group, a succession of allochthonous oceanic foredeep sequence originally deposited in the Neotethys and displaced onto the Samana Hill Ranges prior to the deposition of the Patala Formation. This serves earliest signature of India-Afghan collision (Beck et al., 1995), which is restricted to the Samana Ranges of the Kurram region and is characteristically absent in the rest of the Outer Lesser Himalayas in Pakistan.

Our studies in the Kurram region concur with earlier findings (Meisner et al., 1975; Beck et al., 1995; 1996) that the thrust sheets derived from the Neothetys shelf-oceanic basin transition zone including

ophiolites (Khost-Waziristan), Kahi Group (deep-marine foredeep), Kurram-Khaisora Group (outer passive-margin shelf) over-thrust the inner Indian-Plate passive margin shelf in the Late Paleocene, which is now exposed only in thrust-fault bounded anticlines as window structures. However, some new findings further highlight these India-Afghan collision related structures. In the northern part of the Samana Ranges we have mapped a south-verging anticline (Chamkani Anticline) cored by the Kurram-Khaisora Group, with inner Indian-plate shelf sequence ranging from Jurassic Samana Suk Formation to Late Paleocene Patala Formation occupying the limbs of this anticline (Fig. 1). This contrasts with better known anticlines in the southern Samana Range (e.g.,Darsamnad, Khadimak; Beck et al., 1995, 1996) where the core is occupied by Hill Range sequence and Kurram-Khaisora thrust sheet occupies the intervening synclonoriae (as klippe). This structural relation suggests that the Western Samana Ranges in the Kurram Region show interaction between three thrust sheets 1) a basal allocthon of the Hill Range sequence, 2) a middle allocthon of the Kurram Group, and 3) an upper alocthon of the Hill Range Sequence. The upper thrust sheet of the Hill Range sequence is preserved only in the northern part of the Samana Ranges, whereas in the southern parts of the Hill Ranges only the two basal thrust sheets are preserved.

This work shows that the Kurram region in NW Pakistan is unique in NW Himalayas where thrust sheets derived from the Himalayan collision involving the northern passive margin shelf sequence were being emplaced southwards into the Hill Ranges simultaneously with thrust sheets derived from Indian Plate western shelf resulting from the India-Afghan collision.

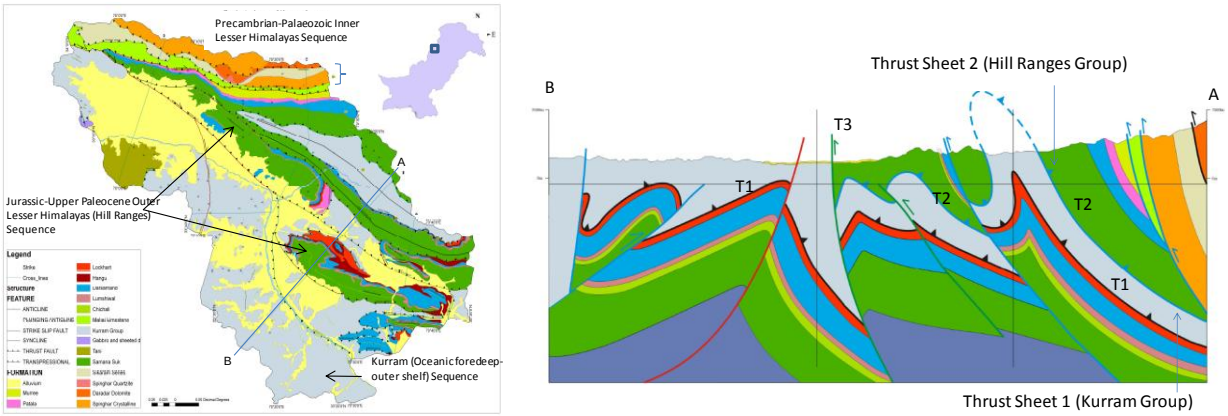

Figure 1. A) Geological sketch map of Kurram Tribal Agency, NW Pakistan, B) Cross-Section across the Samana Ranges, Kurram Agency.

References

Beck, R. A., and 17 others, 1995, Stratigraphic evidence for an early collision between northwest India and Asia, Nature, 373, 55-58.

Beck, R. A., Burbank, D. W., Sercombe, W. J., Khan, M.A., and Lawrence, R.D. 1996, Late Cretaceous ophiolite obduction and Paleocene India-Asia collision in the westernmost Himalaya, Geodinamica Acta, 9, 114-144.

Coward, M.P., Butler, R.W.H., Chambers, A.F., Graham, R.H., Izatt, C.N., Khan, M.A., Knipe, R.J., Prior, D.J., Treloar, P.J., Williams, M.P. 1988, Folding and imbrication of the Indian crust during Himalayan collision. Philosophical Transactions of the Royal Society, A, 326, 89-116.

Izatt, C.N. 1990, Variations in thrust front geometry across the Potwar Plateau and Hazara/Kalachitta Hill Ranges, northern Pakistan. PhD thesis. Imperial College, London.

Meissner, C.R., Hussain, M., Rashid, M.A. and Sethi, U.B. 1975, Geology of Parachinar Quadrangle, Pakistan. U.S Geological Survey, Professional Paper 716-F, 20.

Pivnik, D.A. and Sercombe, W.J. 1993, Compression- and transpression-related deformation in the Kohat Plateau, NW Pakistan Geological Society, London, Special Publications, 74, 559-580.

Metamorphism, melting, and exhumation of the Leo Pargil Dome, NW India

Jackie Langille[1], Micah Jessup[1], John Cottle[2], Graham Lederer[2], Talat Ahmad[3]

[1] University of Tennessee, Knoxville, TN 37996, USA, jlangill@utk.edu
[2] University of California, Santa Barbara, CA 93106, USA
[3] University of Delhi, Delhi -110007, India

The Leo Pargil Dome

The Leo Pargil dome, NW India, is a 30-km-wide, northeast-southwest striking structure composed of amphibolite-facies metamorphic rocks and leucogranites that is bound by oppositely dipping normal sense shear zones that accommodated orogen-parallel extension. The Leo Pargil shear zone defines the west flank of the dome and separates the footwall rocks of the dome from the Haimanta Group and the overlying metasedimentary rocks in the hanging wall to the west (Thiede et al., 2006; Hintersberger et al., 2010, in press).

Metamorphism and Melting

Thermobarometry and in-situ U-Th-Pb monazite geochronology of metamorphic rocks from the dome, the Leo Pargil shear zone, and the immediate hanging wall were combined with U-Th-Pb monazite geochronology of the leucogranite injection complex within the dome to evaluate the relationship between metamorphism, crustal melting, and the onset of exhumation.

These data indicate that rocks in the footwall and the hanging wall of the Leo Pargil shear zone experienced prograde Barrovian metamorphism during crustal thickening until 30 Ma. This was followed by top-down-to-the-west to northwest shearing and near-isothermal decompression of the footwall rocks during orogen-parallel extension by 23 Ma. Our leucogranite ages combined with ages from other studies (Leech, 2008; Lederer et al., 2010) suggest that leucogranite injection began at 30 Ma and continued until 18 Ma.

Tectonic Implications

Exhumation of the Leo Pargil dome may have been accommodated by protracted crustal melting beginning at 30 Ma and buoyancy-driven flow of the melted crust into the areas of extension by 23 Ma. The onset of orogen-parallel extension resulted in decompression of the Leo Pargil dome rocks. This was accompanied by further melting in the core of the dome from 23-18 Ma in response to exhumation. Bouyancy driven flow of this leucogranite melt potentially enhanced exhumation of the dome.

References

Hintersberger, E., Thiede, R. C., and Strecker, M.R., in press, The role of extension during brittle deformation within the NW Indian Himalaya, Tectonics.

Hintersberger, E., Thiede, R. C., Strecker, M. R., and Hacker, B., 2010, E-W extension in the NW Indian Himalaya, Geological Society of America Bulletin, 122, 1499-1515.

Lederer, G., Cottle, J., Jessup, M., Langille, J., and Ahmad, T., 2010, Petrochronologic constraints on partial melting in the Leo Pargil Dome, NW India, 25th Himalaya-Karakoram-Tibet Workshop, San Francisco, CA.

Leech, M. L., 2008, Does the Karakoram fault interrupt mid-crustal channel flow in the western Himalaya?, Earth and Planetary Science Letters, 276, 314-322.

Thiede, R.C., Arrowsmith, J.R., Bookhagen, B., McWilliams, M., Sobel, R., and Strecker, M., 2006, Dome formation and extension in the Tethyan Himalaya, Leo Pargil, northwest India, Geological Society of America Bulletin, 118, 635−650.

Geology of the Upper Tama Kosi/Rolwaling Valley Region, east-central Nepal

KYLE P. LARSON[1], Dawn Kellett[2], and Richard From[1]

[1] Department of Geological Sciences, University of Saskatchewan, Saskatoon, SK, Canada, kyle.larson@usask.ca
[2] Department of Earth Science, University of California, Santa Barbara, CA 93106, USA

The Tama Kosi/Rolwaling area of east-central Nepal is underlain by the exhumed mid-crustal core of the Himalaya. The uppermost portion of the Tama Kosi valley has not been mapped previously and as such this study represents an important piece in completing our basic geologic knowledge within the Himalaya. The geology of the area consists of anatectite-bearing Greater Himalayan sequence phyllitic schist, paragneiss and orthogneiss that generally increases in metamorphic grade and anatectite content up structural section. The top of the Greater Himalayan sequence in the map-area is intruded by an undeformed, pegmatitic leucogranite stock. Relationships in adjacent areas constrain the age of similar leucogranite to be older than middle Miocene (Jessup and Cottle, 2010). Preliminary U-Th-Pb geochronologic analyses indicate monazite growth in the Greater Himalayan sequence during the early and middle Miocene in kyanite and sillimanite grade rocks, and during the late Miocene in staurolite grade rocks. It is not yet known how this growth relates to the metamorphic and anatectic episodes recorded in the study area. All metamorphic rocks are pervasively deformed and commonly record top-to-the-south sense shear. In contrast to previous studies that have overlapped with portions of the present study (Ishida, 1969; Ishida and Ohta, 1973; Schelling,1992), the Main Central thrust fault is not mapped in the study-area; it is interpreted to crop-out farther to the south. The entire exhumed midcrustal package has been subject to late-stage folding during the formation of the Tama Kosi window, a structural culmination that may reflect out-of-sequence adjustment of the orogenic wedge or, alternatively, an inversion of primary basin morphology (Long et al., 2011).

References

Ishida, T., 1969, Petrography and structure of the area between the Dudh Kosi and Tamba Kosi, East Nepal: Journal of the Geological Society of Japan, 75(3), 115-125.

Ishida, T. and Ohta, Y., 1973, Ramechhap-Okhaldhunga region, *in* Hashimoto, S., Ohta, Y. et al., Geology of the Nepal Himalayas, Sapporo, Japan, Saikon Publishing Company, p.39-68.

Jessup, M. and Cottle, J., 2010, Progression from south-directed extrusion to orogen-parallel extension in the southern margin of the Tibetan plateau, Mount Everest Region, Tibet. The Journal of Geology, 118(5), 467-486.

Long, S., McQuarrie, N., Tobgay, T. and Grujic, D., 2011, Geometry and crustal shortening of the Himalayan fold-thrust belt, eastern and central Bhutan. Geological Society of America Bulletin, 123(7/8), 1427-1447.

Schelling, D., 1992, The tectonostratigraphy and structure of the Eastern Nepal Himalaya: Tectonics, 11(5), 925-943.

Discovery of the relict of the Tsangpo foreland basins in Renbu tectonic mélange and its implication for the initial collision between India and Eurasian plates

Guangwei Li [1], Zhiqin Xu [1], Xiaohan Liu[2], Xiaobing Liu [2], Lijie Wei [2]

[1] State Key Laboratory for Continental tectonics and Dynamics, Institute of Geology, Chinese Academy of Geological Sciences, Beijing 100037, China, guangweili2010@gmail.com
[2] Institute of Tibetan Plateau Research, Chinese Academy of Sciences, Beijing, 100085, China

The existence and distribution of the peripheral foreland basins in the Yarlung-Tsangpo suture zone and Gandese zone remains controversial (DeCelles et a1., 2001; Najman, 2006). Recently, Ding et al. established the foreland basin systems in the Gandese-Himalayan collisional orogen belt (Ding et al., 2005, 2009), which recorded the course of the collision between Indian and Eurasian plates. Here we report the in-situ detrital zircon U-Pb and Hf isotopic analysis of sandstone rock from a sedimentary relict (including the siliceous rock, argillite, silty sandstone and coarse sandstone, from below), paraconformably covering the ophiolite relicts in the Renbu mélange belt, Dejilin town, Renbu County. Nine detrital zircon grains out of 54 grains have ages from ~83 to ~121Ma and three grains have ages of 197±3, 203±5 and 208±5Ma. The majority of these young zircons are characterized by high $^{176}Hf/^{177}Hf$ isotopic ratios and positive Hf(T) values that are similar to magmatic zircons from the Gangdese batholith, indicating the latter has been a predominant source provenance of the sedimentary relict. It's the first time to discover the Late Cretaceous deposition in this area. It may be a part of the foreland basin systems (Tsangpo peripheral foreland basin) in the Gandese-Himalayan collisional orogen belt, which plays a significant indicator of the initial collision between India and Eurasian plates.

References

DeCelles, P.G., Robinson, D.M., Quade, J., et al., 2001, Stratigraphy, structure, and tectonic evolution of the Himalayan fold-thrust belt in western Nepa1. Tectonics, 20(4), 487- 509.

Najman, Y., 2006. The detrital record of orogenesis: A review of approaches and techniques used in the Himalayan sedimentary basin. Earth-Science Review, 74(1-2), 1-72.

Ding, L., Kapp, P., Wan X.Q., 2005, Paleocene-Eocene record of ophilite obduction and initial India-Asian collision, south central Tibet. Tectonics, 24(3): 1-18.

Ding L, Cai FL, Zhang QH, et al., 2009, Provenance and tectonic evolution of the foreland basin systems in the Gandese-Himalayan collisional orogen belt. Chinese Journal of Geology, 44, 1289-1311 (in Chinese with English abstract).

Indosinian epoch collsional orogenic belt in the Lhasa terrane, Tibet: geochronology, distribution and evolution

Li Hua-Qi, Xu Zhi-Qin, Yang Jing-Sui and Tang Zhe-Min

Institute of Geology, Chinese Academy of Geological Sciences, Beijing, 100037, China, muzi_7540@163.com

The Lhasa terrane, a huge Tectonic-magmatic belt (2500km long and 150-300km wide), locates between the Yarlung-Tsangpo and Bangong-Nujiang suture zones. The continental crust basement and Paleozoic cover of the Lhasa terrane, together with the Himalaya terrane, is generally considered as the northern margin of Gondwanaland (Yin, A. and Harrison, T. M., 2000; Xu et al., 2006). The Lhasa terrane was finally separated from the Gondwana land with the formation of Yarlung Tsangpo Neo-Tethyan ocean.

However, the discovery of eclogite belt northeast of Lhasa city shed new light in contrast to the above-mentioned general understanding of the Lhasa terrane. The petrography, chronology and geochemistry studies indicate that the protolith of the eclogites might be from the Paleo-Tethyan oceanic crust during Carboniferous-Permian periods. The metamorphic age of eclogite facies is 262±5 Ma, which indicates the existence of a new Paleo-Tethyan suture zone in the Lhasa terrane (Yang et al., 2009).

Regional structure analysis and muscovite 40Ar-39Ar dating of muscovite-quartz schist, eclogite and retrograde eclogite indicates that the closure of the Paleo-Tethyan ocean basin and the following collision of northern and southern parts of the Lhasa terrane occurred at 220-240 Ma. It was an Indosinian epoch collsional orogenesis. This Indosinian orogenesis is further confirmed by the regional sedimentary characteristics, magmatic activity and ophiolite mélange. These evidences suggest that the Indosinian orogenic belt in the Lhasa terrane is widely distributed from the Coqen county in the west, and then extends eastward through the Nanmulin county, Ningzhong and Sumdo area, finally turns around the eastern Himalayan syntaxis into the Bomi region(Figure1).

Based on the evolutionary process, the geological development of the Lhasa terrane from early Palaeozoic to early Mesozoic can be divided into seven stages: ①During Ordovician-Devonian (O-D), the Lhasa terrane should be as a part of northern margin of Gondwana land with stable carbonate platform sediments②During Early - Middle carboniferous (C1-C2), the northern Lhasa terrane should have been departed from Gondwana.An initial ocean basin was formed.③During Middle-Late carboniferous(C2-C3), the initial ocean basin might develop into a mature ocean basin. ④During Late Carboniferous-Early Permian(C3-P1), the Paleo-Tethyan ocean basin should start the subduction process. eclogite oldest single zircon age (293±13Ma) confirms this inference(Yang et al., 2009). ⑤During Late Permian -Early Triassic(P3-T1), most of oceanic crust might be subducted and a remnant ocean basin was left, with large scale eclogites formed then. ⑥During Middle-Late Triassic(T2-T3), the Paleo-Tethyan ocean basin disappeared and an Indosinian collisional orogenesis occurred at 220 -240Ma, with the eclogite exhumation at the same time. ⑦During Late Triassic -Early Jurassic(T3-J1), the Indosinian orogenesis might go to the end and then late-orogenic granitic magmatic activities occurred, forming a large scale Indosinian epoch granite belt in the Lhasa terrane, with accurate zircon ages of 217-190 Ma.

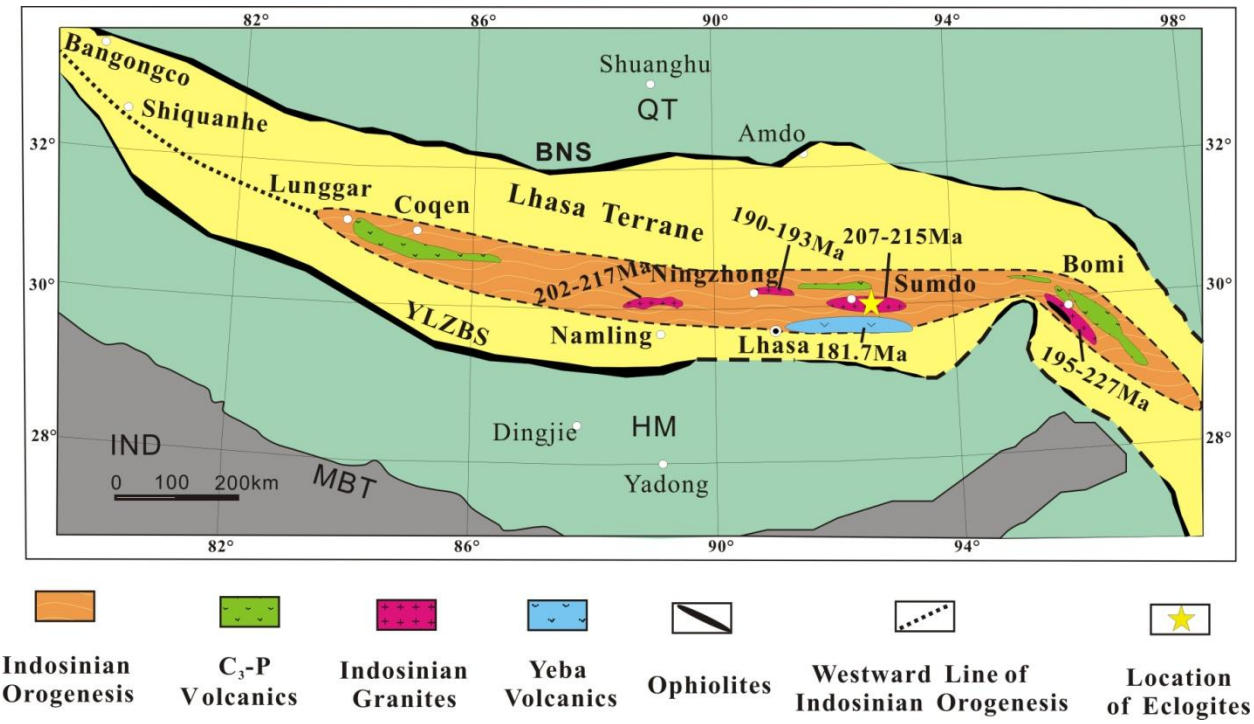

Figure1. The spatial distribution of Indosinian orogenic belt in the Lhasa terrane and the related igneous rocks of Neopaleozoic- early Mesozoic. QT- Qiangtang terrane; HM- Himalaya terrane; IND- India block; MBT- Main boundary fault; BNS- Bangong-Nujiang suture zone; YLZBS- Yarlung Tsangpo suture zone

All the above seven stages reveal a perfect evolutionary process of the Paleo- Tethys ocean between northern Lhasa terrane and southern Gondwana land. The Indosinian orogenisis is a significant event for the evolution of the Lhasa terrane as well as the Tibetan plateau.

References

Xu, Z.Q., Li, H.B. and Yang, J.S., 2006, An orogenic plateau---the collage and orogenic types of the Qinghai-Tibet plateau. Earth Science Frontiers, 13, 1-17.

Yang, J.S., Xu, Z.Q., Li, Z.L., Xu, X.Z., Li, T.F., et. al., and Robinson, P.T., 2009, Discovery of an eclogite belt in the Lhasa block, Tibet. A new border for Paleo-Tethys?, Journal of Asian Earth Sciences, 34, 76-89, doi:10.1016/j.jseaes.2008.04.001.

Yin, A. and Harrison, T. M., 2000, Geologic evolution of the Himalayan-Tibetan orogen, Annual Review of Earth and Planetary Sciences, 28, 211-280, doi:10.1146/annurev. earth.28.1.211.

The collision of India and Asia – paleomagnetic investigations on the Lhasa Block and the Tethyan Himalayan sediments

Ursina Liebke[1], Erwin Appel[1], Fabian Setzer[1], Ding Lin[2], Rouven Volkmann[1]

[1] Department of Applied Geosciences, University of Tuebingen, D-72076, Germany, ursina.liebke@uni-tuebingen.de
[2] Institute of Tibetan Plateau Research, Chinese Academy of Sciences, Beijing 100085, China

The timing of initial collision of India and Eurasia is a key issue for models of the formation of the Tibetan Plateau and the Himalayan mountain range. In spite of decades of research it is still highly debated with ages ranging from 34 Ma to about 60 Ma (e.g. Ding et al. 2003; Aitchison et al. 2007; Najman et al. 2010). To determine the collision age it is crucial to know the shape of the colliding continents prior to the collision. Paleomagnetism is the only method to directly determine the paleolatitudinal positions of the pre-collisional southern margin of Eurasia and northern margin of India. Recently several paleomagnetic investigations were carried out on the Lhasa block on the Linzizong volcanic rocks (LVR) (Chen et al. 2010; Dupont-Nivet et al. 2010; Liebke et al. 2010; Sun et al. 2010; Tan et al. 2010). Mean values for the different formations of the LVR yield paleolatitudes ranging from 6.7 to 16.8°N (summary in Najman et al. 2010). Our new paleomagnetic investigation on a dyke swarm (LD B) in the Linzhou basin confirmed this by a paleolatitude of 15.4±7.3°N. Averaging all results of recent paleomagnetic investigations on the Lhasa block yields a paleolatitude for the pre-collisional southern Eurasian margin of 12.7°N (Fig. 1) for a reference point at the suture zone (90°E/29°N).

Paleomagnetic investigations on sediments of the Tethyan Himalayas (Zongpu Fm) of Patzelt et al. (1996) in the Gamba and Duela areas revealed a paleolatitude for the pre-collisional northern margin of India of 4.7°N for about 58.5 Ma at the reference point. New results from the Dibling limestone in the Zanskar area, northern India, are very promising and yield a paleolatitude of 0.4°N for western India (34°N/76.5°E) for the deposition age of the Dibling limestone, i.e.late early Paleocene - late Paleocene (Nicora et al. 1987). These results are only preliminary and further investigations are necessary in order to test for a primary magnetization and to yield sufficient data for statistical analyses on all submembers of the Dibling limestone and thus get a better temporal resolution. In Figure 1 the paleomagnetic results for India and Eurasia are summarized. By intersection of the pre-collisional southern Eurasian and northern Indian margins a collision age of 53 Ma and 55 Ma was calculated for central and western Tibet (provided that the southern Eurasian margin has a similar paleolatitude in western Tibet than in the central part), respectively. The amount of crustal shortening can be determined by comparing the paleolatitudes from the present day shaped continents given by the apparent polar wander paths (APWPs) and the paleolatitiudes of the extended continents. The above results imply crustal shortening along the southern Eurasian margin at 90°E of about 1790 km since the collision and along the northern Indian margin of about 1290 km (Patzelt et al.1996) and 1400 km (results of Dibling limestone) (Fig. 1).

Furthermore, paleomagnetic investigations were carried out on the Tethyan Himalaya in the Tingri area in central Tibet. The results indicate a synfolding remanence with a possible remanence acquisition age between 49 Ma and 58 Ma. Thus folding of the sediments of the Tingri area started within that time span. Assuming that the folding is directly related to the India-Eurasia collision we yield a constraint for the latest possible collision age of about 49 Ma, supporting our prior results.

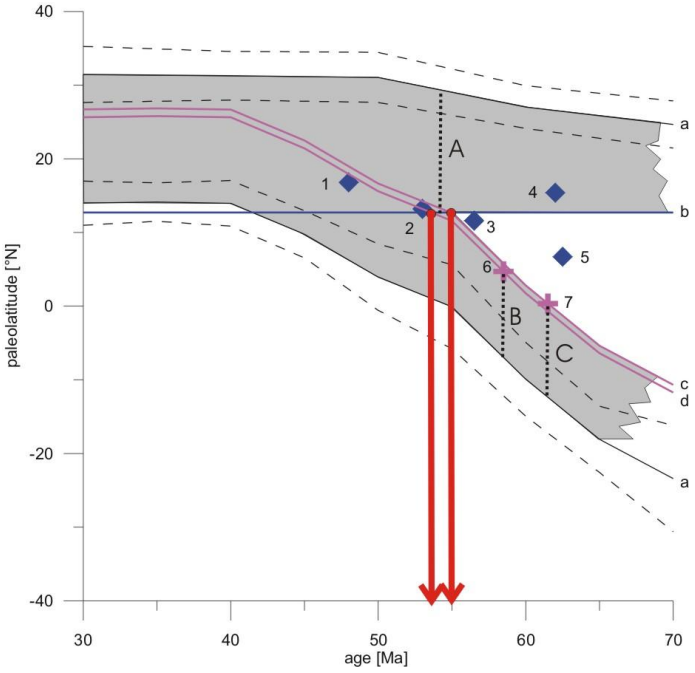

Figure 1. Results of paleomagnetic investigations on the Lhasa block and the Tethyan Himalayan sediments together with the APWPs of India and Eurasia. Diamonds show paleolatitudes for the southern Eurasian margin: 1: mean of Pana Fm, 2: dykes of Liebke et al. 2010, 3: mean Nianbo Fm, 4. LD B, 5: mean Dianzhong Fm. Crosses show paleolatitudes for the northern Indian margin: 6: Patzelt et al. 1996; 7: preliminary results of the Dibling limestone. Solid lines: a: APWPs of India and Euraisa (Besse & Courtillot 2002) with A95 errors indicated by dashed lines, b: paleolatitude of the southern Eurasian margin (mean of all diamonds), c,d: paleolatitude of northern India calculated by c: results of Dibling limestone and d: Patzelt et al. 1996. The red arrows indicate the collision age. Dotted lines illustrate the amount of crustal shortening: A: along the southern Eurasian margin, B, C: along the northern Indian margin based on results of B: Patzelt et al. 1996 and C: Dibling limestone.

References

Aitchison, J.C., Ali, J.R. and Davis, A.M., 2007, When and where did India and Asia collide?, Journal of Geophysical Research, 112, B05423, doi:10.1029/2006JB004706.

Besse, J. and Courtillot, V., 2002, Apparent and true polar wander and the geometry of the geomagnetic field over the last 200 Myr, Journal of Geophysical Research, 107**,** 2300.

Chen, J., Huang B. and Sun, L., 2010, New constraints to the onset of the India-Asia collision: Paleomagnetic reconnaissance on the Linzizong Group in the Lhasa Block, China, Tectonophysics, 489, 189–209, doi:10.1016/j.tecto.2010.04.024.

Ding, L., Kapp, P., Zhong, D.L. and Deng, W.M., 2003, Cenozoic volcanism in Tibet: Evidence for a transition from oceanic to continental subduction, Journal of Petrology, 44**,** 1833-1865.

Dupont-Nivet, G., Lippert, P.C., van Hinsbergen, D.J.J., Meijers, M.J.M. and Kapp, P., 2010, Paleolatitude and age of the Indo-Asia collision: Paleomagnetic constraints, Geophysical Journal International, 182, 1189–1198, doi:10.1111/j.1365-246X.2010.04697.x.

Liebke, U., Appel, E., Ding, L., Neumann, U., Antolin, B. and Xu, Q.A., 2010, Position of the Lhasa terrane prior to India-Asia collision derived from palaeomagnetic inclinations of 53 Ma old dykes of the Linzhou Basin: Constraints on the age of collision and postcollisional shortening within the Tibetan Plateau, Geophysical Journal International, 182,1199–1215, doi:10.1111/j.1365-246X.2010.04698.x.

Najman, Y., Appel, E., Boudagher-Fadel, M., Bown, P., Carter, A., Garzanti, E., Godin, L., Han, J., Liebke, U., Oliver, G., Parrish, R. and Vezzoli, G., 2010. Timing of India-Asia collision: Geological, biostratigraphic, and palaeomagnetic constraints, Journal of Geophysical Research, 115**,** B12416.

Nicora, A., Garzanti, E. and Fois, E., 1987, Evolition of the Tethys Himalaya continental shelf during Maastrichtian to Paleocene (Zanskar, India), Rivista Italiana di Paleotologia STratigrafia, 92, 439-496.

Patzelt, A., Li, H.M., Wang, J.D. and Appel, E., 1996, Palaeomagnetism of Cretaceous to Tertiary sediments from southern Tibet: Evidence for the extent of the northern margin of India prior to the collision with Eurasia, Tectonophysics, 259**,** 259-284.

Sun, Z., Jiang, W., Li, H.B., Pei, J.L. and Zhu, Z.M., 2010, New paleomagnetic results of Paleocene volcanic rocks from the Lhasa Block: Tectonic implications for the collision of India and Asia, Tectonophysics, doi:10.1016/j.tecto.2010.05.011.

Tan, X. D., Gilder, S., Kodama, K.P., Jiang, W., Han, Y.L., Zhang, H., Xu, H.H. and Zhou, D., 2010, New paleomagnetic results from the Lhasa Block: Revised estimation of latitudinal shortening across Tibet and implications for dating the India-Asia collision, Earth Planetary Science Letters, doi:10.1016/j.epsl.2010.03.013.

Comparing analysis of hydroclimatic changes in glacier-fed rivers between the Tibet- and Bhutan-Himalayas

Jingshi Liu[1], Zhongyan Wang[1,4], Tongliang Gong[2], Tenzey Uygen[3]

[1] Institute of Tibetan Plateau Research, Chinese Academy of Sciences, Beijing 100085, China. jsliu@itpcas.ac.cn
[2] Water Resources and Hydrology Bureau of the Tibetan Autonomous Region, Lhasa, China
[3] Bhutan College of Science and Technology, Phuentsholing, Bhutan
[4] Graduate school of Chinese Academy of Sciences, Beijing 100082, China

Both glacier and climate changes have increased the amount of water supplying the Himalayan rivers. Kurichu River in the Bhutan-Himalayas(BH) and Karuxung River in the Tibetan Himalayas(TH) were selected as representative glacier-fed watersheds with high glacier coverage of 20.8% and 14.6% and long term data of 20 years (1986–2006) respectively. The Mann-Kendall trend test and correlation analysis were employed to analyze hydrometeorological data at the gauge stations (1600 m and 4550 m) and a related meteorological stations (2600 m and 4450 m). The results indicate that there are close correlations between monthly air temperature and discharge in the studied watersheds. However the annual runoff have significant increasing trends with increasing air temperature and precipitation in TH, but decrease in BH with increasing air temperature and decreasing precipitation. Monthly runoff was the parameter most sensitive to climatic warming, especially during the autum and winter. It was concluded that far more trends were observed than were expected to be occur by chance. In the past 20 years, the mean annual air temperature has risen dramatically by 0.38°C in TH and 0.68°C in BH each decade, the latter is 0.26°C warmer than that in TH. The increasing trend in runoff rate of TH varied during different times of the year, increased by 44% from October to February in the winter flow, by 24% in the spring flow and by 27% in the summer flow, but the streamflow decreased in BH. The change in runoff is affected mostly by climatic warming from April to June in TH, whereas when the Indian Monsoon prevails in BH, the runoff is affected by both air temperature and precipitation, and the summer rainfall has unpredictable influences on the runoff. During the non-monsoon period, the change in runoff is significantly influenced by air temperature and subsurface water, and the runoff loss in BH is supplied by the increase in TH.

New advisement of tectonic model in south Tibet

Xiaohan Liu [1], Yitai Ju[2], Guangwei Li[3], Xiaobing Liu[1], Lijie Wei[4], Xuejun Zhou[1] & Xingang Zhang[5]

[1] State Laboratory for Continental collision and uplift, Institute of Tibetan Plateau Research, Chinese Academy of Sciences, Beijing, 100085 China, xhliu@mail.iggcas.ac.cn
[2] China Metallurgical Geology Bureau, Beijing 100025, China
[3] State Laboratory for Continental tectonics and Dynamics, Institute of Geology, Chinese Academy of Geological Sciences, Beijing 100037, China
[4] Institute of Geology and Geophycs, Chinese Academy of Sciences, Beijing 100029 China
[5] College of Earth Science, Graduate University of Chinese Academy of Science Beijing 100049, China

New field tectono-sedimentary investigations crossing the Yarlung Zangpo ophiolite zone show a geological features different from the subduction-collision models. A tectonic window exists within the Bailang ophiolite body. Conformable contact lies between the ophiolite deep sea sequence and country flysch layers, without shear zone in north-south orientation. Intrusion-like ophiolite bodies outcroped in Renbu, where country layers maintain sub-concordant contact to the ultramafic bodies with contact metamorphic aureole. The ophiolite zone diverges westward into branches, separated by country flysch. In the Lhasa region, sedimentary facies are similar between both north and south sides of the Zangpo Valley, recording of an intact basin system (Hsu et al., 1995; 1998; Liu et al., 2009; 2010). Li et al. (2010) reported that the north portion of Tethyan Himalaya sequence yield U–Pb detrital zircon age probability spectra and εHf values that are in stark contrast with Tethyan sequence strata of known Indian affinity. We conclude thus the Zangpo ophiolite zone has tectonic affinity of back-arc basin with its spasmodical juvenile oceanic crust. Some new petrological and geochemical studies on the ophiolite rocks reveal similar conclusions (Zheng et al., 2003; Pan and Ding, 2004; Geng et al., 2004; Bédard et al., 2009). The Zangpo back-arc basin developed due to the large amount of Neotethys oceanic crust subducted under the Himalaya-Tibet lithosphere. The collapse of this back-arc basin, with limited subduction and mélange, occurred subsequent to about the Eocene. The ophiolite of the Zangpo back-arc basin became exposed during regional uplifting and rifting in a north-south direction since Middle Miocene.

The real Indian-Asia suture, the Neotethys more likely corresponds to the High Himalayan Central Gneiss belt, supported by its strong shear system with unique vergence, protracted history (Paleocene to middle Miocene) of re-mobilized high pressure metamorphism in middle to lower crust (e.g., Baig, 1990; Ding and Zhong, 1999; Ding et al., 2001; Catlos, 2001; Kaneko et al., 2003; Leech et al., 2005; Liu et al., 2007; Zhang et al. 2008, 2010a; Cottle et al., 2009b; Xu et al. 2010), and the shear activities migrated progressively younger southward, with bulk of shear slip absorbing the Indian and south Tibet crust. Total amount of crust uplift in Himalayan gneiss belt yielded of 30-40 km, mich more than that in Zangpo back-arc basin where the Cenozoic deposits (Kailas conglomerate, Liuqu conglomerate, Linzizong volcanic layers, etc) exist well.

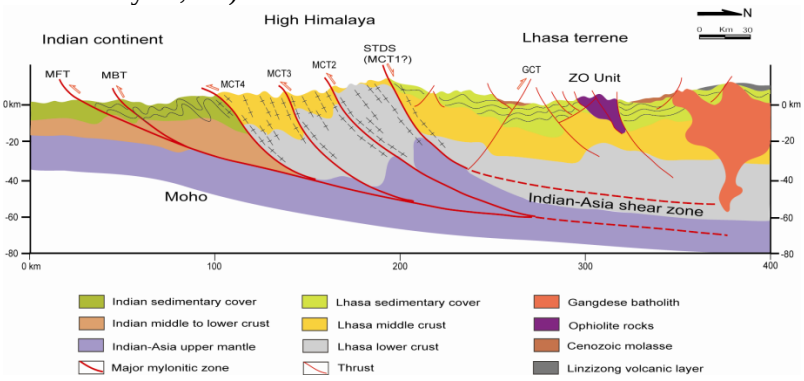

Figure 1: Tectonic model of south Tibet

The Indian sub-continent collided against the Himalayan frontal arc and underthrusted under the arc, proceeding behind the Neotethys oceanic crust at probably the location of the South Tibet Detachment System (STDS). This collision resulted in crust thickening and local uplift. The stress concentration

resulted from such continent-arc collision then migrated younger southward and produced second collision shear plane, while the gravity gradient led to the change of the STDS from a compressive thrust to extension. This process was then repeated southward, producing next mylonitic zones step by step, till to the Main Frontal Thrust. The estimation of the amount of N-S uniform slip shearing based on analysis of microstructural mechanisms on major mylonitic zones, with whole shear gneiss and pelitic shale outcropping in the High Himalaya Central Gneiss could exceed hundreds of kilometers, absorbing the Indian crust. Recent geophysical studies reveal that the main Himalayan shear system extends from a shallow depth under Nepal to the mid-crust under southern Tibet. The crust/mantle interface beneath Tibet is anisotropic, and the dipping mantle fabric suggests that the Indian mantle is subducting in a diffuse fashion along some sub-parallel structures (J. Nabelek et al., 2009). This feature supports to our tectonic model of south Tibet.

References

Baig, M.S., 1990. Structure and geochronology of pre-Himalayan and Himalayan orogenic events in the northwest Himalaya, Pakistan, with special reference to the Besham area. PhD thesis, Oregon State University, Corvallis, 300 pp.

Bédard, E., Hébert, R., Guilmette, C., Lesage, G., Wang, C.S., Dostal, J., 2009. Petrology and geochemistry of the Saga and Sangsang ophiolitic massifs, Yarlung Zangbo Suture Zone, Southern Tibet: Evidence for an arc-back-arc origin. Lithos 113, 48-67.

Catlos, E.J., Harrison, T.M., Kohn, M.J., Grove, M., Ryerson, J.J., Manning, C.E. & Upreti, B.N., 2001. Geochronologic and thermobarometric constraints on the evolution of the Main Central Thrust, central Nepal Himalaya. Journal of Geophysical Research 106, 16177-16204.

Cottle, J.M., Searle, M.P., Horstwood, M.S.A., Waters, D.J., 2009b. Timing of midcrustal metamorphism, melting, and deformation in the Mount Everest Region of southern Tibet revealed by U(-Th) -Pb geochronology. The Journal of Geology, 117, 643-664.

Ding, L. and Zhong, D.L., 1999. Metamorphic characteristics of HP granulite facies in the Namche Barwa region and its tectonic application. Science in China D, 29(5), 385-397.

Ding, L., Zhong, D., Yin, A., Kapp, P., Harrison, T.M., 2001. Cenozoic structural and metamorphic evolution of the eastern Himalayan syntaxis (Namche Barwa). Earth and Planetary Science Letters 192, 423-438.

Geng, Q.R., Pan, G.T., Zheng, L.L., 2004. Petrochemistry character and metamorphism condition of quartzite in the Yarlung Zangpo tectonic belt of Namcha Barwa region. Mineral Petrology 24(1), 76-82. (in Chinese)

Hsü, K.J., Pan, G.T., Sengör, A.M.C., 1995. Tectonic evolution of the Tibetan Plateau: A working hypothesis based on the archipelago model of orogenesis. International Geology Review 37, 473-508.

Hsü, K.J., Sun, S., Wang, Q.C., Chen, H.H., Li, J.L., 1998. Tectonic facies map of China. Science Press, Beijing, pp. 155. (in Chinese)

Kaneko, Y., Katayama, I., Yamamoto, H. et al., 2003. Timing of Himalayan ultrahigh pressure metamorphism: sinking rate and subduction angle of the Indian continental crust beneath Asia. Journal of Metamorphic Geology, 21, 589-599.

Leech, M.L., Singh, S., Jain, A.K., Klemperer, S.L., Manickavasagam, R.M., 2005. The onset of India-Asia continental collision: early, steep subduction required by the timing of UHP metamorphism in the western Himalaya. Earth and Planetary Science Letters, 234, 83-97.

Liu, X.H., Ju, Y.T., Wei L.J. & Li G.W., 2010. Re-examination of tectonic model of the Yarlung Zangpo Suture Zone. Science in China (D) 53 (1), 27-41. doi: 10.1007/s11430-0177-x.

Liu, X.H., Li, G.W., Liu, X.B., Ju, Y.T., Wei L.J. & Zhou X.J., 2009. Regional tectono-sedimentary feature of the Yarlung Zangpo suture zone. Chinese Journal of Geology 44 (4), 1312-1326. (in Chinese with English abstract)

Liu, Y. and Zhong, D., 1998. Tectonic framework of the eastern Himalayan syntaxis. Progress in Natural Science, 8, 366-370.

Liu, Y., Yang, Z., Wang, M., 2007. History of Zircon Growth in a High-Pressure Granulite within the Eastern Himalayan Syntaxis, and Tectonic Implications. International Geology Review, 49, 215-230.

Nabelek, J., Hetenyi, G., Vergne, J., Sapkota, S., Kafle, B., Jiang, M., Su, H., Chen, J., Huang, B.S. & the CLIMB Team, 2009. Underplating in the Himalaya-Tibet Collision Zone Revealed by the Hi-CLIMB Experiment. Science 325, 1371-1374.

Pan, G.T., Ding, J., 2004. Introduction of the Geological map of Tibetan Plateau and its vicinage (1/1500000). Mapping Press, Chengdu, pp. 133. (in Chinese)

Xu Wang-Chun, Hong-Fei Zhang, Randall Parrish, Nigel Harris, Liang Guo, Hong-Lin Yuan, 2010. Timing of granulite-facies metamorphism in the eastern Himalayan syntaxis and its tectonic implications. Tectonophycs, 485 (2010) 231–244.

Zhang, Z.M., Wang, J.L., Zhao, G.C., Shi, C. 2008. Geochronology and Precambrian tectonic evolution of the Namche Barwa complex from the eastern Himalayan syntaxis, Tibet. Acta Petrologica Sinica, 24, 1477-1487.

Zhang, Z.M., Zhao, G.C., Santosh, M., Wang, J.L., Dong, X. & Liu, J.G., 2010a. Two stages of granulite facies metamorphism in the eastern Himalayan syntaxis, south Tibet: petrology, zircon geochronology and implication for the subduction of Neo-Tethys and the Indian continent beneath Asia. Journal of Metamorphic Geology 28, 719-733.

Zheng, L.L., Geng, Q.R., Ou, C.S., 2003. Geochemical character of vitro-andesite in the ophiolite of the Namcha Barwa region, south-east Tibet, and its geological application. Geological Bulletin of China 22 (11-12), 908-911. (in Chinese)

Site Characterization of the Sedimentary Cover at the Himalayan Foothills using Active and Passive Seismic sources for estimation of Earthquake Hazard

A.K. Mahajan and Nitesh Rai

Wadia Institute of Himalayan Geology, 33, General Mahadeo Singh Road, DEHRA DUN. India, akmahajan@rediffmail.com

The characterization of the sediments, down to bedrock, is very important from the seismological point of view in order to study the possible earthquake effects (site effects). Shear wave velocity and the thickness of the subsoil above bed rock are the key parameters in estimating the seismic hazard of any site. Several non–invasive geophysical methods are increasingly applied for geotechnical investigations as they can identify material properties and material boundaries as well as variation in space and time of relatively large volume of soil. However, the depth of penetration using different methods always remains a matter of concern for sediments having thickness more than 100 m in frontal part of the Himalaya and Gangetic plains. The thickness of the soft sediments above bedrock in frontal part of the Himalaya varies from few meters to more than 100 m, whereas in Gangetic plain (Ganga basin) the thickness goes beyond 400-500 m. In order to deal with this problem we have used active and passive seismic sources with different field configuration to target bedrock level. Different soil investigation methods have been applied around the Himalayan foothills and Ganga foreland basin, focusing on three sites with different soil characteristics in northwest Himalaya (Fig.1). Active and passive array experiments were carried out using: Multichannel Analysis of Surface Waves (active MASW), Passive Remote MASW and F-k technique. A dispersion curve was estimated for every site covering a wider frequency band rather than if only one method would have been used. Combining the information provided from active and passive experiment using MASW has provided the information down to 150 m in Doon valley and 300 m down to Ganga basin thus reaching the bedrock level in Doon valley (Fig.2). However the use of F-k method in the same sites provided depth penetration more than 500 m thus, reaching the bedrock level in Ganga basin as well (Mahajan et al., 2011). Combining the information provided by all the methods and after applying neighbourhood algorithm, the best suitable shear (S) wave velocity profiles were estimated for each area (Fig.3). In this way, soil sediments were characterized by the resonance frequency, the soil thickness and the mean S-wave velocity. The study has demonstrated that the use of different methods give coherent and more robust results than when only one method is applied which are required for estimations of site specific seismic hazard.

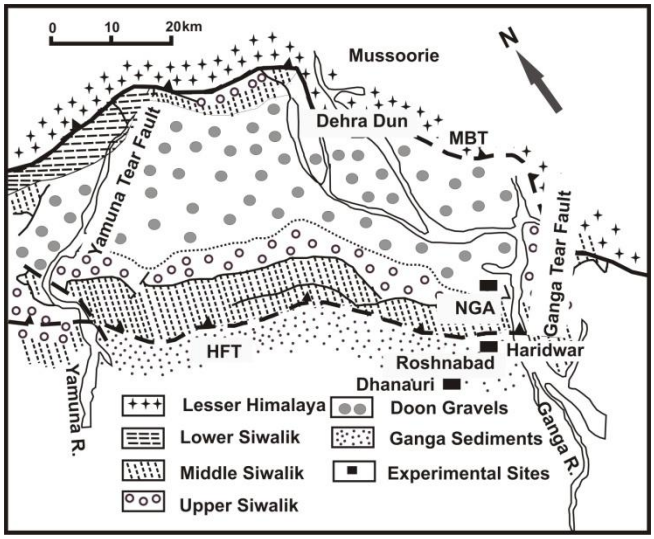

Figure 1: Location map of experimental sites in northwest Himalaya for that span from the Doon valley the site characterisation using active and passive seismic methods

Reference

Mahajan, A.K., Galiana-Merino, J.J., Lindholm C., Mundepi A.K., Rai, N. and Chuahan, N., 2011. Characterization of the sedimentary cover at the Himalayan foothills using active and passive seismic technqieus..Journal of Applied Geophysics, 73, 196-206.

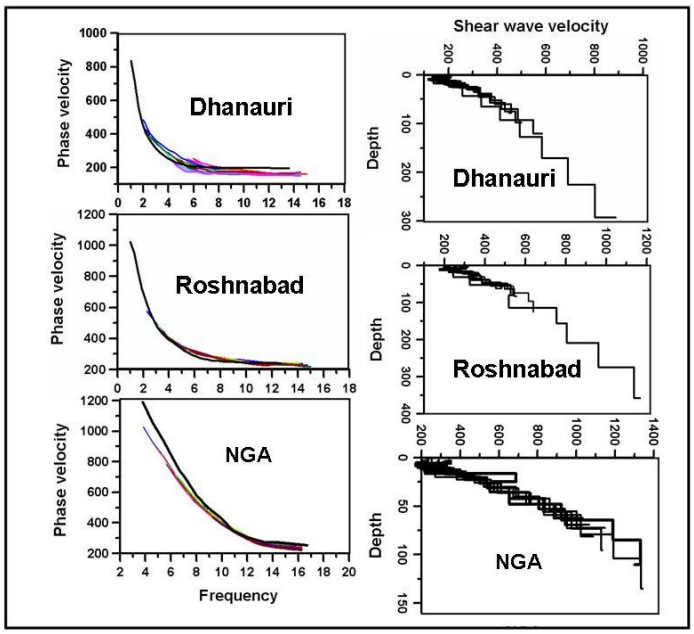

Figure 2: Dispersion curves and associated Vs profiles using different 12 offset positions in active MASW and circular array in MASW passive experiment.

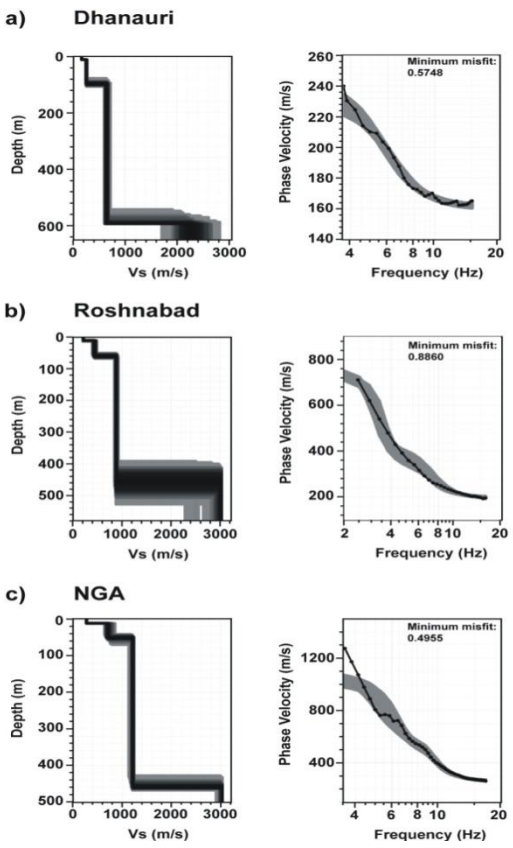

Figure 3: Vs profile and associated dispersion curves estimated for the three sites Dhanauri (a) Roshnabad (b) and NGA(c) (Modified after Mahajan et al., 2011).

Pre-Cenozoic peak metamorphism and deformation of Lesser Himalayan rocks in Nepal

Aaron J. Martin[1], Mihai N. Ducea[2]

[1] Department of Geology, University of Maryland, College Park, MD 20742, USA, martinaj@geol.umd.edu
[2] Departmnet of Geosciences, University of Arizona, Tucson, AZ 85721, USA

Several lines of evidence indicate that the stratigraphically lower part of the Lesser Himalayan series in Nepal, the Nawakot unit, reached peak metamorphic conditions prior to the Cenozoic:

(1) We used a three point Sm/Nd isochron to date crystallization of a single garnet from the Benighat Formation in the uppermost Lesser Himalayan thrust sheet exposed in the Modi river valley of central Nepal. The three points come from isotopic analyses of a whole rock powder, an unleeched garnet aliquot, and a garnet aliquot leeched in two steps with HCl. The three point isochron age is 1230 ± 180 Ma (95% confidence level, MSWD=9). The unleeched garnet analysis plots very near a two point isochron between the leeched garnet and the whole rock analyses, indicating at most minimal heterogeneity of the $^{143}Nd/^{144}Nd$ ratio at the time of garnet crystallization and/or very minor gain or loss of Sm or Nd from the analyzed rock. The dated garnet and other garnets in a thin section cut from a sample taken from the same outcrop preserve growth zoning of major elements, and garnet-ilmenite Fe-Mn exchange thermometry yields a peak temperature of 580 ± 70 °C. For the garnets in the thin section, and probably the dated garnet as well, the presence of internal foliations, their curvature inside the garnets, and their rotation relative to the external foliation indicate garnet growth during deformation. The interpretation that most consistently integrates the Sm/Nd isochron age, major element growth zoning in the garnets, microstructural evidence for garnet growth during deformation, and peak temperature estimate is that the sampled formation reached amphibolite facies conditions and was deformed at c. 1230 Ma. There is no evidence for garnet growth or temperatures near the overall metamorphic peak during the Cenozoic Era.

(2) Muscovite from the uppermost Lesser Himalayan thrust sheet commonly preserves pre-Cenozoic $^{40}Ar/^{39}Ar$ ages revealed as old age steps produced during step heating analyses (summarized by Herman et al., 2010). These old age steps nearly always reach into the Mesozoic and sometimes into the Proterozoic. The preservation of these pre-Cenozoic age steps requires that the Cenozoic maximum temperature did not exceed the closure temperature for diffusive Ar loss from muscovite. The closure temperature for white mica cooling during metamorphism in a continental fold-thrust belt currently is the subject of debate: it may be 380-430 °C (Harrison et al., 2009) or 550-600 °C (Villa, 2006). The overall peak metamorphic temperature attained by these rocks was 550-600 °C (Martin et al., 2010 and references therein). Thus if the lower closure temperature is correct, these Lesser Himalayan rocks must have attained their peak temperature prior to the Cenozoic.

(3) Monazite $^{232}Th/^{208}Pb$ ages also support the interpretation that the lower part of the Lesser Himalayan series enjoyed metamorphism in the Proterozoic. Catlos et al. (2001) analyzed two spots in one monazite crystal from structurally high Lesser Himalayan rocks that yielded latest Paleoproterozoic $^{232}Th/^{208}Pb$ ages. These authors also found a few grains in the same sample and in a nearby sample that produced Mesozoic and Paleozoic spot ages, which presumably result from mixing Proterozoic and Cenozoic generations of monazite during analysis (cf. Martin et al., 2007).

The recognition that the Benighat Formation in the uppermost Lesser Himalayan thrust sheet exposed in the Modi river valley was deformed and reached its peak metamorphic temperature during the Mesoproterozoic, not the Cenozoic, leads to three implications. First, it places a constraint on the minimum depositional age of the Benighat Formation of 1050 Ma, considering the uncertainty on the isochron age (see also Martin et al., 2011). Second, it points to a previously unrecognized orogeny that affected at least part of the northern margin of India at c. 1200 Ma. This orogeny could be related to initial amalgamation of Rodinia. And third, it indicates that tectonic models that use the conclusion that Lesser Himalayan rocks attained their peak temperatures during the Cenozoic must be revised if the Mesoproterozoic age is found to be broadly applicable to Lesser Himalayan rocks across the thrust belt.

References

Catlos, E. J., Harrison, T. M., Kohn, M. J., Grove, M., Ryerson, F. J., Manning, C. E., and Upreti, B. N., 2001, Geochronologic and thermobarometric constraints on the evolution of the Main Central Thrust, central Nepal Himalaya: Journal of Geophysical Research, v. 106, p. 16177-16204.

Harrison, T. M., Celerier, J., Aikman, A. B., Hermann, J., and Heizler, M. T., 2009, Diffusion of 40Ar in muscovite: Geochimica et Cosmochimica Acta, v. 73, p. 1039-1051, doi:10.1016/j.gca.2008.09.038.

Herman, F., Copeland, P., Avouac, J.-P., Bollinger, L., Maheo, G., Le Fort, P., Rai, S. M., Foster, D., Pecher, A., Stuwe, K., and Henry, P., 2010, Exhumation, crustal deformation, and thermal structure of the Nepal Himalaya derived from the inversion of thermochronological and thermobarometric data and modeling of the topography: Journal of Geophysical Research, v. 115, B06407, doi:10.1029/2008JB006126.

Martin, A. J., Gehrels, G. E., and DeCelles, P. G., 2007, The tectonic significance of (U,Th)/Pb ages of monazite inclusions in garnet from the Himalaya of central Nepal: Chemical Geology, v. 244, p. 1-24, doi:10.1016/j.chemgeo.2007.05.003.

Martin, A. J., Ganguly, J., and DeCelles, P. G., 2010, Metamorphism of Greater and Lesser Himalayan rocks exposed in the Modi Khola valley, central Nepal: Contributions to Mineralogy and Petrology, v. 159, p. 203-223, doi:10.1007/s00410-009-0424-3.

Martin, A. J., Burgy, K. D., Kaufman, A. J., and Gehrels, G. E., 2011, Stratigraphic and tectonic implications of field and isotopic constraints on depositional ages of Proterozoic Lesser Himalayan rocks in central Nepal: Precambrian Research, v. 185, p. 1-17, doi:10.1016/j.precamres.2010.11.003.

Villa, I. M., 2006, From nanometer to megameter: isotopes, atomic-scale processes, and continent-scale tectonic models: Lithos, v. 87, p. 155-173, doi:10.1016/j.lithos.2005.06.012.

The Main Central Thrust Zone in Western Nepal

Chiara Montomoli & Rodolfo Carosi

Dipartimento di Scienze della Terra, via S. Maria 53, 56126 Pisa, Italy, montomoli@dst.unipi.it

The Main Central Thrust covers a key role in the dynamic of the Himalayan belt and it has been traced for more than 2000 km from NE India to Pakistan and an open debate exists regarding the different criteria used to define and map it (Searle et al., 2008 and references therein).

The Main Central Thrust Zone (MCTZ) has been studied along several sections in western Nepal, Dolpo region. Here the MCTZ is represented by a thick highly-deformed zone several kilometers thick. The main fabric is a pervasive mylonitic ductile foliation overprinted by later ductile/brittle and brittle shear zones developed during the exhumation of the Greater Himalayan Sequence.
The ductile deformation developed under non-coaxial deformation in which stable porphyroclast analysis, following Passchier (1987) and Wallis (1995), points to simple shear and pure shear acting together during exhumation and to an increase in simple shear component of deformation approaching the high strain zone (Carosi et al., 2007, Larson & Godin, 2009). Shear planes strike N110-120 and moderately to steeply dip to the NE: stretching lineation trend N40-50 and plunge 50-60° to the NE. Kinematic indicators indicate a top-to-SW sense of shear.

Brittle reverse faults and n-type flanking folds (Fig.1) have been recognized overprinting the ductile mylonites. Brittle faults are associated to centimetre up to decimetre thick cataclasites and drag folds pointing to a top-to-the SW sense of shear. Foliated cataclasites are often associated to shear planes as well as Riedel shears. These brittle structures testify a later compressive reactivation of the MCT zone after the main ductile phase at upper structural levels (Mcfarlane, 1993; Harrison et al., 1997; Catlos et al., 2002; 2004).

An inverted metamorphic sequence has been recognized along the study sections.

P-T conditions have been constrained using geothermobarometers in high temperature mylonites while to constraint the P-T conditions during the ductile to brittle tectonic evolution of the MCTZ zone fluid inclusion analyses have been performed on quartz lenses from kyanite bearing gneisses and micaschists sampled from the Main Central Thrust Zone and in quartz inclusions trapped in garnet crystals.

The studied fluid inclusions, found either in isolated clusters and along trails, are two-phase (liquid water + liquid carbonic fluid) at room temperature. They usually show a constant ratio between the liquid water and the carbonic fluids and they are characterized by quite regular negative crystal shapes even if sometimes irregular morphologies have been observed. Microthermometric analyses point CO_2 homogenization temperature (Th-CO_2) ranging between 9.7 and 11.8 °C, while CO_2 melting temperature (Tm-CO_2) is always below the triple point of the pure CO_2 and varies between –58.6 and –59°C, suggesting the presence of CH_4 and/or N_2 coexisting with CO_2. Clathrate dissociation temperatures have been observed between 10.2 and 10.6°C.

The isochores for representative fluid inclusions, computed using Bakker's (1999) method, based on the adaptation of Bowers and Helgeson's (1983) equation of state, compared with the geothermobarometric data and mineral assemblages in the host rock, indicate lower pressure- temperature conditions for their trapping in accordance with the retrograde P-T evolution found in the MCT zone of Garhwal Himalaya (Sachan et al., 2001).

The study sector of the MCT zone recorded a metamorphic event at higher PT conditions up to amphibolite facies followed by a lower grade metamorphism and deformation acquired during exhumation reaching the PT conditions of 2-4 Kbar and 300-400°C at nearly 14-17 Ma determined through Ar/Ar datings on white micas and biotites recrystallized along the mylonitic foliation pointed out a cooling age for the MCTZ (Montomoli et al., in prep.; Vannay & Hodges, 1996).

The presence of reverse thrusts overprinting the mylonites of the MCT zone could also suggest that deformation after the MCT activity proceeded both toward the foreland and by out of sequence thrusts.

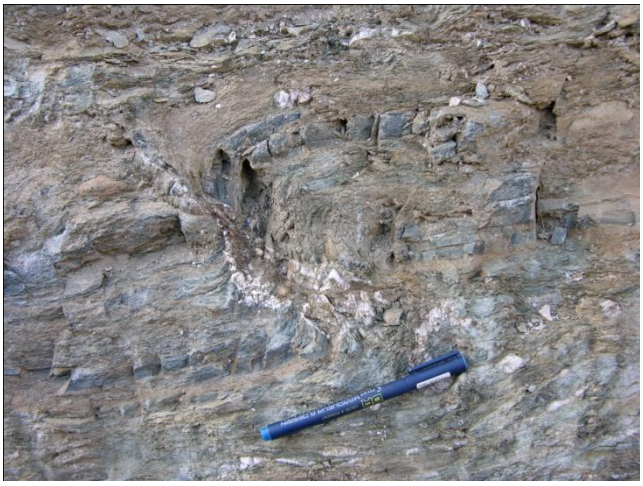

Figure 1. N-type flanking fold showing a top - to - the –SW sense of shear in phyllites of the Main Central Thrust Zone. Cross-cutting element is a quartz vein.

References

Bakker, R.J., 1999, Adaptation of the Bowers and Helgeson (1983) equation of state to the H_2O-CO_2-CH_4-N_2-NaCl system, Chem. Geol.,154, 225-236.

Bowers, T.S. and Helgeson, H.C., 1983, Calculation of the thermodynamic and geochemical consequences of non ideal mixing in the system H2O–CO2–NaCl on phase relations in geologic systems: equation of state for H2O–CO2–NaCl fluids at high pressures and temperatures, Geochim. Cosmochim. Acta, 47, 1247-1275.

Carosi, R., Montomoli, C. and Visonà, D., 2007, A structural transect in the Lower Dolpo: Insights on the tectonic evolution of Western Nepal, J. Asian Earth Sci., 29, 407–423.

Catlos E.J., Harrison, T.M., Manning, C.E., Grove, M., Rai, S.M., Hubbard, M.S. and Upreti, B.N. 2002, Records of the evolution of the Himalayan orogen from in situ Th- Pb ion microprobe dating of monazite: Eastern Nepal and western Garhwal, J. Asian Earth. Sci., 20. 459-479.

Catlos, E.J., Dubey, C.S., Harrison, T.M. and Edwards, M.A., 2004, Late Miocene movement within the Himalayan Main Central Thrust shear zone, Sikkim, north-east India, J. Metam. Geol., 22. 207-226.

Larson, K.P. and Godin, L. 2009, Kinematics of the Greater Himalayan sequence, Dhaulagiri Himal: implications for the structural framework of central Nepal, Journal of the Geological Society, London, 166, 25-43.

Macfarlane, A. M., 1993, Chronology of tectonic events in crystalline core of the Himalaya, Langtang National Park, central Nepal, Tectonics, 12/4, 1004-1025.

Passchier, C. W., 1987, Stable position of rigid objects in non-coaxial flow: study in vorticity analysis, J. Struct. Geol., 9. 679-690.

Sachan, H.K., Sharma, R., Sahai, A and Gururajan, N.S., 2001, Fluid events and exhumation history of the main central thrust zone Garhwal Himalaya (India), J. Asian Earth. Sci., 19. 207-221.

Searle, M., Law R., Godin, L., Larson, K., Streule, M., Cottle, J., Jessup, M., 2008, Defining the Himalayan Main Central Thrust in Nepal, J.Geol. Soc. London 165**,** 523-534

Vannay, J.C. & Hodges, K. 1996, Tectonometamorphic evolution of the Himalayan metamorphic core between the Annapurna and Dhaulagiri, central Nepal, J. Metam. Geol., 14. 635-656.

Wallis, R. S. 1995, Vorticity analysis and recognition of ductile extension in the Sanbagawa Belt, SW Japan, J. Struct. Geol., 17. 1077-1093,

Shedding light on the Main Central Thrust Controversy, Sikkim Himalaya

Catherine M. Mottram[1], Nigel B. W. Harris[1], Randy. R. Parrish[2], Tom W. Argles[1] and Clare J. Warren[1], Saibal Gupta[3]

[1] Department of Earth and Environmental Sciences, The Open University, Walton Hall, Milton Keynes, MK7 6AA, U.K.
c.m.mottram@open.ac.uk
[2] NERC Isotope Geosciences Laboratory, Kingsley Dunham Centre, Keyworth, Nottingham NG12 5GG, U.K.
[3] Department of Geology & Geophysics, I.I.T., Kharagpur – 721 302, India.

The Main Central Thrust (MCT) is generally defined as a major orogen-parallel thrust fault or zone which separates the Greater Himalayan Sequence (GHS) from the Lesser Himalayan Sequence (LHS), each with distinctive geochronological and chemical signatures (Parrish and Hodges, 1996). The MCT plays a pivotal role in tectonic models such as channel flow (Beaumont et al. 2001) and wedge extrusion (Kohn, 2008), but its location is in dispute in many transects (Searle et al. 2008) and poorly known in some areas. There is therefore a crucial gap in our knowledge of this thrust, especially in the east of the orogen. Sikkim presents a nearly-unique exposure of the MCT, thereby allowing an in-depth study of it in three-dimensional space (Fig. 1). As with other traverses across the Himalaya the precise location of the MCT in Sikkim remains equivocal, essentially because it has been difficult to identify structural discontinuities across a region of widespread ductile deformation (Gupta et al. 2010) and to distinguish between the lower GHS and LHS on lithological grounds.

The LHS is a Palaeoproterozoic sequence that has been intruded by ~1.8 Ga granites, whereas the GHS is a Neoproterozoic +/- Early Palaeozoic sequence, typically intruded by ~500 Ma granites (Parrish and Hodges, 1996). On the basis that these major lithological packages are now largely juxtaposed by movement on the MCT, the LHS-GHS boundary can be 'mapped' using isotope geochemical/geochronological data. In the first part of this study, we collected samples from the wide zone of ductile deformation in Sikkim broadly coinciding with the MCT.

LA-MC-ICPMS U-Pb zircon crystallisation ages were obtained from several orthogneiss and metasedimentary samples. The data indicate that the rocks from within the 'MCT zone' in Sikkim are all of LHS affinity with either crystallisation ages ~1.8Ga or detrital zircon provenance >1.7 Ga. Four samples indicate Tertiary (36-11Ma) ages of metamorphism or anatexis.

In a latter stage of the study we aim to compare P-T-t-d paths in the more clearly defined 'MCT zone', and integrate this with the tectonics to obtain a clearer understanding of the movement of the MCT.

The new data outlined in this study allows the MCT, as currently recognised in Sikkim, to be characterised as a package of rocks of Lesser Himalayan affinity that have been deformed by movement on the thrust into a zone of ductile deformation, several kilometres thick. This zone was later folded into the distinctive antiformal structure of the Teesta dome (Fig. 1).

A combination of poor exposure and a lack of consistent definition of the MCT have left the precise location and nature of the MCT in Sikkim somewhat enigmatic. This new data provide the first U-Pb zircon geochronology study of the Sikkim orthogneisses and allows confident extrapolation into Sikkim of the MCT zones from both east and west. This work will build upon other studies of the Sikkim Himalaya (Catlos et al. 2004 and Dasgupta et al. 2009) to produce a more informed understanding of the MCT.

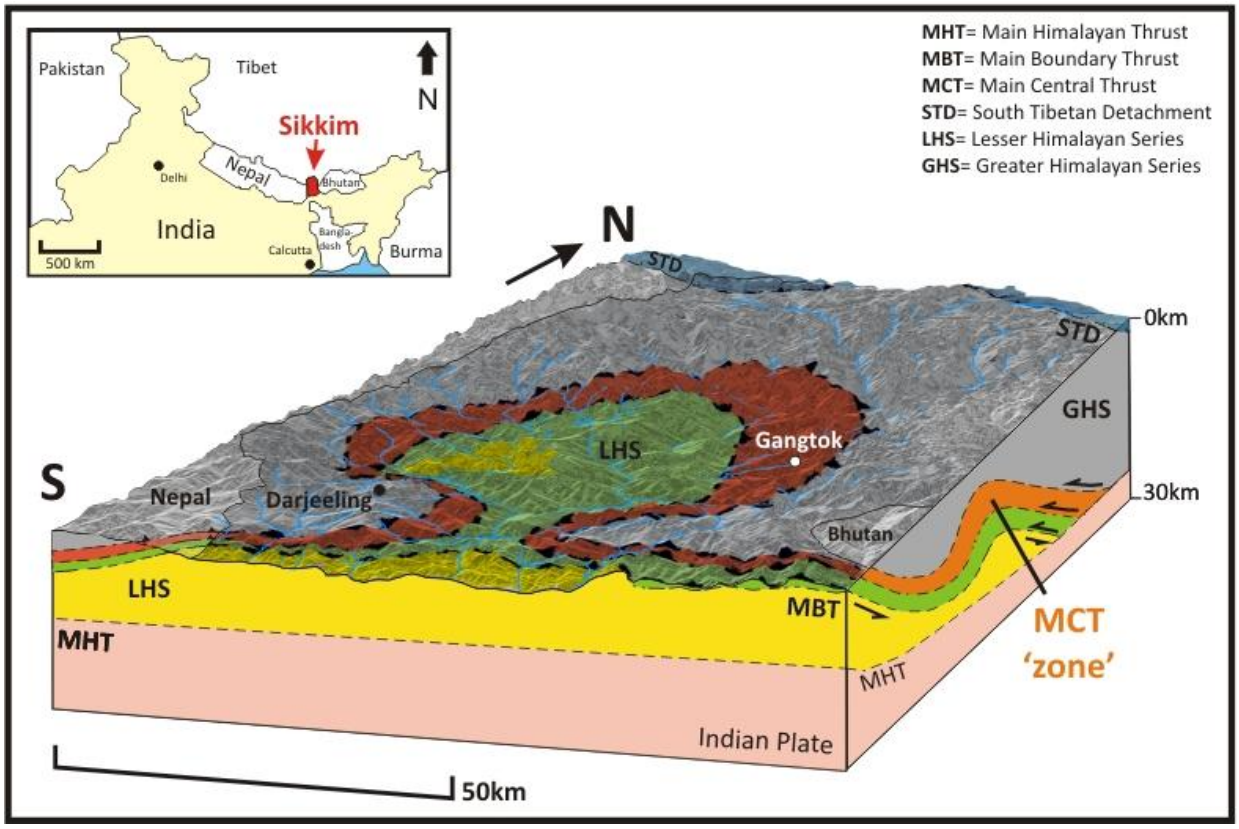

Figure 1: 3D cross section of Sikkim, NE India, with draped geological map. Geology from Goswami (2005). Schematic cross section view shows the deformation of the thrusts into the Teesta dome. Inset shows location of Sikkim.

References

Beaumont, C., Jamieson, R., Nguyen, M. and Lee,B. 2001, Himalayan tectonics explained by extrusion of a low-viscosity crustal channel coupled to focused surface denudation Nature 414, 738.

Catlos, E. J., Dubey, C. S., Harrison, T. M., and Edwards, M. A., 2004, Late Miocene movement within the Himalayan Main Central Thrust shear zone, Sikkim, north-east India, Journal of Metamorphic Geology, 22, 207.

Dasgupta, S., Chakraborty, S., and Neogi, S., 2009, Petrology of an inverted Barrovian sequence of metapelites in Sikkim Himalaya, India: constraints on the tectonics of inversion, American Journal of Science, 309, 43.

Goswami, S. 2005, Inverted metamorphism in the Sikkim-Darjeeling Himalaya: structural, metamorphic and numerical studies. Doctor of Philosophy, University of Cambridge.

Gupta, S., Das, A., Goswami, S., Modak, A., and Mondal, S., 2010, Evidence for Structural Discordance in the Inverted Metamorphic Sequence of Sikkim Himalaya: Towards Resolving the Main Central Thrust Controversy: Journal of the Geological Society of India, 75, 313.

Kohn, M. J. 2008, P-T-t data from central Nepal support critical taper and repudiate large-scale channel flow of the Greater Himalayan sequence, Geological Society of America Bulletin 120, 259.

Parrish, R.R. and Hodges, K.V. 1996, Isotopic constraints on the age and provenance of the Lesser and Greater Himalayan sequences, Nepalese Himalaya, GSA Bulletin 108, 904.

Searle, M.P., Law, R.D., Godin, L., Larson, K.P. Streule, M.J. et al. 2008, Defining the Himalayan Main Central Thrust in Nepal, Journal of the Geological Society of London 165, 523.

A strain-heating model for the seismic low-velocity zone along the Main Himalaya Thrust

Peter I. Nabelek[1] and John L. Nabelek[2]

[1] Department of Geological Sciences, University of Missouri, Columbia, MO 65211, USA, nabelekp@missouri.edu
[2] College of Oceanic and Atmospheric Sciences, Oregon State University, Corvallis, OR 97331, USA

Seismic low-velocity zone along the MHT

Recent Hi-CLIMB seismic experiment, using an 800 km long, densely spaced seismic array across Nepal and southern Tibet has revealed a low-velocity zone along the Main Himalaya Thrust (MHT; Nabelek et al, 2009). The narrow low-velocity zone extends approximately from the 28.5°N latitude, dipping to ~40 km depth at the latitude of the Yarlung Tsangpo Suture, and then continues horizontally beneath the Lhasa Block to approximately 32°N latitude. Nabelek et al. (2009) interpreted this deep low-velocity zone to be the result of increased ductility and partial melting. The narrowness of the low-velocity zone along most of the length of the MHT requires a mechanism by which the partial melting is localized. Strain heating along the ductile portion of the MHT provides such a mechanism.

Parameters of numerical models

A finite-difference model that incorporates strain-heating produces a narrow, localized partial melting zone along the MHT thrust (Fig. 1). The 600 km x 140 km model domain had 1 km grid spacing. The initial conditions were steady-state with subduction of the Indian lithosphere beneath the Himalayas and Tibet; however, topography was ignored. Temperature at the surface was held at 25°C and at the bottom of the lithosphere at 1300°C. Radiogenic heat production in the Indian crust was constant at 2 $\mu W/m^3$ in the upper 20 km and 0.7 $\mu W/m^3$ in the lower 15 km. This heat production results in surface heat flow of 70 mW/m^2 that is the average for the stable northern Indian crust. Given the preponderance of lithologies of oceanic sedimentary provenance and granites above the MHT, heat production in the upper plate was assumed to be 2 $\mu W/m^3$ throughout. Heat production in the lithospheric and convecting mantle was assumed to be 0.01 $\mu W/m^3$. In the initial steady state, the subduction of the Indian lithosphere at 3 cm/y keeps the crust above the MHT refrigerated.

The numerical calculations followed those in Nabelek et al. (2010). They accounted for temperature-dependent thermal diffusivities and rheologies of crustal materials. Thermal diffusivities (D) of crustal lithologies vary exponentially from >1.5 mm^2/s at 25 °C to as low as 0.4 mm^2/s at >600 °C (Whittington et al., 2009). The inverse correlation of D with T results in model steady-state lithospheric geotherms that are straighter in comparison with geotherms calculated with the frequently-used constant D of 1 mm^2/s. This makes heating of the crust to melting temperatures in heat flow models more challenging than most previous models would suggest. Moreover, the inverse correlation shows that hotter rocks retain their heat longer.

Volumetric strain heating due to deformation in the ductile regime is given by $A_{sh} = \tau \times \dot{e}$, where τ is the shear strength of a rock and $\dot{e}$ is the strain rate. Strain rate for a 3 km wide shear zone undergoing simple shear resulting from 3 cm/y subduction is $3 \cdot 10^{-13}$. Assuming power-law temperature dependence of τ for quartz (Rutter and Brodie, 2004), the volumetric heat production at this strain rate is ~100 $\mu W/m^3$ at 550°C and ~10 $\mu W/m^3$ at 750°C (Nabelek et al., 2010). Thus, heat production by simple shear at this tectonically driven strain rate far exceeds the heat production from reasonable concentrations of radioactive elements, and it is even higher for dry pyroxene, olivine, and feldspar.

Model results

In calculations, strain heating was assumed to occur along the length of the MHT, but only within the ductile regime of the crust, the extent of which increases as temperatures become more elevated. The depth dependence of the schist solidus is from Patiño-Douce and Harris (1998). With subduction only, shearing along the MHT produces by 20 m.y., when steady-state begins to be approached, a molten zone between 450 km and the 600 km right boundary of the model domain. A more rapid subduction, hence a larger strain rate, does not produce a significantly longer molten zone because increased strain heating is offset by increased refrigeration by the subducting plate. However, when southward thrusting of the upper

plate at 1 cm/y is introduced into the model, then a narrow, partially molten zone becomes more extended, from 310 km to the end of the model domain (Fig. 1). The partially molten zone is underlain by an inverted temperature gradient. The southward thrusting compresses isotherms near the surface from the Himalayas to southern Tibet. The compression of isotherms results in model heat flow of >100 mW/m^2 that is consistent with published values. Thus, although no provision was made in this preliminary model for topography of the India-Tibet transect and the depth of MHT is not precisely located in the model, the calculations nevertheless demonstrate the feasibility of producing the observed low-velocity, partially-molten zone along the MHT in the deep crust.

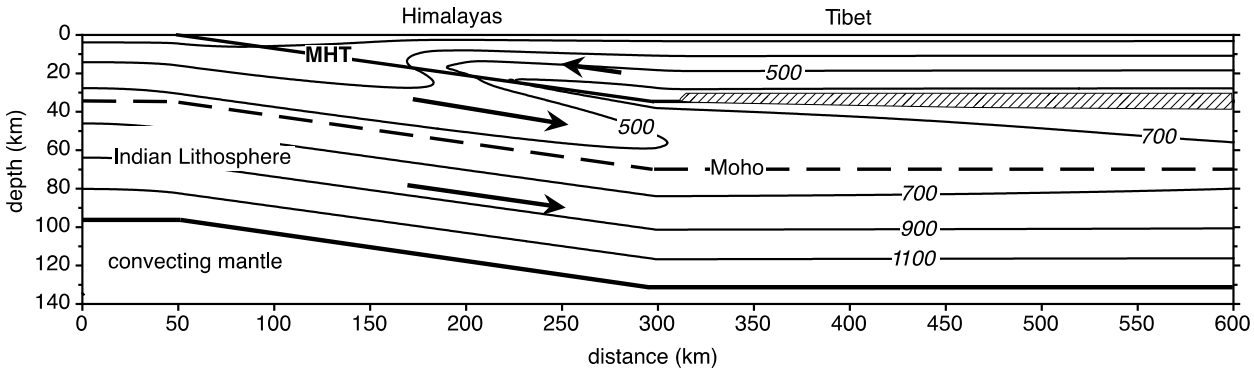

Figure 1. Model domain showing subducting Indian lithosphere beneath the Himalayas and Tibet. Below the lithosphere is convecting mantle that constraints temperature in the bottom of the lithosphere to 1300°C. Dashed line is the Moho. Isotherms in 200° intervals (italics) are shown for a model with strain heating occurring along the ductile portion of the Main Himalaya Thrust (MHT) for 20 m.y.. Striped band shows region where temperatures of the schist solidus were reached in the model.

References

Nabelek, J.L. et al., 2009, Underplating in the Himalaya-Tibet collision zone revealed by the Hi-CLIMB Experiment, Science, 325, 1371-1374.

Nabelek, P.I., Whittington, A.G., and Hofmeister, A.M., 2010, Strain heating as a mechanism for partial melting and ultrahigh temperature metamorphism in convergent orogens: Implications of temperature dependent thermal diffusivity and rheology, J. Geophys. Res., 115, B12417.

Patiño-Douce, A.E. and Harris, N., 1998, Experimental constraints on Himalayan anatexis, J. Petrol., 39, 689–710.

Rutter, E.H. and Brodie, K.H., 2004, Experimental grain size sensitive flow of hot pressed Brazilian quartz aggregates, J. Struct. Geol., 26, 2011–2023.

Whittington, A. G., Hofmeister, A.M., and Nabelek, P.I., 2009, Temperature dependent thermal diffusivity of Earth's crust and implications for magmatism, Nature, 458, 319–321.

Duration of metamorphism in the Karakoram Metamorphic Complex, North Pakistan

R.M. Palin[1], D.J. Waters[1], M.P. Searle[1], M.A. Horstwood[2] and R.R. Parrish[2]

[1] Dept. of Earth Sciences, Oxford University, Oxford, OX1 3AN, United Kingdom, richard.palin@earth.ox.ac.uk
[2] NERC Isotope Geosciences Laboratory, Kingsley Dunham Centre, Keyworth, Nottingham NG12 5GG, UK

Metamorphic modelling of zoned garnets from peraluminous metapelites from two separate regions of the Karakoram metamorphic complex, North Pakistan, has produced new insights into the P-T-t evolution of the deep crust along the Asian margin of the India-Asia collision zone. P-T pseudosections have been constructed in the MnNCKFMASHTO system using THERMOCALC v3.33 on a total of six samples to model peak metamorphic conditions, and U-Pb geochronology of metamorphic monazites has provided age constraints. Two previously unverified metamorphic events in the thermo-tectonic evolution of the Hunza Valley have been documented; an andalusite-grade metamorphic event associated with the closure of the Shyok Suture Zone (c. 105.52 Ma) before the India-Asia collision, and a kyanite-grade overprint on sillimanite-grade rocks (c. 28.22 Ma) after the collision. A kyanite-grade event observed in the Baltoro with similar peak P-T conditions has had peak metamorphism dated at c. 21.81 Ma, suggesting that metamorphism and deformation for this event may be diachronous between the two regions. However previous studies have also suggested that this kyanite-grade event commenced in the Baltoro as early as 28.0 Ma, indicating prolonged duration at peak metamorphic conditions before exhumation commenced. A calculated P-T path for this kyanite-grade event in the Baltoro indicates that primitive garnet growth occurred on an initially high geothermal gradient (~30°C) followed by a near-isothermal rapid increase in pressure. This event is thought to represent early stages of intrusion and lateral migration of the Baltoro batholith, comparable with tectonic models of magmatic over-accretion producing similar shaped P-T paths.

Peak P-T conditions and prograde P-T paths were calculated using compositionally zoned garnets. Where possible, to assess the reliability of calculated peak P-T conditions, the fractionation of major cations from the matrix during porphyroblast growth was modelled in THERMOCALC. When garnet makes a significant contribution to the rock bulk composition, results suggest that the fractionation of cations during growth affects the assemblage and individual phase proportions calculated at peak metamorphic conditions. In this example, employing fractionation resulted in more petrographically reliable assemblages and proportions, therefore it is suggested that, if possible, the use of fractionation should be employed for future work to allow more accurate modelling of chemical equilibrium in natural systems.

The thermal structure and composition of Tibetan crust and upper mantle

Keith Priestley and Dan McKenzie

Bullard Laboratories, Madingley Rise, Madingley Road, Cambridge, CB30EZ, United Kingdom, kfp10@cam.ac.uk

Surface-wave tomography studies by a number of groups shows that material with high shear-wave velocity is currently present everywhere beneath the Tibetan Plateau. A variety of other seismic observations such as regional Sn propagation and teleseismic S-wave delays support the surface-wave observations. These seismic observations suggest that most of the plateau has been underthrust by high wave-speed Indian mantle from the south and possibly, to a lesser extent, high wave-speed Asian mantle from the north.

Low shear-wave velocities in the upper mantle beneath northern Tibet have previously been noted and these, along with the recent volcanism in northern Tibet, led one of us to propose that the lithosphere beneath Tibet had delaminated as a result of a convective instability caused by shortening (Houseman, McKenzie and Molnar, 1981). However, more recent seismic observations show that these low shear-wave velocities are a relatively shallow feature (less than about 130 km) and conversion of the shear-wave velocity structure to temperature (Priestley and McKenzie, 2006) demonstrate that at deeper depths the Tibetan upper mantle is cool with respect to the surrounding mantle. Therefore, the lithosphere extends to almost 300 km depth beneath most, if not all, the plateau. Consequently, the delamination proposed by Houseman et al is wrong. Thermal modeling suggests that the low velocity sub-Moho mantle beneath central and northeast Tibet results from radioactive heating of the thickened Tibetan crust. With increasing time, this crustal radioactive heating causes a temperature inversion which heats the lower crust and uppermost mantle, thus lowering the sub-Moho shear velocity. Therefore, cold lithosphere has not been removed by delamination, and, at least in the northern part of the plateau, the mantle beneath the Moho is hotter than that at greater depths.

This unexpected behavior can be understood if the density of the lithosphere is a function of both its temperature and its composition. Mantle nodules brought to the surface by melts show that much of the continental lithosphere has been depleted by melt removal, leaving a harzburgite whose density is substantially less than that of the fertile mantle. The trace element composition of basaltic rocks from northern Tibet shows that their source rocks were harzburgites that had been enriched by a few percent of metasomatic melt. The melting must be occurring in the mantle, probably at shallow depths beneath the Moho, where the shear wave velocity is low and where the temperature is increasing because of downward conduction of heat generated by radioactive decay within the crust. The density of the harzburgitic source rock for the magmas is about 63 kilograms per cubic meter less than the density of fertile mantle. Therefore, while the Tibetan lithosphere has been thickened by shortening, it is stabilized by its lower density relative to the density of the fertile upper mantle. A similar upper mantle lithosphere is currently forming beneath the Zagros compressional belt in western Iran and trace element analysis of the volcanics within the compressional belt indicate a similar depleted and low density source for the magmas. However, gravity and GPS observations demonstrate that the Tibetan lithosphere is mobile and where it is not constrained by old, strong lithosphere, it flows and thins.

References

Houseman, G. A., D. P. McKenzie, and P. Molnar, 1981, Convective instability of a thickened boundary layer and its relevance for the thermal evolution of continental convergent belts, J. Geophys. Res., 86(B7), 6115–6132.

Priestley, K. and D. McKenzie, 2006, The thermal structure of the lithosphere from shear wave velocities, Earth and Planetary Science Letters, 244, 285-301.

Quantifying crustal flow in Tibet with magnetotelluric data

Dennis Rippe[1], Martyn Unsworth[1,2], Denghai Bai[3]

[1] Department of Physics, University of Alberta, Edmonton, AB, T6G 2E9, Canada, dennis.rippe@ualberta.ca
[2] Department of Earth and Atmospheric Sciences, University of Alberta, Edmonton, AB, T6G 2E3, Canada
[3] Institute of Geology and Geophysics, Chinese Academy of Sciences, Beijing 100029, China

The Himalaya and the Tibetan plateau have been formed by the collision of the Indian and Eurasian plates over the last 40-70 million years (see Yin and Harrison, 2000 for a general overview). A wide range of tectonic processes have been active during the development of this orogen. Many geodynamic models have been developed to explain the evolution of the Himalayan orogen and the Tibetan plateau and to define the overall mass balance required in this continent-continent collision. These include complete continental underthrusting, distributed shortening, indention tectonics and extrusion, delamination and lower crustal flow. The observed deformation may occur through a combination of these tectonic processes that cover the spectrum from brittle deformation localized on a number of major strike-slip faults defining a set of rigid blocks (Tapponnier et al., 2001) to ductile deformation of the crust and upper mantle with spatially continuous distribution over large parts of the plateau (Shen et al., 2001).

Models invoking ductile deformation through crustal flow are based on the assumption that the strength of the middle to lower crust is less than the strength of the upper crust and the underlying mantle. In this case, deformation in the weakened mid- to lower crustal layer may occur as a response to plate motion, topography-induced pressure gradients or a combination thereof. Two regions of crustal flow have been suggested to be active in Tibet. In Southern Tibet, the observation of leucogranites and high grade metamorphic rocks exposed in the High Himalaya, combined with geophysical observations of a partially molten crust (Nelson et al., 1996) led to the suggestion of a southward directed crustal flow driven by topography-induced pressure gradients and surface erosion (Beaumont et al., 2001). In Eastern Tibet, it is observed that large areas have been uplifted with little surface deformation (Royden et al., 1997). This led to the suggestion that outward crustal flow had occurred from regions of the Tibetan plateau with a thickened crust (Clark and Royden, 2000).

For crustal flow to occur, the crust must be relatively weak, such that it is susceptible to deformation by pressure gradients caused by the topography. The strength of the crust is controlled by its composition, temperature and the presence of fluid phases such as partial melt. Laboratory measurements on partially molten rocks suggest that melt fractions of 5-10 % reduce the crustal strength by one order of magnitude (Rosenberg and Handy, 2005). By relating these laboratory measurements to magnetotelluric observations, which are sensitive to the presence of partial melts, it is possible to establish a direct relationship between the electrical conductance and the flow parameters associated with flow in this weak lower crustal layer (Fig. 1; Rippe and Unsworth, 2010).

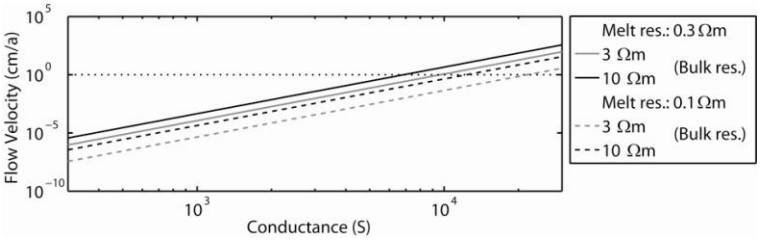

Figure 1. Topography induced flow velocity as a function of conductance for granite. Constant bulk resistivities of 3 and 10 Ωm and melt resistivities of 0.1 and 0.3 Ωm were assumed.

Magnetotelluric exploration uses variations in the naturally occurring electromagnetic fields at the Earth's surface to determine the subsurface electrical resistivity structure. Magnetotelluric data collected as part of the International Deep Profiling of Tibet and Himalaya (INDEPTH) project and the Eastern Himalayan Syntaxis 3D (EHS3D) project (Fig. 2) indicate a low-resistivity layer at mid- to lower crustal depths beneath the southern Lhasa block and the Qiangtang terrane extending from central Tibet to the eastern margin of the plateau. A joint interpretation of the magnetotelluric data with other geophysical observations suggests that the observed low-resistivity layer can be best explained by a layer of partial melting at mid- to lower crustal depths (Klemperer, 2006).

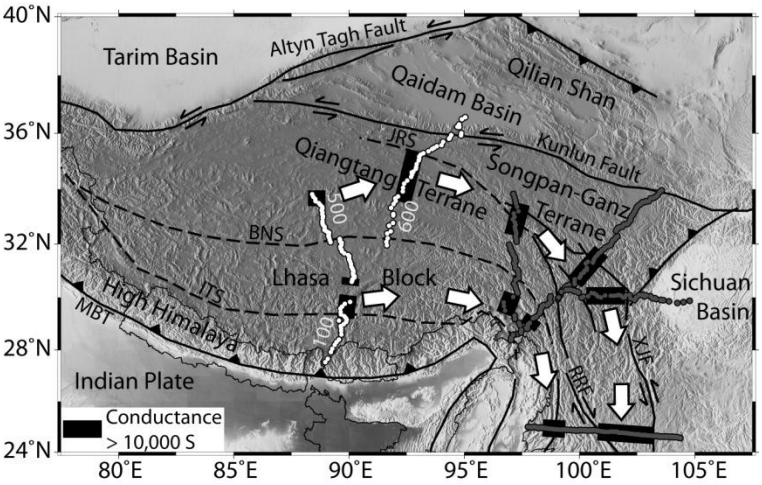

Figure 2. Topographic map of Tibet showing major tectonic features and boundaries (MBT: Main Boundary Thrust, ITS: Indus Tsangpo Suture, BNS: Banggong-Nuijang Suture, JRS: Jinsha River Suture, RRF: Red River Fault, XJF: Xiaojiang Fault, KF: Kunlun Fault). Locations of INDEPTH magnetotelluric measurements are shown as white dots. Locations of EHS3D magnetotelluric measurements are shown as grey dots. White arrows indicate suggested crustal flow pattern (after Bai et al., 2010).

Depending on the strength, the mid-to lower crustal low-resistivity layer might be weak enough for crustal flow to develop. For the Central Tibetan Plateau, if the weak lower crustal layer consists of partially molten felsic rocks, calculations show that conductances in the range 7000 - 27,000 S will produce flow velocities of the order 1 cm/a (Fig. 1, Rippe and Unsworth, 2010). Beneath the southern part of the Lhasa block and the Qiangtang terrane magnetotelluric studies indicate conductances of up to 20,000 S (Bai et al., 2010; Unsworth et al., 2005). These conductances suggest effective viscosities of $2.5 \cdot 10^{18}$ - $3 \cdot 10^{20}$ Pa s, corresponding to flow velocities between 0.02 and 4.5 cm/a (Rippe and Unsworth, 2010). Together with higher pressure gradients near the margins of the plateau, these flow parameters clearly support ductile deformation through crustal flow in these parts of Tibet.

Previous geophysical observations have not constrained the pattern of crustal flow beneath the Tibetan plateau. The magnetotelluric data suggest two flow channels with conductances exceeding 10,000 S extending horizontally over distances of 800 km from the Central Tibetan Plateau into southwestern China (Fig. 2; Bai et al., 2010). The suggested flow pattern supports the hypothesis of hydraulic uplift of large areas in Eastern Tibet caused by a topography-induced outward flow of crustal material, while revealing a more complex deformation pattern than previously suggested (Clark and Royden, 2000).

References

Bai, D. et al., 2010. Crustal deformation of the eastern Tibetan plateau revealed by magnetotelluric imaging. Nature Geoscience, 3(5), 358-362.

Beaumont, C., Jamieson, R.A., Nguyen, M.H. and Lee, B., 2001. Himalayan tectonics explained by extrusion of a low-viscosity crustal channel coupled to focused surface denudation. Nature, 414(6865), 738-42.

Clark, M.K. and Royden, L.H., 2000. Topographic ooze: Building the eastern margin of Tibet by lower crustal flow. Geology, 28(8), 703.

Klemperer, S.L., 2006. Crustal flow in Tibet: geophysical evidence for the physical state of Tibetan lithosphere, and inferred patterns of active flow. Geological Society, London, Special Publications, 268(1), 39-70.

Nelson, K.D. et al., 1996. Partially Molten Middle Crust Beneath Southern Tibet: Synthesis of Project INDEPTH Results. Science, 274(5293), 1684-1688.

Rippe, D. and Unsworth, M., 2010. Quantifying crustal flow in Tibet with magnetotelluric data. Physics of the Earth and Planetary Interiors, 179(3-4), 107-121.

Rosenberg, C.L. and Handy, M.R., 2005. Experimental deformation of partially melted granite revisited: implications for the continental crust. Journal of Metamorphic Geology, 23(1), 19-28.

Royden, L.H. et al., 1997. Surface Deformation and Lower Crustal Flow in Eastern Tibet. Science, 276(5313), 788-790.

Shen, F., Royden, L.H. and Burchfiel, B.C., 2001. Large-scale crustal deformation of the Tibetan Plateau. Journal of Geophysical Research, 106(B4), 6793-6816.

Tapponnier, P. et al., 2001. Oblique stepwise rise and growth of the Tibet plateau. Science, 294(5547), 1671-7.

Unsworth, M. et al., 2004. Crustal and upper mantle structure of northern Tibet imaged with magnetotelluric data. Journal of Geophysical Research, 109(B2), B02403.

Unsworth, M.J. et al., 2005. Crustal rheology of the Himalaya and Southern Tibet inferred from magnetotelluric data. Nature, 438(7064), 78-81.

Yin, A. and Harrison, T.M., 2000. Geologic Evolution of the Himalayan-Tibetan Orogen. Annual Review of Earth and Planetary Sciences, 28(1), 211-280.

Crustal-scale deformation history of the Longmen Shan polyphased range located at the eastern border of the Tibetan plateau

Alexandra Robert[1] , Manuel Pubellier[1] , Julia de Sigoyer[1] , Abdeltif Lahfid[2] , Pierre Lanari[3] , Jérôme Vergne[4] , Olivier Vidal[3] and Valérie Bosse[5]

[1] Laboratoire de Géologie, Ecole Normale Supérieure de Paris, 24, rue Lhomond, 75231 Paris Cedex 5, arobert@geologie.ens.fr
[2] B.R.G.M., 3 avenue Claude-Guillemin, 45060 Orléans, France
[3] ISTerre, Université Joseph Fourier, BP 53 - 38041 Grenoble Cedex 9, France
[4] E.O.S.T., 5 rue René Descartes, 67084 Strasbourg Cedex, France.
[5] Laboratoire des Magmas et Volcans, 5 rue Kessler, 63038 Clermont-Ferrand Cedex, France

The Longmen Shan range is a very peculiar margin of the Tibetan plateau because high mountains with a steep topographic gradient subsists whereas GPS measurements indicate almost no present day horizontal shortening across the range (Shen et al., 2009). Furthermore, seismological and gravimetric data also indicate that a steep 20km Moho step exists between the Tibetan crust and the Yangtze craton (Robert et al., 2010a,b). Two large crustal provinces were therefore identified in the Longmen Shan : (1) The Songpan Garze unit which is mostly composed of a thick sequence of turbiditic flysch and (2) The Yangtze affinities unit which consists in Neoproterozoic crystalline massifs, their sedimentary cover and mostly platform and continental sediments of the Sichuan Basin. Today, this margin appears as a major boundary between two contrasted crusts (figure 1) whereas original depositional environments indicate this boundary was a passive margin by Triassic times.

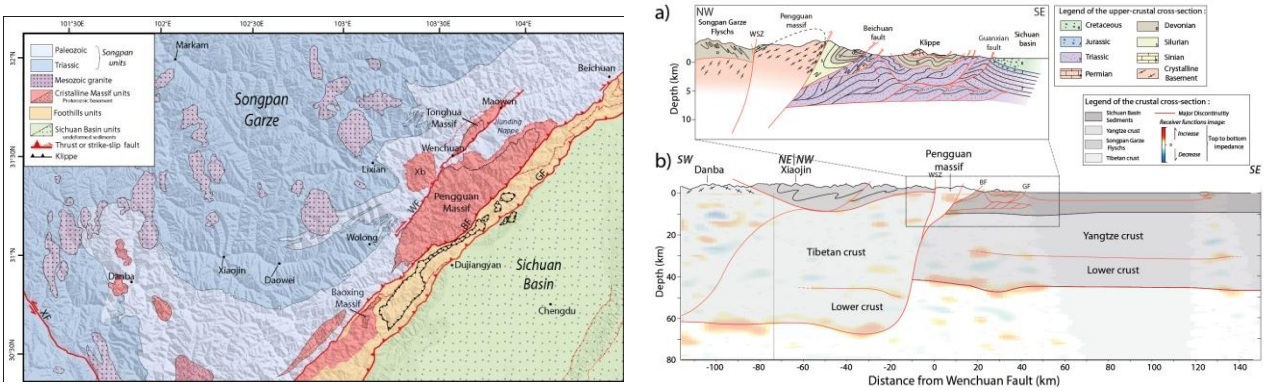

Figure 1. Left : Structural sketch of the Longmen Shan area drapped on SRTM data Right : a) Upper crustal scale cross-section of the Longmen Shan range showing the geometry of the faults structuring the range b) Schematic crustal-scale cross-section across the Longmen Shan from the Receiver functions imaging that indicate the sharp Moho offset between the 63km-thick Tibetan crust and the 45km-thick Yangtze crust. From Robert et al. (2010a).

It is commonly accepted that the tectonic history of this belt began during late Triassic with the Indosinian orogeny, which was synchronous with the collision of the North China block with the South China block (Yangtze craton), and ended with the closure of the Paleotethys (Mattauer et al., 1992). Some authors mentioned a Yanshanian deformation phase that affected the belt but the timing (Middle Jurassic to Cretaceous), and the deformations associated to this phase are not well constrained.The last tectonic phase (8-11Ma) reactivated old structures and was associated with major exhumation of the range (Godard et al., 2010).

Unfortunately, few studies quantify deformation and exhumation history of the range as a consequence of the lack of minerals indexes of metamorphism. Therefore we used especially adapted methods to study this kind of rocks as the RSCM method (Raman Spectroscopy of Carbonaceous Material) (Beyssac et al., 2002) or P-T estimates relying of the multiequilibrium between chlorites and phengites (Vidal et al., 2006 ; Lanari et al. *submitted*). In few samples, the occurrence of synchronous garnets and biotites allows the application of the biotite/garnet geothermometer and pseudo-sections calculations using Perple_X programs (Connolly, 2005).

Our results highlight three major phases of deformation that occurred in the Longmen Shan range:

1) Indosinian orogeny (Late Trias to Early Jurassic) that affects the Songpan Garze flysch is mostly characterized by nappe tectonics with a motion directed toward the South-East. This tectonics was associated with the peak of pressure and temperature (crystallization of garnet, biotites ± staurolite ± kyanite) that is recorded in sediments exhumed in the Wenchuan-Maowen shear zone and in the Danba area (zones of major exhumation). Pseudosections using Perple_X on samples in the Wenchuan-Maowen shear zone indicates pressures of 6.5kbar and temperatures of 550°C for the peak of metamorphism associated with crystallization of garnets. Furthermore, temperatures maxima of about ~500°C were recorded in most parts of the flysch. The end of the Indosinian orogeny could be associated with minor thick-skin tectonics and relatively low exhumation.
2) Late Mesozoic tectonics restricted to the Wenchuan Shear Zone and the Danba area and was associated to greenschists facies metamorphism. In the Wenchuan-Maowen shear zone, structural features indicate a sinistral transpressional event. Chorites-Phengites multiequilibrium P-T estimates point out pressures varying from ~6 to ~3kbar with temperatures of 350°C-400°C suggesting a rapid exhumation of the greenschist rocks. The in situ (LaICPMS) Th-Pb ages for monazites (including chlorite and phengite) indicate ages ranging from 90 to 70Ma.
3) Miocene to Present-day tectonics consists of a reactivation of the front of the Longmen Shan (Beichuan, Guanxian faults and triangular zone of the Sichuan Basin) due to the India-Eurasia collision and is associated with rapid exhumation localized principally on the Beichuan fault.

Indosinian orogeny was mostly characterized by thin-skin tectonics affecting a very thick sedimentary pile and relatively low exhumation was perform during this deformation phase. A late Yanshanian event (90 to 70 Ma) affected the Longmen Shan range and is characterized by a sinistral transpressional event. Our results highlight that important exhumation was performed during this deformation event in the Wenchuan Maowen shear zone. We consider that this event was a prior phase of thickening of the Tibetan crust. The last deformation phase is Miocene and correlated to the India-Eurasia collision and the formation of the Tibetan plateau. This late phase is also associated to diffuse crustal thickening of the whole Tibetan crust. The major role of the tectonic heritage in the crustal-scale geometry of the belt, which conditions the location of the major thrusts and the thickening of the Tibetan crust is pointed out by our study.

References

Beyssac O., et al., 2002, Raman spectra of carbonaceous material in metasediments: a new geothermometer, Journal of Metamorphic Geology, 20, 859-871.

Connolly, J. A. D., 2005, Computation of phase equilibria by linear programming: A tool for geodynamic modelling and its application to subduction zone decarbonation. Earth and Planetary Science Letters 236:524-541.

Godard V., et al. 2010, Late Cenozoic evolution of the central Longmen Shan (Eastern Tibet), insight from (U-Th)/He thermochronometry, Tectonics, 28.

Mattauer M., et al., 1992, La chaîne triasique du Songpan Garze (Ouest Sechuan et Est Tibet) : Une chaîne de plissement-décollement sur marge passive , C.R. Acad. Sci. Paris, 314, 619-626.

Robert A., et al., 2010a, Structural and thermal characters of the Longmen Shan (Sichuan, China), Tectonophysics, 491, 165-173.

Robert A., et al., 2010b, Crustal structures in the area of the 2008 Sichuan earthquake from seismologic and gravimetric data, Tectonophysics, 491, 205-210.

Shen Z.K., et al., 2009, Slip maxima at fault junctions and rupturing of barriers during the 2008 Wenchuan earthquake, Nature Geoscience, 2.

Vidal O., et al., 2006, P-Tdeformation-Fe3+/Fe2+ mapping at the thin section scale and comparison with XANES mapping. Application to a garnet-bearing metapelite from the Sambagawa metamorphic belt (Japan), Journal of Metamorphic Geology, 24,669-683.

Wang E.C. and Q.R. Meng, 2009, Mesozoic and Cenozoic tectonic evolution of the Longmenshan fault belt, Science in China Series D ; Earth Sciences, 52, 579-592.

Spatial and Temporal Variation in Slip Rate along the Kongur Normal Fault, Chinese Pamir

Lindsay M Schoenbohm[1], Ji Chen[2], Zhaode Yuan[2], Benjamin Kirby[3], Edward R Sobel[4], Lewis A Owen[5]

[1] Department of Chemical and Physical Sciences, University of Toronto Mississauga, Mississauga, ON L5L 1C6, Canada, lindsay.schoenbohm@utoronto.ca
[2] State Key Lab. of Earthquake Dynamics, Inst. of Geology, China Earthquake Admin., PO Box 9803, Beijing, 100029, China
[3] Anadarko Petroleum Corp., Houston, TX, 77380, USA
[4] Institute für Erd- und Umweltwissenschaften, Universität Potsdam, 14476 Potsdam, Germany
[5] Department of Geology, University of Cincinnati, Cincinnati, OH 45221, USA

Much of the interior of the Pamir Mountains experience approximately E-W extension, despite their location within the convergent western Himalayan syntaxis. Extension could reflect radial overthrusting or oroclinal bending of the Pamir, or reflect differential shortening, but the precise driver remains poorly understood. The Kongur normal fault (Fig. 1) in the Chinese Pamir has been extending since ~7-8 Ma in the north and 7-5.5 Ma in the south (Robinson et al., 2004; 2007). The Muji segment of the fault in the north strikes E-W and is dominated by right-lateral strike-slip displacement. To the south, the fault strikes NW-SE or N-S, forming excursions around the anomalously high peaks Kongur Shan (7,719 m) and Muztagh Ata (7,546 m), which sit the in footwall of the fault. These peaks are underlain by deeply exhumed rocks. Exhumation dies off rapidly to the south and is transferred via the NW-dipping Tahaman fault to the E-dipping Tashkorgan fault. The correspondence between the high peaks and large glaciers and an inferred 8-fold acceleration in exhumation rate at ~ 2 Ma (Arnaud et al., 1993), has led to the suggestion that enhanced exhumation is a response to glacial erosion in the Quaternary. However, while glacier morphology does seem to reflect exhumation rate, lithology and erosion along the Gez River appear more closely linked with the degree of unroofing and formation of the high peaks than does glacial erosion (Schoenbohm et al., in review). Additionally, thermochronologic modelling (Robinson et al., 2004; 2010) suggest constant cooling since ~7-8 Ma. To better understand the nature of extension in the Pamir and to test models for climate-tectonic coupling in the footwall of the fault, both short- and long-tem slip rate along the Kongur normal fault need to be defined.

Exhumation along a dipping fault and advection of isotherms makes determination of long term displacement rate from cooling data problematic. Thermo-kinematic modelling has only been completed along a transect through the footwall where the Gez River crosses the range; the study demonstrates that slip along the fault has been steady at ~6.5 mm/yr since 7 Ma (Robinson et al., 2010). Assuming a 40° west-dipping fault this indicates a vertical displacement rate of 4.2 mm/yr (Fig. 2) an E-W extension rate of 5.0 mm/yr and (Fig. 1), nearly identical to the GPS-determined rate of 5.1 ± 0.8 mm/yr (Yang et al., 2008; Zubovich et al., 2010). $^{40}Ar/^{39}Ar$ biotite and muscovite, and zircon (U-Th)/He data show a similar pattern, with the youngest ages near the center of the fault (Fig. 2). These data suggest a consistent pattern of maximum vertical and horizontal displacement rates in the center of the Kongur detachment.

To define short-term rates, offset fluvial terraces and moraines were mapped and dated using ^{10}Be terrestrial cosmogenic nuclides (TCN). Mapping was conducted using real time kinematic GPS. Terraces were dated by collecting a series of samples from 2-m deep pits along the terrace edges and analyzing the samples for ^{10}Be TCN concentration. For moraine dating, 5 samples were collected from the surface of large, partially-embedded boulders. Samples were processed following standard methods and analyzed at the PRIME Lab facility. We modelled TCN concentration using a Monte Carlo method developed by Hidy et al. (2010). Along the dominantly strike-slip Muji segment of the fault, we dated two terraces (9.9 $^{+1.8}_{-1.2}$ ka and 3.3 $^{+0.6}_{-0.6}$ ka) and two moraines (30.8 ± 5.8 ka and 12.3 ± 2.7 ka). The inner riser between the lower and upper terrace, which is offset 37.6 m, has been preserved at least since the abandonment of the lower terrace, and therefore indicates a dextral slip rate of 11.4 mm/yr ± 2.1. The younger moraine is offset 169 m across the fault, indicating dextral slip at 13.7 mm/yr ± 3.0, the same within uncertainty, suggesting an average rate of ~12.6 mm/yr (Fig. 1). This is slightly faster than the 8.1 ± 0.9 mm/yr suggested by GPS data (Yang et al., 2008; Zubovich et al., 2010). Along the northern section of the dip-slip part of the Kongur detachment fault, a terrace offset 20 m vertically was dated at 6.6 $^{+1.0}_{-1.0}$ ka. This suggests a vertical offset rate of 3.0 ± 0.5 mm/yr and an E-W extension rate (assuming a 20° west-dipping

fault because of the oblique extension direction) of 8.3 ± 1.4 mm/yr. This rate is similar to but still slightly higher than the GPS derived rate of 7.5 ± 0.8 mm/yr (Yang et al., 2008; Zubovich et al., 2010). Additional antithetic faults within the hanging wall valley accommodate further extension, and could make up the difference in horizontal extension between the two sites.

Holocene slip rate along the Kongur normal fault is similar to the modern GPS rates, but considerably faster than the long-term slip rate as indicated by thermochronologic data. One explanation may be that the study captures a particularly active period of the earthquake cycle, and our rates are thus not representative. However, an intriguing possibility is that slip rate has recently increased, implying accelerated E-W extension. It is unclear however, what could have driven such acceleration. Further, extension rates are faster in the north, despite the greater exhumation of the central part of the fault.

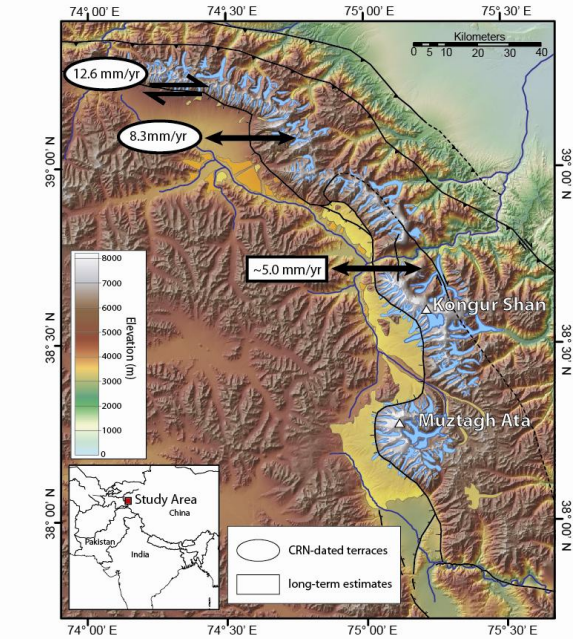

Figure 1. Map (SRTM DEM base) of study region showing E-W horizontal extension along the Kongur normal fault.

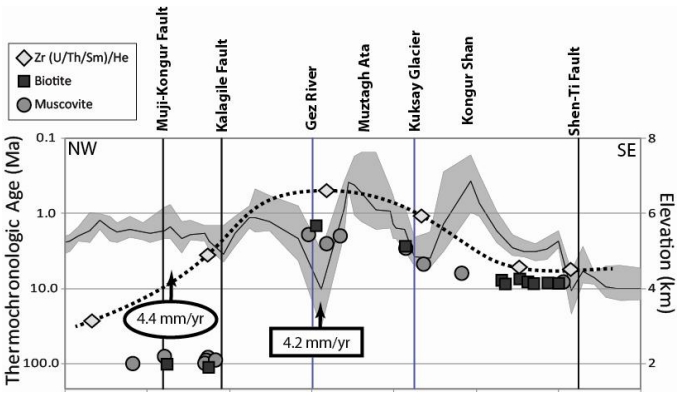

Figure 2. Data from NW to SE along Kongur normal fault. Thermochronologic data from Robinson et al., 2004; 2007 and Schoenbohm et al., in review. Dashed line connects zircon (U-Th)/He data in order to schematically depict maximum cooling rate near center of fault system. grey region with center line shows max, min and mean topography. Symbols for vertical exhumation rate same as for Figure 1.

References

Arnaud, N.O., M. Brunel, J.M. Cantagrel, and P. Tapponnier (1993), High cooling and denudation rates at Kongur Shan, eastern Pamir (Xinjiang, China) revealed by $^{40}Ar/^{39}Ar$ alkali feldspar thermochronology, *Tectonics, 12,* 1335-1346.

Hidy, A.J., J.C. Gosse, J.L. Pederson, J.P. Mattern and R.C. Finkel (2010), A geologically constrained Monte Carlo approach to modeling exposure ages from profiles of cosmogenic nuclides: an example from Lees Ferry, AZ: *Geochemistry, Geophysics and Geosystems*, v. 11, doi: 10.1029/2010GC003084.

Robinson, A.C., A. Yin, C.E. Manning, T.M. Harrison, Zhang S., Wang X (2004), Tectonic evolution of the northeastern Pamir: Constraints from the northern portion of the Cenozoic Kongur Shan extensional system, western China, *Geological Society of America Bulletin, 116,* 953-973.

Robinson, A.C., A. Yin, C.E. Manning, T.M. Harrison, Zhang S. and Wang X. (2007), Cenozoic evolution of the eastern Pamir: Implications for strain-accommodation mechanisms at the western end of the Himalayan-Tibetan orogen, *Geological Society of America Bulletin, 119,* 882-896.

Robinson, A.C., A. Yin, and O.M. Lovera (in press), The role of footwall deformation and denudation in controlling cooling age patterns of detachment systems: An application to the Kongur Shan extensional system in the Eastern Pamir, China, *Tectonophysics,* doi: 10.1016/j.tecto.1020.10.003.

Sobel, E.R., Schoenbohm, L., Chen, J., Thiede, R., Stockli, D., Sudo, M., and Strecker, M.R., 2011, Late Miocene - Pliocene deceleration of dextral slip between Pamir and Tarim: Implications for Pamir orogenesis: Earth and Planetary Science Letters, v. 304, p. 369-378.

Yang S, Li J, Wang Q., 2008, The deformation pattern and fault rate in the Tianshan Mountains inferred from GPS observation: Science in China Series D: Earth Science, v. 51, p. 1064-1080.

Zubovich A V, Wang X Q, Scherba Y G *et al*., 2010, GPS velocity field of the Tien Shan and surrouding region: Tectonics, v. 29, doi: 10.1029/2010TC002772.

Crustal-Lithospheric structure, geological evolution and continental extrusion of Tibet

Michael P. Searle[1], John Elliott[1], Richard Phillips[2] and Sun-Ling Chung[3]

[1] Department of Earth Sciences, Oxford University, South Parks Road, Oxford, OX1 3AN, UK, mikes@earth.ox.ac.uk
[2] Institute of Geophysics and Tectonics, Leeds University, Leeds, UK.
[3] Department of Geosciences, National Taiwan University, Taipei 10699, Taiwan.

Crustal shortening and thickening to ~70-85 km in the Tibetan Plateau occurred both before and mainly after the ~50 Ma India-Asia collision. Potassic-ultrapotassic shoshonitic and adakitic lavas erupted across the Qiangtang (~50-29 Ma) and Lhasa blocks (~30-10 Ma) indicate a hot mantle, thick crust and eclogitic root during that period. The progressive northward underthrusting of cold, Indian mantle lithosphere since collision shut off the source in the Lhasa block at ~10 Ma. Late Miocene-Pleistocene shoshonitic volcanics in North Tibet require hot mantle. We review the major tectonic processes proposed for Tibet including 'rigid-block', continuum and crustal flow as well as the geological history of the major strike-slip faults. We examine controversies concerning the cumulative geological offsets and the discrepancies between geological, Quaternary and geodetic slip rates. Low present-day slip rates measured from GPS and InSAR along the Karakoram and Altyn Tagh faults in addition to slow long-term geological rates can only account for limited eastward extrusion of Tibet since Mid-Miocene time. We conclude that despite being prominent geomorphic features sometimes with wide mylonite zones, the faults cut earlier formed metamorphic and igneous rocks and show limited offsets. Concentrated strain at the surface is dissipated deeper into wide ductile shear zones.

Constraing pre-Himalayan fabric by SHRIMP U-Pb zircon dating

Sandeep Singh[1], Arvind K. Jain[1] and Mark E. Barley[2]

[1] Department of Earth Sciences, Indian Institute of Technology Roorkee, Roorkee – 247 667, INDIA, san662005@gmail.com
[2] The School of Earth and Geographical Sciences, University of Western Australia, 35 Stirling Highway, Crawley 6009, Western Australia, Australia

The Himalayan Orogen is a result of continent-continent collision no later than 57 Ma. The collision tectonics has remobilized the Archean to Proterozoic continental lithosphere in a thick NE-dipping ductile slab-like folded Himalayan Metamorphic Belt (HMB). The Himalayan Metamorphic belt (HMB) forms nappes of regional dimension in the frontal parts within the Lesser Himalaya and the Higher Himalayan Crystallines (HHC) in the inner part within the Higher Himalaya. The Higher Himalayan Crystalllines (HHC) are thrust southward over the Lesser Himalayan Proterozoic sedimentary zone, along the Main Central Thrust (MCT) and associated splays like Jutogh/ Munsiari/ Vaikrita Thrust. The southern part of this belt is thrust southward and exposed as metamorphic klippe within the Lesser Himalaya and is known as the Salkhala Nappe in Kashmir having Paleo-Mesozoic sedimentary cover, the Chamba Nappe and Chail Nappe in Himachal, the Garhwal Nappe including the Banali-Satengal-Lansdown klippe in Garhwal, the Almora- Dudatoli Nappe in Garhwal- Kumaon, and also incorporating the Ramgarh Nappe and Askote- Baijnath- Nandprayag Klippe. The HHC forms the hanging wall of the Main Central Thrust (MCT) and incorporates pelitic, psammitic and quartzite sequences together with thin amphibolite and calc-silicate bands along with granitoids of various ages. It forms the remobilized basement, which is extensively deformed and metamorphosed under middle greenschist to almandine-amphibolite facies due to collisional tectonics and uplifted to the highest elevation in the Himalaya.

Evidence of the pre-Himalayan fabric and associated metamorphism have been inferred from contact relations of 2.0 to 0.50 Ga granitic plutons and revealed extensive involvement of the middle Proterozoic basement in the central Himalayan collision zone. Although several contributors point to such an event, but there is no general agreement regarding the existence of a pre-Himalayan metamorphism. Field investigations within the HHC indicate the pre-Himalayan metamorphism and include the metamorphic banding/ layering having earliest F_1 folds, where tiny mica flakes trend uniformly across their hinges and parallel the lithological layering on their limbs. S_1 foliation has been preserved in the hinge zones of the rootless F_2 folds indicating intense transportation of the earlier structures. Crystallization of minerals such as quartz, muscovite, chlorite, biotite, feldspar, occurred during the development of F_1 folds and are preferably oriented along the axial plane foliation S_1 and, therefore, are related to the D_1 deformation. Presence of this mineral assemblage along the F_1 folds indicates greenschist-facies pre-Himalayan metamorphism. The inherited garnet ages from the Higher Himalayan Crystallines (HHC) have also been corelated to the pre-Himalayan orogeny (Alakhnanda valley: 534±24 Ma; NW Himalaya: 467±3 Ma; Central Nepal: 445±16 Ma; Namche migmatites: 548±17 Ma; Barun Gneiss: 436±8 Ma).

The observation made by us in the Mandi area of Himachal Himalaya indicates contact relationship of the Jutogh Group metamorphism with Mandi Granite. The relationship can be observed along the Mandi-Kulu road section along its eastern margin along the river bank (about 50 m below the road) where the Beas River change its course from NNW to WSW between village Karg and Badanun. The field evidences indicate a sheared contact of Mandi Granite with the Jutogh metamorphic marked by very sharp boundary, where psammites are intensely sheared. The granite contact trends parallel to the older lithological banding having a foliation S_1, which has undergone ductile shearing along S_2 foliation. At this locality both Mandi Granite and the Jutogh Group metamorphic are characterised by a common shear foliation, which is the most prevalent planar fabric of HMB and have been generated as a result of Himalayan collisional tectonics. This shear fabric transforms the older S_1 fabric of Jutogh metamorphic into well defined NW-SE trending planar fabric. This S_1 fabric is lacking in the Mandi granite and from the field evidences it appears that the Mandi Granite is intruded along this foliation plane. Therefore, the dating of Mandi Granite will constrain the age of the pre-Himalayan S_1 fabric. Keeping this in mind the dating of the Mandi Granite has been attempted to constrain the pre-Himalayan fabric by SHRIMP U-Pb technique. One coarse grained undeformed samples were subjected to standard mineral separation to

extract zircons. Cathodoluminescence (CL) imaging of zircons show oscillatory growth and sector zoning of primary magmatic zircons. Sixteen (16) near-concordant analyses on zircon grains on the core and rim of grains gave a mean $^{206}Pb/^{238}U$ age of 469±8 Ma, which is the best constrained age of this body so far.

Field relationship and SHRIMP U-Pb dating of Mandi Granite has revealed that distinct intrusive granite pluton was emplaced within the Himalayan Metamorphic Belt (HMB). Such similar granitic plutons are known to exist, however, their intrusive relationships such as apophyses and xenoliths and structures along the contacts have not been explored so far. However, the contact relationship of the well-exposed contact of Mandi Granite has clearly demonstrated presence of pre-Himalayan deformation fabric, which is atleast 469±8 Ma old.

Using U-Pb and Lu-Hf Isotopes in Zircon to Constrain the Tectonic Provenance of the Himalayan Metamorphic Core, Garhwal Region, India

Christopher J. Spencer, Ron A. Harris, Carl W. Hoiland

Department of Geological Sciences, Brigham Young University, Provo, UT 84602, USA, chrisspencer@byu.edu

We report the U-Pb and Lu-Hf isotopes in zircon from the highly metamorphosed core of the Himalaya in the Garhwal Region of India: the ortho- and paragneiss units of the Greater Himalayan Sequence (oGHS and pGHS, respectively) and the Lesser Himalayan Crystalline Sequence (LHCS). Our data confirm the geochemical distinction of the older LHCS and the younger GHS. Zircons from the Paleoproterozoic metasediments of the LHCS (n=92) yield U-Pb crystallization ages from 1614±14 Ma to 2679±14 Ma with a single distinct peak at 1870 Ma. εHf values from zircon in the LHCS (n=24) range from 1 to -8. Zircons from the Neoproterozoic metasediments of the pGHS (n=146) yield U-Pb crystallization ages from 481±10 Ma to 2560±8 Ma with a single distinct peak at 860 Ma. εHf values from zircon in the metasediments of the pGHS (n=43) range from 13 to -21. Zircons from the oGHS (n=139) yield U-Pb crystallization ages from 416±2 Ma to 2740±2 Ma with a single distinct peak at 472 Ma. These zircons often exhibited older inherited cores ranging from ~800 Ma to ~2740 Ma with Cambro-Ordovician rims (416 Ma to 510 Ma). εHf values from zircon in the oGHS (n=22) have two distinct modes: the inherited zircon cores have similar values to the ~860 Ma zircons from the pGHS (13 to -21), while the ~480 Ma rims range from -7 to -11.

Assuming the deposition of the pGHS was synchronous across the northern margin of India circa 800-480 Ma (Myrow et al., 2010) we compare our U-Pb data from the Garhwal region together with a compiled dataset of U-Pb ages from the literature to the pGHS in Nepal and Bhutan (data compiled from Gehrels et al., in review; McQuarrie et al., 2008; Long et al., 2010). The detrital zircon U-Pb age spectra from the pGHS in various parts of the range show significant variation, which indicates varying provenance for the various regions of deposition (Figure 1).

To further characterise the potential source regions from which the metasediments were initially derived we compare the U-Pb and Lu-Hf data from the Garhwal region to various Gondwana crustal terranes (Figure 2) using the Gondwana reconstructions of Myrow et al. (2010) and Torsvik and Cocks (2009). Using the compiled U-Pb and Lu-Hf data, the εHf values of the LHCS overlap entirely with those of the Aravalli shield of India (Kaur et al., 2011) and partially with those of the Yilgarn Craton of Australia (Griffin et al., 2004). The most juvenile εHf values of the pGHS overlap with the Arabian Nubian Shield (ANS) in Israel (Morag et al., 2011); however, the ANS in Israel is associated with island arc volcanism with little crustal contamination at ~800 Ma, while the detritus from the pGHS have an arc signature with significant crustal contamination ~860 Ma. Other older and younger Gondwana sources (older: Albany Fraser, Eastern Ghats, Prince Charles Mountains; younger: Delamerian, Ross, Kuunga, and East African orogenies) have similar Hf isotopic signatures but do not have overlapping ages (Griffin et al., 2004; Flowerdew et al., 2007; Veevers et al., 2009; Dhuime et al., 2011; Glen et al., 2011; Kirkland et al., 2011). The oGHS have εHf values indicative of a crustal melt sourced from the pGHS. The average $^{176}Hf/^{177}Hf$ evolution trend of the most juvenile and evolved zircons in the pGHS produce match those of the oGHS. Furthermore, the inherited cores of the oGHS zircons have the same U-Pb and Hf values as the pGHS. These evidences indicate the pGHS was a likely source for the oGHS. Low U/Th ratios (<10), magmatic zoning, and euhedral zircons also support an igneous (rather than detrital) source. While the nature of this Cambro-Ordovician igneous event is still poorly understood, it is clear that the Hf isotopes can provide further insight into the petrogenesis of the magmatic rocks associated therewith.

Further Lu-Hf isotopic work is needed both in the detrital rocks as well as the potential source regions to better characterise the source regions and tectonic provenance of the lithotectonic units that make up the Himalayan mountains.

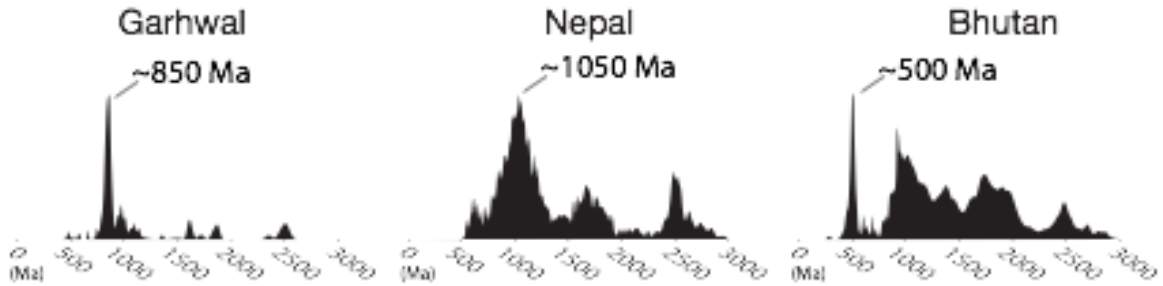

Figure 1. Normalized probability plots for the Greater Himalayan Sequence from the Garhwal region of India, Nepal, and Bhutan (data compiled from Gehrels et al., in review; McQuarrie et al., 2008; Long et al., 2010).

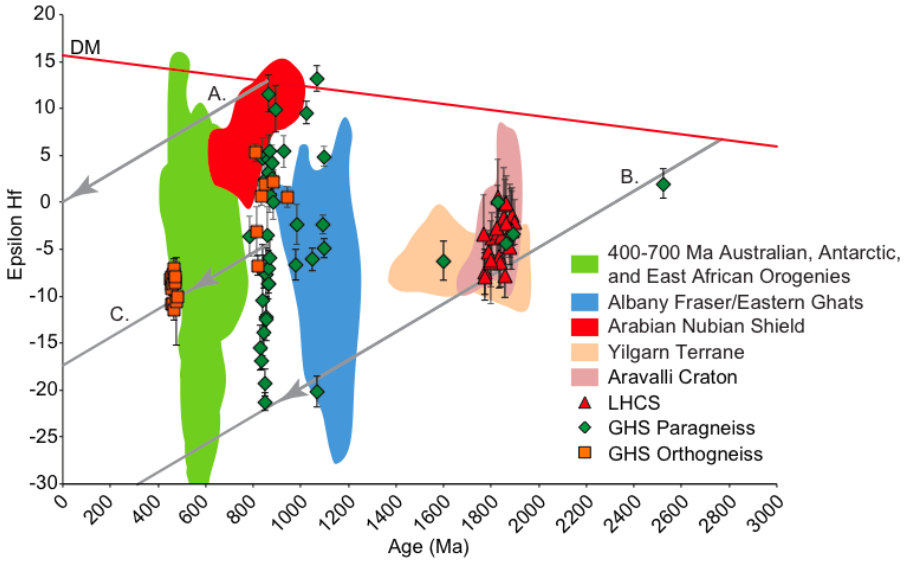

Figure 2. Plots of epsilon Hf vs age for the metamorphic core of the Himalaya and various potential source regions (see text for references). Line A represents the Lu-Hf decay path of the most juvenile zircons from the pGHS; line B represents the decay path of the most evolved pGHS zircons, and line C is the average of paths A and B, which represents a probable decay path of the oGHS.

References

Condie, K.C., Beyer, E., Belousova, E., Griffin, W.L., O'Reilly, S.Y., 2005, U–Pb isotopic ages and Hf isotopic composition of single zircons: The search for juvenile Precambrian continental crust, PC Res, 139, 42-100.

Dhuime, B., Hawkesworth, C.J., Storey, C.D., Cawood, P., 2011, From sediments to their source rocks: Hf and Nd isotopes in recent river sediments, Geology, 39, 407-410.

Flowerdew, M.J., Millar, I.L., Curtis, M.L., Vaughan, A.P.M., Horstwood, M.S.A., Whitehouse, M.J., Fanning, C.M., 2007, Combined U-Pb geochronology and Hf isotope geochemistry of detrital zircons from early Paleozoic sedimentary rocks, Ellsworth-Whitmore Mountains block, Antarctica, GSA Bulletin, 119, 275-288.

Glen, R.A., Saeed, A., Quinn, C.D., Griffin, W.L., 2011, U–Pb and Hf isotope data from zircons in the Macquarie Arc, Lachlan Orogen: Implications for arc evolution and Ordovician palaeogeography along part of the east Gondwana margin, Gondwana Research, 19, 670-685.

Griffin, W.L., Belousova, E.A., Shee, S.R, Pearson, N.J., O'Reilly, S.Y., 2004, Archean crustal evolution in the northern Yilgarn Craton: U–Pb and Hf-isotope evidence from detrital zircons, PC Res, 131, 231-282.

Kaur, P., Zeh, A., Chaudhri, N., Gerdes, A., Okrucsh, M., 2011, Archaean to Palaeoproterozoic crustal evolution of the Aravalli mountain range, NW India, and its hinterland: The U–Pb and Hf isotope record of detrital zircon, PC Res, 187, 155-164.

Kirkland, C.L., Spaggiari, C.V., Pawley, M.J., Wingate, M.T.D., Smithies, R.H., Howard, H.M., Tyler, I.M., Belousova, E.A., Poujol, M., 2011, On the edge: U–Pb, Lu–Hf, and Sm–Nd data suggests reworking of the Yilgarn craton margin during formation of the Albany-Fraser Orogen, PC Res, in press.

Long, S., McQuarrie, N., 2010, Placing limits on channel flow: Insights from the Bhutan Himalaya, EPSL, 290, 375-390.

McQuarrie, N., Robinson, D., Long, S., Tobgay, T., Grujic, D., Gehrels, G., Ducea, M., 2008, Preliminary stratigraphic and structural architecture of Bhutan: Implications for along strike architecture of the Himalayan system, EPSL, 272, 105-117.

Myrow, P.M., Hughes, N.C., Goodge, J.W., Fanning, C.M., Williams, I.S., Peng, S., Bhargava, O.N., Parcha, S.K., Pogue, K.R., 2010, Extraordinary transport and mixing of sediment across Himalayan central Gondwana during the Cambrian–Ordovician, GSA Bull, 122, 1660-1670.

Torsvik T.H. and Cocks, L.R.M., 2009, The Lower Palaeozoic palaeogeographical evolution of the northeastern and eastern peri-Gondwanan margin from Turkey to New Zealand, in: Bassett, M.G. (ed.), Early Palaeozoic Peri-Gondwana Terranes: New Insights from Tectonics and Biogeography. Geological Society, London, Special Publications, 325, 3-21.

Veevers, J.J., Saeed, A., 2009, Permian–Jurassic Mahanadi and Pranhita–Godavari Rifts of Gondwana India: Provenance from regional paleoslope and U–Pb/Hf analysis of detrital zircons, Gondwana Research, 16, 633-654.

River systems in Himalaya: looking into the past through the luminescence dating technique

Pradeep Srivastava[1], Yogesh Ray[1], Y.P. Sundriyal[2]

[1] Wadia Institute of Himalayan Geology, 33, GMS Road, Dehradun 248001, Pradeep@wihg.res.in
[2] Department of Geology, H.N.B. Garhwal University, Srinagar (Garhwal)- 246174.

Himalaya, the expression of continent-continent collision and related thrust tectonics, shows highest continental relief, experiences a significant E-W rainfall gradient and variations in surface processes. In an active orogen of such a kind, mass distribution, erosion, intensity of rainfall and their interaction decides upon its large-scale morphotectonic evolution. The river systems that drain through such neotectonically active thrusts bear potential to unravel the past climatic as well tectonic evolutionary history of Himalaya. Fluvial terraces are often used to decipher controlling factors like varying climate and tectonic pulses and time scales of river aggradation and incision in such a tectonically active setting. The researches suggest that the valley scale aggradations may represent the climatic impact while the fluvial incision into the bedrock equals the long-term uplift rate and thus the local rise of the incision rate can be interpreted as an effect of vertical motion along the active tectonic discontinuities and/or increased hydraulic efficiency.

Fluvial systems in the Himalaya are studied for their terrace configurations in terms of bedrock bench and overlying alluvial cover. Depending on the ratio of the thickness of alluvial cover and underlying bedrock, three different kinds of terrace configurations are identified: (1) Cut-fill terraces with thick alluvial cover over the thin bedrock bench; (2) terraces with almost equal thickness of alluvial cover and bedrock bench; and (3) terraces with thicker bedrock bench and thinner alluvial cover. An initiative with such a background combining field investigations and chronological studies on the geomorphological and sedimentological archives of major Himalayan river valleys of (i) Spiti (Arid-Trans-Himalaya, rainfall ~100 mm/a; Phartiyal et al., 2009), (ii) Mandakini, Alaknanda, Bhagirathi (NW Lesser Himalaya, rainfall ~1200 mm/a Ray and Srivastava, 2010), (iv) Nayar valley (monsoon dominated Garhwal Lesser Himalaya), (iii) Marsyandi (Humid, Central Himalaya, Nepal, rainfall 2000 mm/a, Pratt et al., 2004), (iv) Teesta (Eastern Himalaya, Sikkim, Rainfall ~2500 mm/a, Mukul et al., 2007) (v) Kameng and Brahmaputra (NE Himalaya, rainfall ~3000 mm/a; Srivastava et al., 2009; Srivastava and Misra, 2008) indicated that:

1. In the wetter part of the Himalaya, the Alaknanda-Bhagirathi valley experienced two-phased deglaciation from ~63-18 ka, supplied pulses of higher sediment loads and massive valley aggradation in NW Himalayan. The ~40 luminescence ages representing aggradation cluster 50-25 ka and 18-11 ka. The ten dated landslides in the same valley suggested no possible correlation to climate change and thus it is inferred that the rivers in the humidor part of the Himalaya in general follow glacial-periglacial hypothesis of valley developments.
2. The Spiti River, in the drier NW Himalaya, showed deviation nad aggraded till ~6 ka and the published records of palaeolandslide chronology in this region suggests that the valley aggradation was largely controlled by climate controlled phases of excessive landslides.
3. The rivers in NE Himalaya exhibit several phases of incision that are synchronous to aggradation in west. The higher precipitation in the region probably kept sediment-water ratio below a threshold of aggradation. This point towards relatively high erosional stress and associated deformation in the NE Himalaya.
4. Bedrock incision rates, as calculated from dated alluvial covers of strath surfaces indicated the values that are spatially variable and fall in the range of rates reported from across the Himalaya. These estimated rates however are higher than the basin average erosion rates calculated using isotopic mass balance in the riverbed sediments.

References

Mukul, M., Jaiswal, M.K., Singhvi, A.K., 2007, Timing of recent out-of-sequence deformation in the frontal Himalayan wedge: insights from Darjiling sub-Himalaya, India. Geology, 35, 999-1002.

Phartiyal, B., Sharma, A., Srivastava, P., Ray, Y., 2009, Chronology of relict lake deposits in the Spiti River, NW Trans Himalaya: Implications to Late Pleistocene-Holocene climate-tectonic perturbations. Geomorphology, 108, 268-272.

Pratt. S.B., Burbank, D.W., Heimsath, A., Ojha, T., 2004, Landscape disequilibrium on 1000-10,000 year scales Marsyandi River, Nepal, central Himalaya. Geomorphology, 58, 223-241.

Ray, Y., Srivastava, P., 2010, Widespread aggradation in the mountainous catchment of the Alaknanda-Ganga River System: Timescales and implications to Hinterland-foreland relationships. Quaternary Science Reviews, 29**,** 2238-2260.

Srivastava, P., Bhakuni, S.S., Luirei, K., Misra, D.K., 2009, Morpho-sedimentary records at the Brahmaputra River exit, NE Himalaya: climate-tectonic interplay during Late Pleistocene-Holocene. Journal of Quaternary Science, 24, 175-188.

Srivastava, P., Shukla, U.K., 2009, Quaternary Evolution of the Ganga River System: New Quartz Ages and a review of Luminescence Chronology. Himalayan Geology, 30, 85-94

Srivastava, P., Tripathi, J.K., Islam, R., Jaiswal, M.K., 2008, Fashion and phases of Late Pleistocene aggradation and incision in Alaknanda River, western Himalaya, India. Quaternary Research, 70, 68-80.

Srivastava, P., Misra, D.K., 2008, Morpho-sedimentary records of active tectonics at the Kameng river exit, NE Himalaya. Geomorphology, 96**,** 187-198.

Tectonothermal evolution of the Greater Himalayan Series, Sutlej Valley, NW India

Donald W. Stahr, III, Richard D. Law

Department of Geosciences, Virginia Tech, Blacksburg, VA 24061, USA, dstahr@vt.edu

The metamorphic core of the Himalayan orogen comprises medium- to high-grade rocks of the Greater Himalayan Series (GHS). GHS rocks in the Sutlej Valley, NW India, are exposed in an ~16 km thick panel, bounded below by the Main Central thrust (MCT) and above by the Sangla Detachment, a local strand of the South Tibetan Detachment system (STDS) of normal faults. Unlike other exposures of the GHS where pressure at peak temperature increases up structural section, in the Sutlej Valley the GHS displays a nearly isobaric inverted metamorphic temperature gradient. Here peak metamorphic temperatures range from ~610 ºC at the level of the MCT to ~750 ºC at the level of the STDS. Peak temperatures were all attained at ~7–9 kbar (cf. Vannay et al., 1999). To date a single *P–T* path has been extracted from a migmatite at high structural levels that indicated a period of nearly isobaric heating to ~750 ºC that was followed by cooling during decompression (Vannay et al., 1998). This path generally differs from others obtained at similar structural levels where a period of isothermal decompression is inferred to immediately follow attainment of peak temperature.

In this contribution we present new microstructural and petrologic data combined with thermodynamic modelling from the lowest structural levels of the GHS in the Sutlej Valley (within ~1200 m of the MCT). These rocks preserve a remarkably complete record of the microstructural and thermobaric evolution of the GHS and bear directly on the tectonothermal history of rocks incorporated into the MCT zone during mylonitization.

The earliest deformation event recognized in the Sutlej GHS at the level of the MCT is recorded by straight to sigmoidal (S1) inclusion trails of quartz + ilmenite in the cores of large garnet porphyroblasts. S1 is often observed at high angles to the matrix foliation (S2), and is truncated at inclusion-poor garnet rims. Thermodynamic modelling indicates these garnets began growing at ~500 ºC and 5 kbar. Where inclusions are preserved at the interface of garnet cores and rims they are invariably at high angles to S1. This textural relationship indicates either: i) a hiatus in garnet growth along the prograde path while the matrix fabric was reorganized; or ii) minor garnet resorption along the prograde path, or possibly a combination of both. The interpretation of a hiatus during garnet growth is supported by a sharp chemical discontinuity between garnet core and rim compositions. The abruptness of the observed chemical 'unconformity' indicates that this hiatus was relatively short-lived since diffusional relaxation of fast-diffusing major elements (e.g., Mn) was limited.

Microstructures observed in pelitic rocks collected at ~1000 m up structural section reveal a similar microstructural evolution. These rocks reached higher peak temperatures (~675 ºC and 8.4 kbar), and thus do not allow retrieval of conditions at the garnet-in reaction, but a clockwise *P–T* loop is inferred based on microstructures and thermodynamic modelling. The *P–T* paths of both rocks selected for thermodynamic modelling overlap on the cooling path at ~ 600 ºC and 7 kbar suggesting that rocks within ~1000 m of the MCT were coupled soon after the structurally lowest rocks attained peak metamorphic conditions. We also infer that exhumation of rocks at this structural level was rapid due to the preservation of pristine primary growth zoning even though peak temperatures >600 ºC were attained. Preservation of such a detailed record of punctuated porphyroblast growth and microstructural evolution is rare along the length of the Himalaya. These new data support an interpretation whereby the locus of mylonitization in the MCT zone propagated southward into progressively cooler crustal material. Rocks progressively incorporated into the deforming MCT zone were continually juxtaposed against hotter rocks in the hanging wall. As the MCT propagated southward, rocks in the hanging wall were cooled and rapidly exhumed toward the synorogenic topographic surface.

References

Vannay. J.-C., and Grasemann, B., 1998, Inverted metamorphism in the High Himalaya of Himachal Pradesh (NW India): phase equilibria versus thermobarometry, Schweiz. Mineral. Petrogr. Mitt., 78, 107-132.

Vannay, J.-C., Sharp, Z.D., and Graseman, B., 1999, Himalayan inverted metamorphism constrained by oxygen isotope thermometry, Contributions to Mineralogy and Petrology, 137, 90-101.

Titanite geochronology from the mid to lower crust of the Pamir plateau, eastern Tajikistan.

Michael A. Stearns, Bradley H. Hacker, Andrew Kylander-Clark

Department of Earth Sciences, University of California Santa Barbara, Santa Barbara, CA 93106, U.S., mstearns@umail.ucsb.edu

The Pamir plateau contains large exposures of the mid–lower crust, depths not widely exposed in the Tibetan plateau. Determining the spatial and temporal patterns of crustal thickening across the Pamir plateau is critical for understanding how orogenic plateaux are constructed. The dome cores consist of upper amphibolite grade para- and orthogneisses and schists, with the characteristic peak mineral assemblage of kyanite + biotite + garnet ± muscovite in pelites. Thermobarometry indicates peak conditions of 600–750°C and 6–10 kbar, representing exhumation depths of 20–40 km (McGraw et al., in review). U-Pb ages of titanite from orthogneisses from the Pamir domes were determined to investigate the timing of thickening of the mid to lower crust. The closure temperature of titanite (~650–700 °C) makes it an especially useful geochronometer for dating high-grade metamorphism. Ages were obtained using laser ablation inductively coupled plasma mass spectrometry (LA-ICP-MS) following the acquisition of backscattered electron maps to characterize grain zoning and guide LA-ICP-MS spot placement. Ages range from 40 to 10 Ma and define two populations of ~40–32 Ma and ~19–10 Ma. The older ages are restricted to the central Pamir and the youngest ages come from the southern Pamir. We provisionally interpret the oldest ages to indicate titanite growth during burial and the youngest to reflect closure during exhumation. This spatial pattern suggests is consistent with a general pattern of northward plateau propagation and southward-propagating exhumation. These results do not support plateau propagation via westward lower-crustal flow from the topographically higher Tibetan plateau.

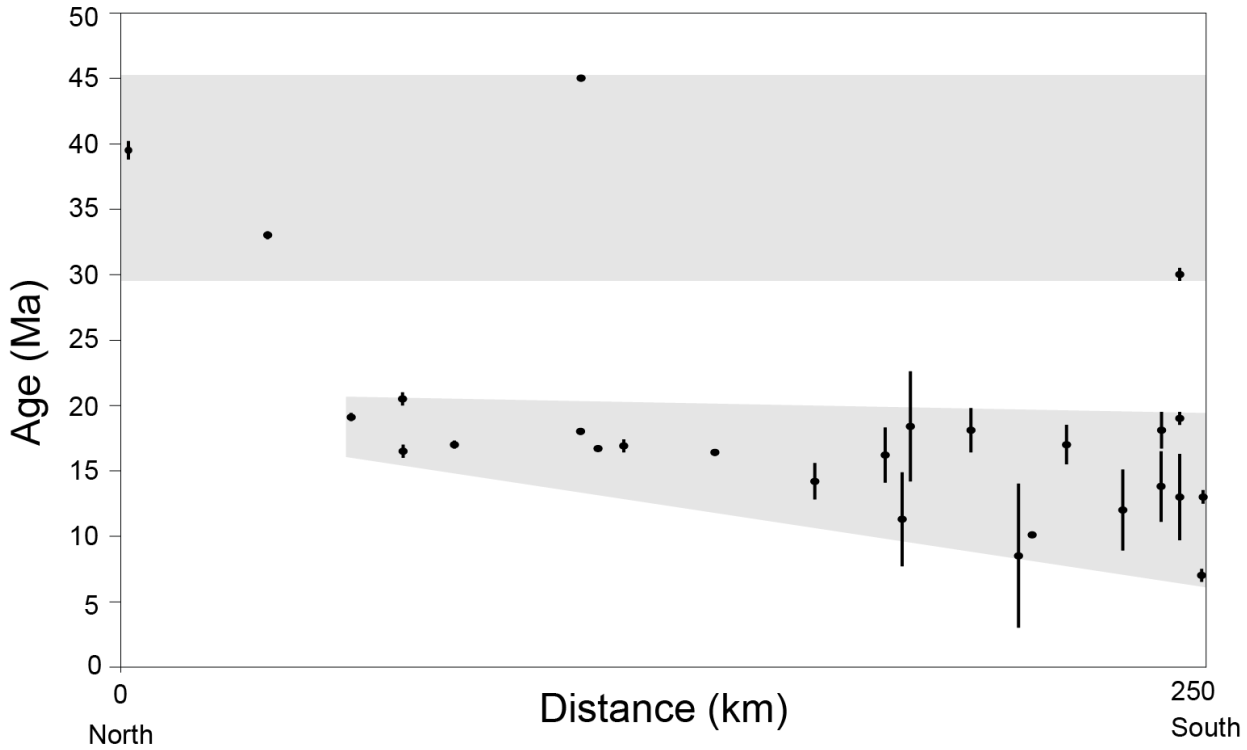

Figure 1. U-Pb titanite ages arranged from north to south on an orogen perpendicular transect. Error bars are 2σ uncertainties. The shaded regions represent interpreted populations of older crystallization ages and younger cooling ages.

References

McGraw, J., Hacker, B.R., Ratschbacher, L., Stuebner, K., Welse, C., Gloaguen, R., Gadoev, M. Oimahmadoc, I., and Minaev, V., 2011, Cenozoic deep crust exposed in the Pamir Collision Zone: Geology, in press.

Himachal Himalaya: shallowest and oldest exposure of the orogenic metamorphic core

Konstanze Stübner[1], Djordje Grujic[2], Keno Lünsdorf[1], Randall Parrish[3], and Talat Ahmad[4]

[1] Geowissenscaftliches Zentrum, Georg-August Universität Göttingen, Germany, konstanze.stuebner@geo.uni-goettingen.de
[2] Department of Earth Science, Dalhousie University, Halifax, Canada
[3] NERC Isotope Geosciences Laboratory, Keyworth, Nottingham, UK
[4] Department of Geology, University of Delhi, Delhi, India

An intriguing feature of the Himalayas is the apparent continuity of the major tectonic units and tectonic contacts along the entire strike of the mountain range from the eastern to the western syntaxes. Shallower levels of the orogen's metamorphic core are, however, exposed in the western compared to the central and eastern part. These different levels of exposure reflect the evolution of the Himalayas and provide an opportunity to investigate the interactions between the main structures of the orogen in space and time, and thus to study some of the fundamental mechanisms of mountain building.

In Himachal Pradesh, northwest India, the Main Central thrust (MCT) separates the low-grade rocks of the Lesser Himalayan sequence (LHS) from greenschist to amhibolite-grade metamorphic rocks of the Haimanta unit. The Haimanta has been interpreted as part of the Greater Himalayan crystalline (GHC; e.g. Steck, 2003, Searle et al., 2007). However, other authors correlate the Haimanta with the Tethyan Himalayan sequence (e.g., Thakur, 1998, Webb et al., 2007) and propose that the GHC in northwest India is limited to a narrow band around the Kishtwar and Kulu-Rampur tectonic windows. Related to this controversy are the questions of: (1) How does the South Tibetan detachment (STD) continues west of the Sutlej valley?, (2) How much top-to-the-Northeast displacement related to the emplacement of the GHC is present in Himachal Pradesh, and (3) Where is the GHC located?

To answer these questions we examine a number of possible geodynamic scenarios for northwest India and compare these regarding their respective predictions on geometry of metamorphic isograds, cooling paths, and deformation histories of rocks throughout the MCT hanging wall.

We present new SHRIMP-RG U/Pb zircon ages that record ~485 Ma emplacement of Deo Tibba and other granitic rocks in the MCT hanging wall with only one sample showing a Miocene metamorphic overprint. New LA-MC-ICPMS Th/Pb ages of metamorphic allanite from samples of the Haimanta unit constrain the timing of peak metamorphic conditions. New $^{40}Ar/^{39}Ar$ cooling ages from the Beas and Chandra valleys are interpreted as early Miocene ductile extrusion and emplacement of the GHC.

Raman spectroscopy on carbonaceous material on samples from the Bajaura nappe (LHS), structurally immediately above the base of MCT deformation, indicates peak temperatures of 500 - 550 °C. One sample from the Haimanta unit ca. 500 m above the MCT yields indistinguishable peak temperatures of 550 °C. Although preliminary in nature, these data further constrain the inverse metamorphic gradient recorded within the GHC (650 to 700 °C; Wyss, 2007), and are consistent with the equivalent data obtained further west in the Garwhal Himalaya.

References

Searle, M., Stephenson, B., Walker, J., and Walker, C., 2007, Restoration of the Western Himalaya: implications for metamorphic protoliths, thrust and normal faulting, and channel flow models, Episodes 30, 242–257.

Steck, A., 2003, Geology of the NW Indian Himalaya, Ecl. Geol. Helv. 96, 147–196.

Thakur, V.C., 1998, Structure of the Chamba nappe and position of the Main Central Thrust in Kashmir Himalaya, J. Asian Earth Sci. 16, 269–282

Webb, A., Yin, A., Harrison, M., Célérier, J., and Burgess, P., 2007, The leading edge of the Greater Himalayan Crystalline complex revealed in NW Indian Himalaya: Implications for the evolution of the Himalayan orogen. Geology 35, 955–958.

Wyss, M., 2000, Metamorphic evolution of the northern Himachal Himalaya: Phase equilibria constraints and thermobarometry, Schweiz. Mineral. Petrogr. Mitteil. 80, 317–350.

Miocene gneiss domes in the Pamir: extension in a convergent setting

Konstanze Stübner[1,2], Lothar Ratschbacher[2], Raymond Jonckheere[2], Jörg Pfänder[2], Bradley Hacker[3], István Dunkl[1], Klaus Stanek[2], Vladislav Minaev[4], and the TIPAGE Team

[1] Geowissenschaftliches Zentrum, Georg-August Universität Göttingen, Germany, konstanze.stuebner@geo.uni-goettingen.de
[2] Geologie, TU Bergakademie Freiberg, Germany
[3] Earth Research Institute, University of California, Santa Barbara, USA
[4] Tajik Academy of Sciences, Institute of Geology and Seismology, Dushanbe, Tajikistan

The Pamir Mts. of Central Asia have absorbed several hundred kilometers of Cenozoic north-south shortening due to the India–Asia collision. Shortening in the Pamir occurred over a narrow zone of ~500 km N–S distance, compared to >1200 km across the Tibet–Himalaya system further east. In contrast to the Tibetan plateau, high-grade metamorphic rocks are widely exposed in the Pamir and comprise >30 % of the surface outcrops. These rocks occur in at least seven gneiss domes that form E-trending, northward convex belts. As exemplified by detrital U-Pb zircon geochronology, the domes mostly comprise Paleozoic and Early Mesozoic metasedimentary rocks, which experienced Barrovian metamorphism with local migmatization (~600-700°C, ~9-14 kbar). Exhumation from mid- to lower crustal depths was attained during the Miocene; similarities in structure and exhumation histories suggests a common formation mechanism for several of these domes.

The composite Shakhdara–Alichur dome is the largest dome (~300 x 100 km). Doming in the Shakhdara dome started at ~20 Ma and continued until at least 3 Ma. Exhumation was mainly accomplished by a major south-dipping normal shear zone along the southern dome boundary, the South Pamir detachment. To the east, in the Alichur dome, vergence of exhumation switches to top-to-N along the less prominent Yashikul detachment; in the southeastern Pamir plateau, further diminished extension occurred within the Mesozoic cover sediments. The Central Pamir domes (Yazgulom, Gudara, Muzkol-Sarez) show similar north-south extension and Miocene onset, but earlier termination of exhumation.

Apatite (U-Th)/He ages from the Shakhdara may indicate a renewed episode of rapid cooling starting in the late Pliocene or Pleistocene, likely related to incision of the Pjansch river system. The pronounced difference in relief between the Shakhdara dome and the eastern Pamir plateau argues against a purely climatic cause for Pleistocene river incision.

We attribute doming and extension to overall transpressional thickening with long-wavelength–low-amplitude buckling of the entire crust. Concurrent to subsequent mid-upper crustal extension compensates for excess thickening. The tectonics of the southern and central Pamir may be driven by shallow underthrusting of the western edge of the cold and rigid Indian lithosphere, which has detached from the Hindu Kush slab to the west, beneath the hot and thick Pamir crust. In contrast, in the northern Pamir Cenozoic deformation is mostly brittle, started late (Late Miocene-Pliocene), and dome formation (northwestern Pamir Kurgovat dome) involves only 5-10 km of Cenozoic exhumation. Syn-orogenic extension and gneiss dome formation of the amount documented in the central and southern Pamir is unparalleled in the Tibet orogen and provides insights into mid-crustal processes largely concealed in Tibet; it offers new possibilities for understanding collisional orogeny.

Tectonic attribute about Mesozoic-Cenozoic Basement of South Qiangtang Basin in Tibet, China

Genhou Wang, Guo-Li Yuan, and Xiao Liang

The School of Earth Sciences and Resources, China University of Geosciences, Beijing, 100083, China, wgh@cugb.edu.cn

South Qiangtang Basin (SQTB) is clamped between Longmucuo-Shuanghu-Lancangjiang and Bangonghu-Nujiang tectonic belts, and covered with Mesozoic-Cenozoic strata. Except Mesozoic-Cenozoic Strata, four series of metamorphic complexes could be observed in shapes of ellipse and oblong, such as Gemuri, Nierong, Jitang, and Jiayuqiao metamorphic complexes. However, there are some different viewpoints about metamorphic ages of these metamorphic complexes, cause of formation and tectonic attribute (Wang CS et al.2001; Huang JJ et al.2001, 2003; Kapp P et al. 2000, 2003).

Some researchers consider that, the basement of Qiangtang Basin is buildup by two-layers of Proterozoic metamorphic rocks, lower crystal "rigid basement", upper metamorphic "plastic basement", and middle angular unconformity (Wang GZ et al.2001; Wang CS et al.2001). Nonetheless, these four metamorphic complexes are systematically studied in order to well understand the basement of SQTB. Under the theory of rock rheology, structural analysis was carried out with comprehensive methods, such as micro-structure and macro-structure, structural deformation and metamorphic, isotopic geochronology. Based on such a research, we presume that Mesozoic-Cenozoic Basement of SQTB is mostly Paleozoic subduct-accretionary complex rock. Some evidences are shown here. Jitang metamorphic complexes: 40Ar/39Ar age of Phengite in Mica-quartzose Schist 230±1 Ma (Wang GH, 2008); Gemuri metamorphic complexes: Ar-Ar age of Glaucophane 222Ma, Crossite 223-220Ma or 221Ma, and Phengite 215Ma (Table 1); Jitang metamorphic complexes in this study: 40Ar/39Ar ages of Phengite in Mica-quartzose Schist 219.1±1, 218.1±1.3, 228.8±1.2, 228±1.3 Ma et al.

In summary, all of ages proved that Lanling Blueschists was formed at Late Triassic. Though Large-scaled geological mapping, structure analysis, and isotopic geochronology, it could be proposed that subduct-accretionary complex was formed during Indosinian.

Table 1 Metamorphic Ages of metamorphic rocks in Lanlin

Sampling site	Rocks	Mineral	Age (Ma)	Reference
East Lanling	Blueschist	Glaucophane	222	Kapp et al.2003
East Lanling	Blueschist	Crossite	223-220	Kapp et al.2003
West Jiaomuri	Blueschist	Crossite	221	Kapp et al.2003
West Jianaizangbu	muscovite schist	Phengite	215	Li C. et al. 2009

Heating the Over-Thickened Lithosphere, downward from Crust or upward from Mantle?

Yang Wang, Suhua Cheng

School of Earth Sciences and Resources, China University of Geosciences, Beijing, 100083, China, allen_thalassa@sina.com

Surface wave tomography shows that the thickness of the lithosphere beneath Tibet plateau is now about 300 km (Priestley and McKenzie, 2006). Their result suggests that the process that generated the thickened crust beneath Tibet plateau has resulted in thick lithosphere that extends beneath the whole plateau. Meanwhile, there is no evidence of large scale lithospheric removal since the formation of the plateau; thus, the thick lithosphere must be stabilized against convective instability, most probably by depletion (McKenzie and Priestley, 2008). They argued that the thick depleted lithospheric mantle to have been produced by shortening, to transport the depleted material downwards to form the mantle "keel". The downward conduction of heat generated by radioactive decay within the over-thickened crust causes the increasing of temperature and melting in the deep crust and the shallow mantle, and results in regional metamorphism and magmatism. When the crustal temperatures exceed the granite solidus, melting will occur, and the upward movement of melt will transport the elements that generate heat to the upper part of the crust. After the upper 30–40 km of this thickened crust has been removed by erosion, the Tibet will eventually become a craton. However, we find that the heat production rate used in the modelling of McKenzie and Priestley (2008) is too high. In their model, the upper and lower crustal thickness are 20 km and 5 km, with heat production rates of 2 $\mu W/m^3$ and 0.4 $\mu W/m^3$ respectively. This means that the average heat production rate of crust is 1.68 $\mu W/m^3$, two times of the global average for continental crust (Rudnick and Gao, 2003; Wang, 2006). Accordingly, crustal heating model can not explain the lithospheric thermal evolution of Tibet plateau.

Instead we propose the mantle heating model in here. If lithospheric removal has not occurred beneath Tibet, the only other heat source available should be mantle radioactivity. The lithospheric mantle beneath Tibet had been enriched from poly-phase subduction. Thus, after shortening the entire lithosphere, the radioactive elements fertile mantle became very thick, and the heat generation within the lithospheric mantle contributed a rather large portion of mantle heat flow. If the fertile mantle has average heat production rate are 0.1 $\mu W/m^3$, the mantle heat flow by radioactive decay in the 120 – 150 km thick mantle varies from 12 mWm^{-2} to 15 mWm^{-2}. This enhanced mantle heat flux can produce the same thermal effects as the crustal heating model suggested by McKenzie and Priestley (2008). The upward conduction of heat generated by radioactive decay within the over-thickened fertile lithospheric mantle will cause the increasing of temperature in the deep crust and the shallow mantle, and results in the decrease of seismic velocity in the shallow mantle, which is observed in the north part of Tibet plateau. When the temperatures in shallow mantle exceed the peridotite solidus, melting will occur, and the upward movement of melt will transport the heat-producing elements to the crust. Eventually, the over-thickened lithospheric mantle loses a lot of heat-producing elements, and cools down. Compared to the Archean undifferentiated crust, heat-producing elements are enriched in upper part of the Phanerozoic continental crust. Thus, we prefer the mantle upward heating rather than the crust downward heating to explain the thermal evolution of the over-thickened continental lithosphere formed in Phanerozoic epoch, such as Tibet plateau.

This study is supported by China 973 Program (Grant No. 2008CB425704), the National Natural Science Foundation of China (40572128, 40376013, 40104003), and the Fundamental Research Funds for the Central Universities (No. 2010ZD15 and 2010ZY23).

References

McKenzie, D. Priestley, K., 2008, The influence of lithospheric thickness variations on continental evoution, Lithos, 102, 1-11.

Priestley, K., McKenzie, D., 2006, The thermal structure of the lithosphere from shear wave velocities, EPSL, 244, 97-112.

Rudnick, R.L. and Gao, S., 2004, Composition of the Continental Crust. In: Holland, H.D., Turekian, K.K. (Eds.), Treatise of Geochemistry, vol. 3. Elsevier, Amsterdam, 1-64.

Wang, Y., 2006, Thermal State, Rheological Strength and Crustal Composition of North and South China. Geological Press, Beijing, 1-91 (in Chinese).

Constraining the cooling history of the Greater Himalayan Sequence in NW Bhutan

Clare J. Warren[1], Djordje Grujic[2], John M. Cottle[3], N.W. Rogers[1]

[1] Department of Earth and Environmental Sciences, The Open University, Milton Keynes, MK76AA, UK, c.warren@open.ac.uk
[2] Department of Earth Sciences, Dalhousie University, Halifax, Canada, BH3 4R2
[3] Department of Earth Science, University of California, Santa Barbara, CA 93106-9630, USA

Rutile from a mafic granulite, intermediate granulite and mafic amphibolite within juxtaposed litho/tectonostratigraphic units in the Greater Himalayan Sequence (GHS) of NW Bhutan yield overlapping laser ablation multi-collector inductively-coupled plasma mass spectrometry (LA-MC-ICPMS) U-Pb lower intercept cooling ages of 10.1 ± 0.4 Ma, 10.8 ± 0.1 Ma and 10.0 ± 0.1 Ma, respectively. Titanite that grew during an exhumation-related amphibolite-facies overprint on an eclogite-facies mineral assemblage from the neighbouring Jomolhari Massif yields a U-Pb lower intercept cooling age of 14.6 ± 1.2 Ma. The interpretation of cooling rate by linking thermochronometer ages to a single closure temperature, T_C (Dodson, 1973), is shown to not provide as useful insight into cooling rates as matching analysed ages with those calculated from diffusion models. Certain assumptions made in calculating T_C, specifically the assumption of high starting temperature and cooling rate proportional to 1/time, are not applicable to Himalayan timescales and temperature paths. Additionally, T_C requires knowledge of the cooling rate, commonly the unknown parameter of interest. Given the increasing precision of available geochronological data and the computationally undemanding nature of simple diffusion models, there is now little reason not to progress beyond Dodson's 1973 T_C formulation in the quest for determining cooling rates. Numerical diffusion models constrained by previously published temperature-time (Warren et al. 2011) and Pb-diffusion data (Cherniak 2000) suggest that the rutile ages from NW Bhutan may be explained by rapid cooling (>50 °C/Ma) from peak P-T conditions of ca. 800 °C and 1.0 GPa at 14 Ma in the granulite-bearing unit and ca. 650 °C at 12 Ma in the amphibolite-bearing unit. The good fit between the model and analysed ages confirms the relatively high retentivity of Pb in rutile suggested by experimental data (Cherniak 2000). Diffusion modelling additionally suggests that the titanite age is too old to be consistent with the temperature-time paths inferred for the other analysed samples. Instead, the titanite data suggest that the Jomolhari Massif cooled at a rate of ca. 40 °C/Ma from ca. 650 °C at an earlier time of 17-15 Ma. This suggests that the high-grade rocks in the Jomolhari Massif experienced a different cooling history from the rest of the GHS in NW Bhutan. Together these data show that high-grade rocks from three apparently different structural levels of the GHS in NW Bhutan experienced rapid cooling following high temperature metamorphism, but at different times. The highest grade granulite-facies rocks were exhumed from deeper structural levels that are not exposed, preserved, or remain unrecognized west of eastern Nepal. A progressive eastwards change in tectonic regime, metamorphic history and/or exhumation mechanism across the orogen is implied by these thermochronologic data.

References

Cherniak, D. J., 2000. Pb diffusion in rutile: Contributions to Mineralogy and Petrology, 139, 198-207.

Grujic, D., Warren, C. J., and Wooden, J. L., in review. Syn-convergent exhumation of elusive Himalayan crustal eclogites: Earth and Planetary Science Letters.

Warren, C.J., Grujic, D., Cottle, J.M., Rogers, N.W., in review. Constraining the cooling history of NW Bhutan from rutile and titanite chronology and diffusion modelling: Journal of Metamorphic Geology.

Structural, metamorphic and magmatic evolution of the SE Tibetan crust

Owen Weller[1], Mike Searle[1], Marc St-Onge[2], Dave Waters[1], Nicole Rayner[2], Jingsui Yang[3], Sun-Lin Chung[4]

[1] Department of Earth Sciences, University of Oxford, OX1 3AN, UK, owen.weller@earth.ox.ac.uk
[2] Geological Survey of Canada
[3] Chinese Academy of Geological Sciences
[4] National Taiwan University

The Tibetan plateau is the largest area of high average elevation (~5 km) and thick crust (~70-90 km) on the planet. It is composed of a series of terranes progressively accreted from the north since the early Mesozoic, and is bounded to the south by the collision of India with Asia ~50 Ma. Understanding the formation of the plateau is fundamental to understanding how collisional orogenies develop, how the lithosphere deforms and even how climate changes. However the timing of crustal thickening and surface uplift of the plateau has been the subject of much speculation and debate. Models proposed range from pre-collisional uplift, through gradual uplift following collision to sudden uplift ~7-8 Ma (England & Searle, 1986; Molnar *et al.*, 1993).

A major problem has been the lack of exhumed Tertiary high-grade metamorphic rocks in the plateau region. This is because Tibet is arid with low relief and little erosion so rocks are not readily exhumed. Therefore inferences are made about the Tibetan crust using alternative methods, such as analogue studies of the Karakoram, mantle xenoliths, volcanic distributions and receiver function studies (Searle *et al.*, 2010; Chan *et al.*, 2009; Chung *et al.*, 2005; Tilmann & Ni, 2003). However not all of Tibet is flat. The SE corner has high relief and is relatively unexplored. Recently high-grade metamorphic rocks have been discovered in the Eastern Nyenchen Tanglha Range, including cordierite and sillimanite grade gneisses and migmatites, providing a unique window into the lower crust of Tibet.

The age of metamorphism is currently unknown but in-situ and grain mount U-Pb SHRIMP dating of monazites and zircons from a suite of samples collected from this region in September 2010 is being conducted in May 2011, the results of which will be announced at the conference. Combined with pseudosection analysis, it is hoped that firm constraints can be placed on the various models of the evolution of Tibet. The ultimate aim of the project is (1) to determine the structural evolution of the crust along the southern margin of the Asian plate in the Lhasa block, (2) determine the pressure-temperature conditions of metamorphism and (3) determine the age of peak metamorphism, crustal thickening and exhumation of the Asian margin prior to, during and following the collision of India ~50 Ma.

References

England, P. and Searle, M., 1986, The Cretaceous-Tertiary Deformation of the Lhasa Block and its Implications for Crustal Thickening in Tibet, Tectonics, 5, 1-14.

Molnar, P., England, P., and Martinod, J., 1993, Dynamics, Uplift of the Tibetan Plateau, and the Indian Monsoon, Reviews of Geophysics, 4, 357-396.

Searle, M. *et al*., 2010, Anatomy, age and evolution of a collisional mountain belt: the Baltoro granite batholith and Karakoram Metamorphic Complex, Pakistani Karakoram, Journal of the Geological Society, 167, 183-202.

Chan, G. *et al*., 2009, Probing the basement of southern Tibet: evidence from crustal xenoliths entrained in a Miocene ultrapotassic dyke, Journal of the Geological Society, 166, 45-52.

Chung, S. *et al.*, 2005, Tibetan tectonic evolution inferred from spatial and temporal variations in post-collisional magmatism, Earth-Science Reviews, 68, 173-196.

Tilmann, F., and Ni, J., 2003, Seismic Imaging of the Downwelling Indian Lithosphere, Beneath Central Tibet, Science, 300, 1424-1427.

Coeval extrusion and lateral flow of the Greater Himalaya: New insights from structural and geochronological data in southern Tibet

Zhiqin Xu[1], Qin Wang[2], Fenghua Liang[1], Xuexiang Qi[1], Huaqi Li[1], Zhihui Cai[1], Zeng lingsen[1]

[1] State Laboratory of Continental tectonics and Dynamics, Ministry of Land and Resources. Institute of Geology, Chinese Academy of Geological Sciences, Beijing 100037, China, xzq@ccsd.cn
[2] State Key Laboratory for Mineral Deposits Research, Department of Earth Sciences, Nanjing University, Nanjing 210093, China

Orogen-parallel structures have been recognized in the Greater Himalayan Crystalline Complex (GHC). However, because the top-to-the-north and top-to-the-south shear fabrics are predominant in the north-dipping Main Central thrust (MCT) below and the South Tibet detachment (STD) above across the entire GHC, the tectonic significance of the orogen-parallel deformation in exhumation of the GHC was often ignored. Based on new field structural data, kinematic and geochronological analyses along the line of Pulan-Nyalam-Yadong in the GHC, we determined the east-west lateral flow between the GHC basement and its sedimentary covers. The lattice preferred orientations (LPO) of quartz and sillimanite from mylonite and mylonitic gneiss were measured using the electron backscatter diffraction (EBSD) technique. The kinematic fabrics in the wide shear zone and asymmetric LPOs of quartz and sillimanite indicate a consistent top-to-the-east shear sense in the eastern GHC, both top-to-the-east and top-to-the-west shear sense in the central GHC, and a top-to-the-west shear in the western GHC. The characteristic fabrics of quartz and sillimanite indicate the lateral flow occurred in the middle crust. However, the stretching lineation turns to north-south trending when close to the MCT and STD. Therefore the GHC is characterized by an extruded recumbent-shaped structure, which developed the top-to-the-north fabric and normal metamorphism sequence near the STD, and top-to-the-south fabric and inverse metamorphism sequence near the MCT. SHRIMP dating on zircon indicates that the orogen-parallel deformation initiated at 28-26 Ma in the eastern GHC, and 22-16 Ma in the western GHC. In addition, 40Ar/39Ar dating on biotite and muscovite yields 14-11 Ma for the eastern GHC. Our dating results are consistent with the activation age of the MCT (23-20 Ma) and STD (20-16 Ma), implying coeval orogen-parallel and orogen-perpendicular deformation during extrusion of the GHC. We propose a new channel flow model to interpret the architecture and extrusion of the GHC, in which the coeval east-west extension and north-south shortening occurred under pure shear during the India-Asia collision. The relatively fast strain rate in the middle of the channel resulted in the lateral flow of material in the GHC, and ductile detachment between the crystalline basement and the sedimentary cover in the middle crust.

Third Pole Environment (TPE) program: a new base for the study of "water–ice–air–ecosystem-human" interactions on the Tibetan Plateau and surrounding areas

Tandong Yao[1], Lonnie G. Thompson[2], Volker Mosbrugger[3], Xiaohan Liu[1], Yaoming Ma[1], Fan Zhang[1], Xiaoxin Yang[1], Daniel R. Joswiak[1]

[1] Institute of Tibetan Plateau Research, Chinese Academy of Sciences, China, xhliu@mail.iggcas.ac.cn
[2] Byrd Polar Research Center, the Ohio State University
[3] Senckenberg Research Center for Nature Study

Centered on the Tibetan Plateau, the Third Pole region stretches from the Pamir and Hindu Kush in the west to the Hengduan Mountain in the east, from the Kunlun and Qilian mountains in the north to the Himalayas in the south, covering an area over 5000 km^2 with an elevation higher than 4000m. Like the Arctic and Antarctica, the Third Pole is one of the most sensitive areas responding to global climate change due to its high altitude and the presence of permafrost and glaciers, which are most sensitive to global warming. Supported by the Chinese Academy of Sciences and some international organizations, the Third Pole Environment Program (TPE) is now being implemented to attract international research institutions and academic talents to focus on a theme of "water–ice–air–ecosystem-human" interactions in the Third Pole region, to reveal environmental change processes and mechanisms on the Third Pole and their influences on and regional responses to global changes, and thus to serve for enhancement of human adaptation to the changing environment and realization of human-nature harmony (www.tpe.ac.cn/en/).

Cenozoic Bimodal Volcanic Rocks of the Northeast boundary of Tibet Plateau: implication for the collision-deduced mantle flow in Tibetan Plateau and the rifting genesis of North-south tectonic belt

Xuehui Yu, Xuanxue Mo, Zhida Zhao, Guochen Dong, Su Zhou

China University of Geoscience, Beijing, 100083, China, xhy532@yahoo.com.cn

Cenozoic bimodal volcanic rocks of the Northeastern boundary of Tibet Plateau located in the area of West Qinling, Gansu Province in China, which belong to the west boundary of Ordos block and also north section of North-South tectonic belt in tectonics. The longitude is E104°30'-105°36' and the latitude is N33°35'-34°40'in geography. The bimodal volcanic rocks like to East Africa rift, consisted of kamafugite, carbonatite, Shoshonite, rhyolite and/or trachyte. The age of the bimodal volcanic rocks is between 23Ma to 7.1Ma determined by isotopic dating of K/Ar and $^{39}Ar/^{40}Ar$. The $^{87}Sr/^{86}Sr$ = 0.704031-0.70525, $^{206}Pb/^{204}Pb$ = 18.408-19.062, $^{207}Pb/^{204}Pb$ = 15.476-15.677, $^{208}Pb/^{204}Pb$ = 38.061-39.414 and εNd = 0.3-5.3 of the volcanic rocks, all of these are similar to the feature of Neo-Tethyan mantle geochemical end member represented by Yaluzangbu ophiolites, and also to the volcanic rocks related to Onto Java and FOZO mantle plume (Yu et al., 2009, 2011). It showed the Cenozoic bimodal volcanic rocks have the geochemical feature of Indian Ocean mantle geochemical domain. and the genesis of the bimodal volcanic rocks may be related to mantle plum, the magmatic resources of the volcanic rocks should be a depleted mantle.For this reason, we guess the origin and genesis of Cenozoic bimodal volcanic rocks related to northeastward migration and upwelling of the collision-deduced mantle flow along the interface of 400 km depth beneath the Tibetan plateau, and also responses to eastward expanding of the Tibetan plateau.

Cenozoic bimodal volcanic rocks in Western Qinling providing ideal lithoprobes for understanding North-south tectonic belt and proved North-south tectonic belt is a rift However, we should take notice of the West Qinling has been located compression geobackground coming from North Asia continent, West Pacific tectonic domain and Southwest Tethyan domain since Mesozoic to Cenozoic(Zhang et al., 2006). The crustal thickness is 52Km and the deep of the lithopheric bottom is >120Km in West Qinling revealed by geophysics (Lin et al., 1995). The geothermal of West Qinling is higher than that of Huabei Craton and near to oceanic geothermal line determined by mantle xenoliths bearing on the kamafugite (Shi et al., 2003). Therefore, West Qinling is not a typic Craton and is a Cratonic blocks composed of many litter of blocks linked by oroginic belts (Deng et al., 1996). Among of the blocks have been seprated by East Kunlun faults and Nouth boundary fault systems of West Qinling with complex structure. For these reason mentioned above, we guess the rifting of North-south tectonic belt is not similar to Baikal rift, and is also not like East Africal rift formed in typic Craton. The feature and genesis of the rift of North-south tectonic belt not only controlled by northeastward migration and upwelling of the asthenosphere flow along the interface of 400 km depth beneath the Tibetan plateau, but also related to the differences of move velocity and direction between the blocks, and to the stress differences of compression, strike-slip, shear and stretch of the blocks and faults. So the North-south tectonic belt is an active tectonic belt and is a developing boundary of plates.

Characteristics and Transformation of Polybrominated Bipenyl Ethers in Tibetan Plateau Soil Contrasting to the East Area in China

Guo-Li Yuan and Genhou Wang

School of the Earth Sciences and Resources, China University of Geosciences, Beijing, 100083, China, yuangl@cugb.edu.cn

Polybrominated Bipenyl Ethers (PBDEs) is a new-style persistent organic pollutants, mainly originated from brominated Flame Retard in electric products, which is found to be toxic and bioaccumulative. In Tibetan plateau, PBDEs was found in surface soil and atmosphere. However, it is well known that, PBDEs contaminant in Tibetan plateau, especially the sites far away from Lahsa, is not local origination and transported from other area. Although there are some speculations about source area of PBDEs in Tibet, little evidences to prove those conclusions [1,2]. So, our study intends to found whether PBDEs in Tibet is relative to those in East China by analysis of PBDEs congers' characteristics in soils. In addition, transformation of PBDEs absorbed in soil is similar or not while they are in Tibet or East China. PBDEs have 209 congers from PBDEs-1 to PBDEs-209, while number of bromine atom in compound change from 1 to 10. Commonly, degradation of PBDEs in media is from high to low bromine. Figure 1 shows the sampling sites of soil in Tibetan and the east China.

Based on contrasting composes of PBDEs congers in Tibetan and East China Soil, it is found that:
(1) Ratio of light congers (∑ PBDE1-47/∑PBDE1-209) is ca. 72wt%, and PBDE209 just is 1.3wt% in Tibetan area. In east area, 15.7%wt for sum of light congers and 68.1%wt for PBDEs209.
(2) In east area, the ratio of high brominated congers (∑PBDE153-209/∑PBDE1-209) is linear to that of light congers (∑PBDE1-47/∑PBDE1-209), which indicates that light congers is relative to that high ones, or light congers was transformed from high ones in soils. However, such relationship between high and light congers cannot be found, which also suggested that light congers are not directly originated from degrade of high ones in soils.

Based on analyzing the relativity between the content of clay in soils with PBDEs congers in different degrading level, the transform of PBDEs in soil is found as following:
(3) In Tibetan plateau, the ratio of light congers and high ones are negatively related to the content of clay in soil, which suggests that high or light congers are all undergone photo-degrade by the catalysis of clay in soils. The light congers are also transferred with high ones from other areas.
(4) In East China, the ratio of high congers is negatively related to the content of clay in soil, while ratio of light congers is positively related to the content of clays. It suggested that clay catalyzed photo-degrade from high congers to light ones. Because the source is local, soil firstly absorbed high congers, then degraded into light ones due to the catalysis of clay in soil.

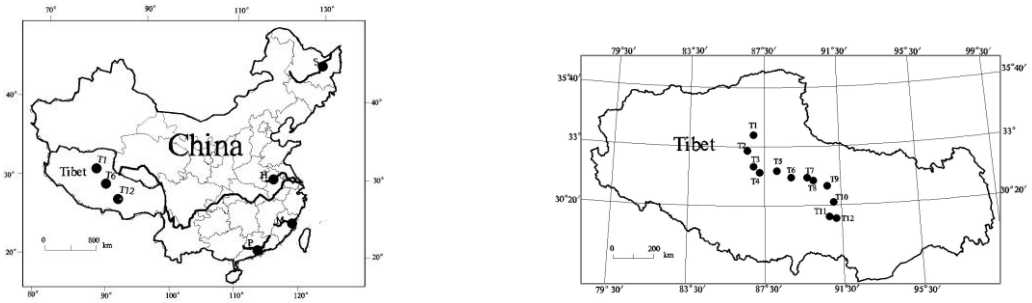

Figure 1. The map of sampling sites

References
Wang XP et al. Environ. Sci. Technol. 2010, 44, 2988-2993.
Wang P et al. Chemosphere 2009, 76, 1498-1504.

Crustal structure of the eastern margin of the Tibetan Plateau from magnetotelluric data

Yan Zhan[1], Guoze Zhao[1], Martyn J. Unsworth[2], Lifeng Wang[1], Jijun Wang[1], Xiaobin Chen[1], Ji Tang[1]

[1] Institute of Geology, China Earthquake Administration, Beijing, 100029,China, zhanyan66@vip.sina.com
[2] Dept. of Earth and Atmospheric Sciences, University of Alberta, Edmonton, Alberta, T6G 2E3, Canada

Introduction

The ongoing collision between India and Asia causes both crustal thickening and strike slip motion on the northeastern and eastern margins of the Tibetan Plateau. Deformation of the crust in this region occurs by a range of processes that includes (a) brittle deformation on major strike slip faults and (b) continuous deformation in the subsurface, including crustal flow. Magnetotelluric (MT) exploration is a powerful tool for imaging crustal structure in regions undergoing active tectonics (Unsworth, 2010). This study presents two new magnetotelluric datasets that have been used to study the geoelectric structure of the Northeastern (HY area) and Eastern (LMS area) margins of the Tibetan Plateau (Fig.1).

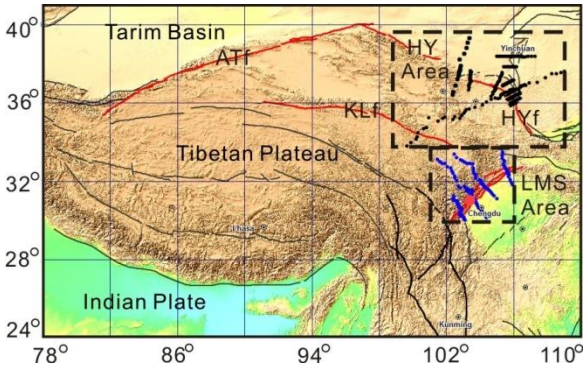

Figure 1 : Map of the India-Asia collision zone showing the two study areas. ATf = Altyn Tagh fault; KLf = Kunlun fault; HYf = Haiyuan fault

Haiyuan area - the Northeastern Margin of the Tibetan Plateau

Surface deformation in Northeastern Tibet is dominated by motion on a series of major strike-slip faults that accommodate the eastward motion of the crust (Altyn Tagh, Kunlun and Haiyuan Faults) (Tapponnier and Molnar, 1977; Burchfiel et al., 1991; Zhang et al, 2004). The Haiyuan fault is the most northerly of these faults (Deng et al., 1984; Li et al., 2009) and has generated a number of major earthquakes in the last century, such as Ms = 8.5 Haiyuan earthquake in 1920 and Ms = 8.0 Gulang earthquake in 1927 (Deng et al, 1986; Gaudemer et al., 1995). The variable topographic gradients of the eastern margin of the Tibetan Plateau have been explained on the basis of crustal flow occurring in regions with weakened lithosphere, and blocked by regions of strong lithosphere (Clark and Royden, 2000; Duvall and Clark, 2010). The tectonics of this area were investigated by a detailed MT survey from 1999 to 2005. The layout of the survey is shown in Figure 2. Data were processed using standard techniques and 2-D inversion was used to generate resistivity models which revealed a mid-crustal low resistivity layer to the south of the Haiyuan fault zone. However, it was absent to the north of the Haiyuan Fault.

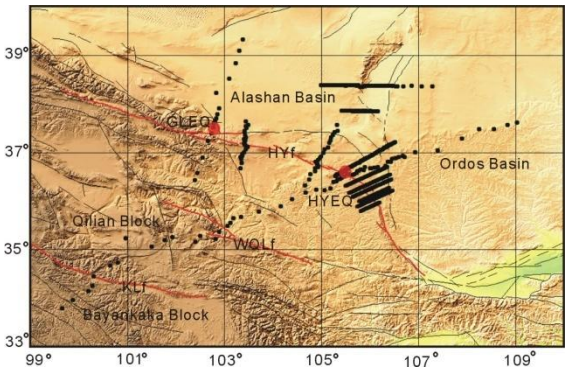

Figure 2 : Map of the Haiyuan MT study area. Black dots mark locations of MT stations. (KLf: Kunlun fault; WQLf: West Qinling fault; HYf: Haiyuan fault.

Longmenshan area-the Eastern Margin of the Tibetan Plateau

In contrast to Northeastern Tibet, the Longmenshan is characterized by a steep topographic boundary between the Eastern Tibetan Plateau and the Sichuan Basin. This steep gradient has been explained on the basis of lower crustal flow being blocked by the strong lithosphere of the Sichuan Basin (Clark and Royden, 2000). There is strong evidence for crustal flow west of the Sichuan Basin from evidence for uplifted landscapes (Clark et al., 2005). Despite the slow convergence rates, sufficient stress accumulated to cause the 2008 Wenchuan earthquake (Burchfiel et al., 2008). After the 2008 earthquake, MT data were collected on a number of profiles that crossed the Longmenshan, in order to understand the mechanisms that caused the earthquake, as shown in Figure 3.The MT data were used to generate 2-D resistivity models. These revealed a major mid-crustal low resistivity layer beneath the Eastern Tibetan

Plateau, similar to that observed beneath large areas of Eastern and Southern Tibet (Unsworth et al., 2005; Zhao et al., 2008; Bai et al., 2010). The resistivity of this layer implies a weak layer that could flow over geological timescales (Rippe and Unsworth, 2010). This weak layer terminated some 20-30 km west of the Longmenshan, which is a zone of high electrical resistivity. This observation clearly supports the hypothesis that uplift of the Eastern Tibetan Plateau has been caused by lower crustal flow (Clark et al.,2005; Burchfiel et al.,2008). Structural studies of the Longmenshan show evidence of folding (Hubbard and Shaw, 2009) but cannot explain the high topography west of the Longmenshan. Locally, a zone of low resistivity is observed surrounding the hypocentre region of the 2008 Wenchuan earthquake. However station spacing and data quality were not sufficient to fully define the geometry of this feature.

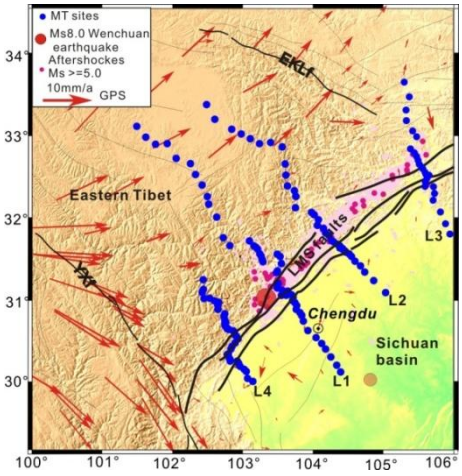

Figure 3. Map of Longmenshan MT study. Blue dots mark locations of MT stations. (YXf:Yushun-Xianshuihe fault; EKLf: East Kunlun fault; LMS faults: Longmenshan faults; GPS vectors are from Shen et al., (2009)

Summary

The study has revealed that a crustal low resistivity layer is observed beneath the northeastern and eastern Tibetan Plateau. The properties suggest that it could flow as suggested by geodynamic models. The layer terminates on the margins of the plateau, as predicted by the geodynamic models and it can explain the pattern of seismicity observed in the area.

References

Bai, D. et al., 2010, Crustal deformation of the eastern Tibetan Plateau revealed by magnetotelluric imaging, Nature Geoscience, 3, 358-362.

Burchfiel, B. C. et al., 1991, Geology of the Haiyuan fault zone, Ningxia Autonomous Region, China and its relation to the evolution of the northeastern margin of the Tibetan Plateau, Tectonics, 10, 1091–1110.

Burchfiel, B. C. et al., 2008, A geological and geophysical context for the Wenchuanearthquake of 12 May 2008, Sichuan, Peoples Republic of China. GSA Today, 18, 4-11.

Clark, M. K. and Royden, L. H., 2000, Topographic ooze: Building the eastern margin of Tibet by lower crustal flow, Geology, 28, 703-706.

Clark M. K. et al., 2005, Dynamic topography produced by lower crustal flow against rheological strength heterogeneities bordering the Tibetan Plateau, Geophys. J. Int., 162, 575–590.

Deng, Q. et al., 1984, Active faulting and tectonics of the Ningxia Hui Autonomous Region, China, JGR, 4427– 4445.

Deng, Q. et al., 1986, Variations in the geometry and amount of slip on the Haiyuan (Nanxihaushan) faultzone, China and the surface rupture of the 1920 Haiyuan earthquake, in Earthquake Source Mechanics, Geophys. Monogr. Ser., 37, edited by S. Das, J. Boatwright, and C. H. Scholz, pp. 169 –182, AGU, Washingtion, D. C.

Duvall, A. and Clark, M. K., 2010, Dissipation of fast strike-slip faulting within and beyond northeastern Tibet, Geology, 38(3), 223-226.

Gaudemer, Y. et al., 1995, Partitioning of crustal slip between linked active faults in the eastern Qilian Shan, and evidence for a major seismic gap, the 'Tianzhu gap', on the western Haiyuan fault, Gansu (China), Geophys. J. Int., 120, 599 – 645.

Hubbard, J. and Shaw, J.H., 2009, Uplift of the Longmenshan and Tibetan plateau, and the 2008 Wenchuan (M=7.9) earthquake, Nature, 458, 194-197.

Li C. et al., 2009, Late Quaternary left-lateral slip rate of the Haiyuan fault,northeastern margin of the Tibetan Plateau, Tectonics, 28, TC5010, 1-26.

Rippe, D. and Unsworth M., 2010, Quantifying crustal flow in Tibet with magnetotelluric data, Physics of the Earth and Planetary Interiors, 179, 107-121.

Shen, Z. et al., 2009, Slip maxima at fault junctions and rupturing of barriers during the 2008 Wenchuan earthquake, Nature Geoscience, 2, 718-724.

Tapponnier, P. and Molnar, P., 1977, Active faulting and tectonics in China, JGR., 82, 2905 –2930.

Unsworth, M. J. et al., 2005, Crustal rheology of the Himalaya and Southern Tibet inferred from magnetotelluric data, Nature, 433, 78-81.

Unsworth, M.J., 2010, Magnetotelluric studies of continent-continent collisions, Surveys in Geophysics, 31(2), 137-161.

Zhang, P. et al., 2004, Continuous deformation of the Tibetan Plateau from Global Positioning System data, Geology, 32(9), 809– 812.

Zhao, G. et al., 2008, Evidence of crustal 'channel flow' in eastern margin of Tibet Plateau from MT measurements. Chinese Sci. Bulletin, 53, 1887-1893.

A Magnetotelluric Study of the Altyn-Tagh Fault in the North Margin of the Tibetan Plateau

Letian Zhang[1,2], Matthew J. Comeau[3], Martyn Unsworth[3], Wenbo Wei[1,2], Sheng Jin[1,2], Gaofeng Ye[1,2], Jianen Jing[1,2], Florian Le Pape[4], Alan G. Jones[4], Jan Vozar[4]

[1] School of Geophysics and Information Technology, China University of Geosciences, Beijing 100083, China, letianOI@gmail.com
[2] Key Laboratory of Geo-detection of Ministry of Education, Beijing 100083, China
[3] Dept of Physics, University of Alberta, Edmonton, AB T6G 2J1, Canada
[4] Dublin Institute for Advanced Studies, Dublin, Ireland

The on-going continent-continent collision between the Indian and Eurasian plates has created the spectacular topography of the Tibetan plateau. The tectonic processes that occurred during this collision process are still not fully understood and different tectonic models have been proposed. Horizontal motions are clearly important, as evidenced by the major strike faults that characterize the Northern and Eastern parts of the Tibetan Plateau. However, the contribution of horizontal motion on these faults to the overall mass balance of the orogen is still not resolved (Yin and Harrison 2000). Another important tectonic process that has been discussed is the possibility of widespread crustal flow, although the spatial extent of this in Northern Tibet is not well defined (Clark and Royden 2000).

The INDEPTH project (InterNational DEep Profiling of Tibet and the Himalaya) has undertaken a series of integrated geological and geophysical studies across the Tibetan Plateau since 1993 (Nelson, et al. 1996). The final stage of the INDEPTH study (INDEPTH-IV) has been focussed on the dynamics of the Northern Tibetan Plateau. As part of this study, a series of magnetotelluric (MT) profiles have been collected across the Altyn Tagh Fault (ATF) in the Qinghai and Gansu provinces (Figure 1). The MT method provides images of subsurface resistivity. This parameter is sensitive to the presence of fluids and temperature and gives important constraints on crustal rheology. MT data has been effectively used in studies of active tectonics, including studies of strike-slip faults (Unsworth and Bedrosian 2004) and the Tibetan Plateau (Bai, et al. 2010, Unsworth, et al. 2005, Wei, et al. 2001). In this paper, we present some preliminary results from the MT data on the ATF-East profile (Figure 2).

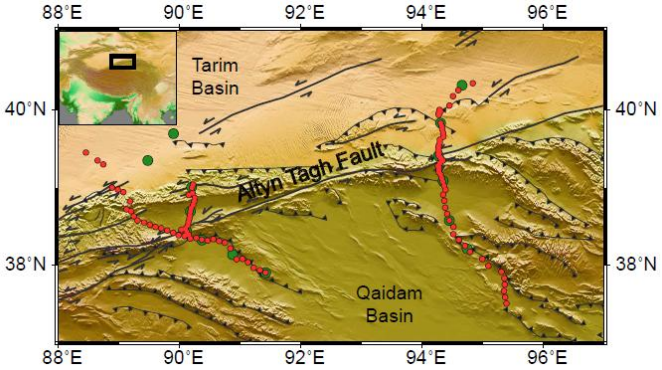

Figure 1. Topography map of the survey area. Red dots are broadband MT stations, and green dots are long-period MT stations.

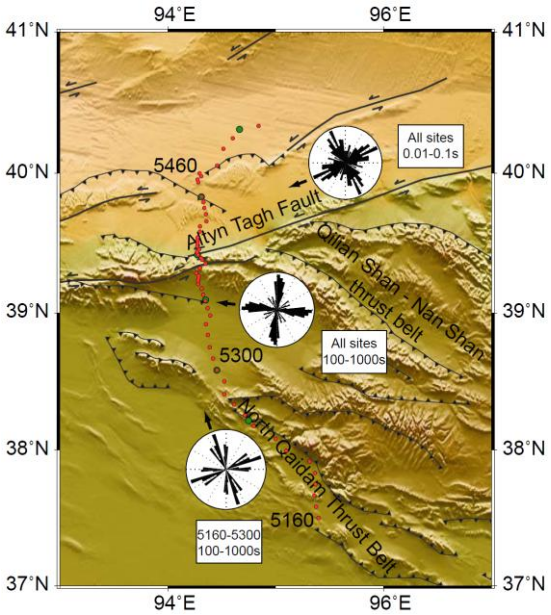

Figure 2. Map of the ATF-East line with rose diagrams showing strike analysis results.

Strike Analysis

The strike direction was determined using the multi-site, multi-frequency tensor decomposition technique of McNeice and Jones (2001). The northern and southern sections of the profile belong to different tectonic domains and have different strike directions. Thus the profile was divided into two sections, and results plotted as rose diagrams in Figure 2. It should be noted that strike directions determined with MT include an inherent 90° ambiguity. Therefore, other geological information is needed to determine the correct strike

direction. The rose diagrams show that the strike direction varies with the period of the EM signal. The shallow structure is sampled by the short period band (0.01 – 0.1 s), that gives a strike direction that is parallel to the surface trace of the Altyn Tagh Fault, as shown in the upper rose diagram on Figure 2. As period increases, the depth sampled increases and the strike direction becomes parallel to the thrust faults in the southern part of the profile. Another notable feature is the different long-period strike direction in the northern and southern parts of the profile. The strike direction of the southern part reflects the North Qaidam Thrust Belt (see the lower rose diagram).

Inversion Model

Giving the complicated geometry implied by the strike analysis, the inversions were focussed on the northern section of the profile. The MT data was rotated to a strike direction of N60°E and inverted with the algorithm of Rodi and Mackie (2001). As shown in Figure 3, conductive anomalies were found directly below the surface trace of the Altyn Tagh Fault. A conductive feature under the Qaidam basin was also detected in the inversion model. This is likely due to fluids in the fractured zone as the moving block of the Tibetan Plateau meets the stable block of Tarim Basin in the North. This large conductor may connect with the conductive layer already known to be widespread in the Tibetan crust. No major feature extending through the entire lithosphere is observed in this model, which implies that the Altyn Tagh Fault is relatively shallow feature at this location. This feature suggest that the eastern segment of the Altyn Tagh Fault is a crustal-scale structure, as suggested by Burchfiel et al., (1989).

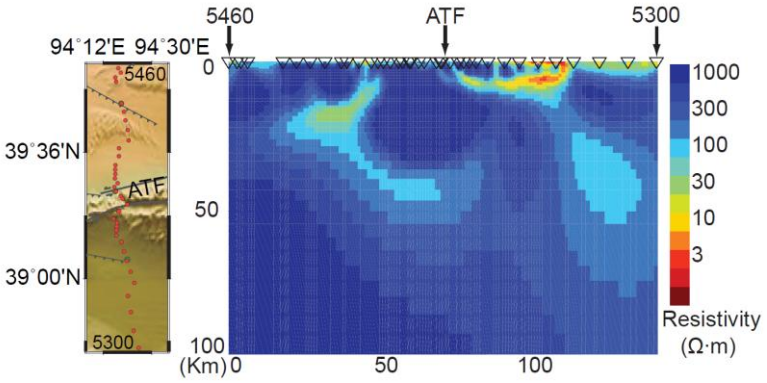

Figure 3. A comparison of the inversion model with the surface topography and geological structures along the northern section of ATF-East profile.

* This work was supported by a grant from the National Natural Science Foundation of China (General Program No. 40974058) and National Science Fund for Distinguished Young Scholars (No. 40904025).

References

Bai, D., et al., 2010, Crustal Deformation of the Eastern Tibetan Plateau Revealed by Magnetotelluric Imaging, Nature Geoscience, 3, 358-362.

Burchfiel, B.C., et al., 1989, Intracrustal Detachment within Zones of Continental Deformation, Geology, 17, 748-752.

Clark, M.K. and Royden, L.H., 2000, Topographic Ooze: Building the Eastern Margin of Tibet by Lower Crustal Flow, Geology, 28, 703-706.

McNeice, G.W. and Jones, A.G., 2001, Multisite, Multifrequency Tensor Decomposition of Magnetotelluric Data, Geophysics, 66, 158-173.

Nelson, K.D., et al., 1996, Partially Molten Middle Crust beneath Southern Tibet: Synthesis of Project INDEPTH Results, Science, 274, 1684-1688.

Rodi, W. and Mackie, R.L., 2001, Nonlinear Conjugate Gradients Algorithm for 2-D Magnetotelluric Inversion, Geophysics, 66, 174-187.

Unsworth, M.J. and Bedrosian, P.A., 2004, Electrical Resistivity Structure at the Safod Site from Magnetotelluric Exploration, Geophys. Res. Lett., 31, L12S05.

Unsworth, M.J., et al., 2005, Crustal Rheology of the Himalaya and Southern Tibet Inferred from Magnetotelluric Data, Nature, 438, 78-81.

Wei, W., et al., 2001, Detection of Widespread Fluids in the Tibetan Crust by Magnetotelluric Studies, Science, 292, 716-719.

Yin, A. and Harrison, T.M., 2000, Geologic Evolution of the Himalayan-Tibetan Orogen, Annual Review of Earth and Planetary Sciences, 28, 211-280.

The initial India-Asia continental collision and foreland basin evolution in the Tethyan Himalaya of Tibet: Evidences from stratigraphy and palaeontology

Qinghai Zhang[1], Helmut Willems[1, 2], Lin Ding[3] , Kai-Uwe Gräfe [1], Erwin Appel [4]

[1] Department of Geoscience, University of Bremen, D-28359 Bremen, Germany, zhang@uni-bremen.de
[2] Nanjing Institute of Geology and Palaeontology, Chinese Academy of Sciences, 210008 Nanjing, China
[3] Institute of Tibetan Plateau Research, Chinese Academy of Sciences, 100085 Beijing, China
[4] University of Tuebingen, Institute for Applied Geosciences, 72076 Tuebingen, Germany

Both Gamba and Tingri are located on the southern Tethyan Himalaya and exhibit Paleogene marine sedimentary strata with similar lithological sequences, from the base up depositing Indian-derived sandstones, larger foraminifera-bearing limestones, green marls and Asian-derived siltstones, and red marly siltstones and mudstones. The green marls and siltstones are proposed to be deposited in the foredeep of a foreland basin, and therefore represent the Initial India-Asia Continental Collision (IIACC) (Najman, et al., 2010; Zhu et al., 2005).

Our studies on the stratigraphy, palaeontology, and palaeoenvironment in Gamba and Tingri show that the cessation of limestone deposition occurring at the Shallow Benthic Zonation 7 (SBZ 7, ~54-55 Ma) in Gamba predates that in Tingri (the base of SBZ 10, ~52.8 Ma), indicating that Gamba fell into the foredeep earlier than Tingri, and consequently Gamba has a potential to provide a maximum age of the IIACC. In addition, on the distal part of a foreland basin (such as Tingri and Gamba), the forebulge will occur earlier than the foredeep, and consequently the age of the forebulge may better constrain the timing of the IIACC. In Gamba, a conglomerate layer immediately above the larger foraminiferal assemblage of SBZ 5 is proposed to represent the first formation of the forebulge during the onset of the foreland basin. The coincidence between the conglomerate layer and the Carbon Isotope Excursion (CIE) provides a precise age of 55.5-55.8 Ma (the Paleocene/Eocene boundary) for the IIACC. In addition, together with the age of the IIACC reported in Ladakh (Garzanti, E., 2008; Green et al., 2008), the synchronicity of the IIACC in the west (Ladakh) and east (Gamba) is approved by us.

References

Garzanti, E., 2008, Comment on "When and where did India and Asia collide?" by Jonathan C. Aitchison, Jason R. Ali, and Aileen M. Davis. J. Geophys. Res. 113, doi:10.1029/2007JB005276.

Green, O.R., Searle, M.P., Corfield, R.I., Corfield, R.M., 2008. Cretaceous-Tertiary carbonate platform evolution and the age of the India-Asia collision along the Ladakh Himalaya (Northwest India). J. Geol. 116, 331-353.

Najman, Y., Appel, E., Boudagher-Fadel, M., Bown, P., Carter, A., Garzanti, E., Godin, L., Han, J., Liebke, U., Oliver, G., Parrish, R., Vezzoli, G., 2010. Timing of India-Asia collision: Geological, biostratigraphic, and palaeomagnetic constraints. J. Geophys. Res. 115, doi:10.1029/2010JB007673.

Zhu, B., Kidd, W.S.F., Rowley, D.B., Currie, B.S., Shafique, N., 2005. Age of Initiation of the India-Asia Collision in the East-Central Himalaya. J. Geol. 113, 265-285.